An Experimental and Simulation Study on Parametric Analysis in Turning of Inconel 718 and GFRP Composite using Coated and Uncoated Tools

A THESIS SUBMITTED IN FULFILLMENT OF

THE REQUIREMENT FOR THE AWARD OF THE DEGREE

OF

Master of Technology (Research)

in

Mechanical Engineering

Submitted

by

Rajiv Kumar Yadav
(Roll No. 612ME311)

Under the Supervision of

Prof. Siba Sankar Mahapatra

Department of Mechanical Engineering

National Institute of Technology, Rourkela 769008

August 2014

Devoted to my best loving family

CERTIFICATE

This to certify that the thesis entitled ñ**An Experimental and Simulation Study on Parametric Analysis in Turning of Inconel 718 and GFRP Composite using Coated and Uncoated Tools**ò being submitted by **Rajiv Kumar Yadav** for the award of the degree of Master of Technology (Research) (Mechanical Engineering) of NIT Rourkela, is a record of bonafide research work carried out by him under our supervision and guidance. **Mr. Rajiv Kumar Yadav** has worked for more than two years on the above problem at the Department of Mechanical Engineering, National Institute of Technology, Rourkela and this has reached the standard fulfilling the requirements and the regulation relating to the degree. The contents of this thesis, in full or part, have not been submitted to any other university or institution for the award of any degree or diploma.

Dr. Siba Sankar Mahapatra
Professor
Department of Mechanical Engineering
National Institute of Technology,
Rourkela

Place: Rourkela
Date:

ACKNOWLEDGEMENT

This thesis is a result of research that has been carried out at **National Institute of Technology, Rourkela**. During this period, I came across with a great number of people whose contributions in various ways helped my field of research and they deserve special thanks. It is a pleasure to convey my gratitude to all of them.

In the first place, I would like to express my deep sense of gratitude and indebtedness to my supervisor **Prof. S.S. Mahapatra** for his advice and guidance from early stage of this research and providing me extraordinary experiences throughout the work. Above all, he provided me unflinching encouragement and support in various ways which exceptionally inspire and enrich my knowledge.

I specially acknowledge **Prof. S. Datta** for his advice, supervision and crucial contribution as and when required during this research. His involvement with originality has triggered and nourished my intellectual maturity that will help me for a long time to come. I am proud to record that I had opportunity to work with an exceptionally experienced professor like him.

I am grateful to **Prof. S.K. Sarangi**, Director and **Prof. K.P. Maity**, former Head of Mechanical Engineering Department, National Institute of Technology, Rourkela, for their kind support and concern regarding my academic requirements. I am very much thankful to all my professors.

I express my thankfulness to the faculty and staff members of the Mechanical Engineering Department for their continuous encouragement and suggestions. Among them, **Sri P. K. Pal** deserves special thanks for his kind cooperation in non-academic matters during the research work. I also thankful to **Prof. S.K. Patel,** Professor Mechanical Engineering Department, **Mr. S. Das,** Technical Assistant Mechanical Engineering Department, for providing me the facility and guidance for performing the experiments.

I am indebted to **Mr. Kumar Abhishek, Ms. Bijaya Bijeta Nayak, Mr. Chhabi Ram Matawale, Mr. Manas Ranjan Singh, Mr. Suman Chatterjee, Mr. Chitrasen Samantra, Mr. Chinmaya Prasad Mohanty, Mr. Vikas Sonkar, Mr. Dilip Kumar Sen, Mr. Anshuman Kumar, Mr. Amit Mehar, Mr. Swayam Bikas Mishra** and **Ms. Sanjita Jaipuria** for their support and co-operation which is difficult to express in words. The time spent with them will remain in my memory for years to come.

There goes a popular maxim, ñOther things may change us, but we start and end with familyò Parents are next to God and I would like to thank my parents **Mr. Bachchu Singh Yadav** and **Mrs. Shanti Devi** for their numerous sacrifices and ever increasing unconditional love for me. A stock of loving appreciation is reserved for my elder brother **Mr. Ram Sewak Yadav, Mr. Jai Prakash Yadav, Mr. Prakash Yadav** and **Mr. Paras Yadav** and elder sisters **Mrs. Paravati Devi** and **Mrs. Chinta Devi** for their extreme affection, unfathomable belief and moral support for me. The thesis is dedicated to my family members.

Last, but not the least, I thank the one above all of us, the omnipresent God, for giving me the strength during the course of this research work.

Rajiv Kumar Yadav

ABSTRACT

Process simulation is one of the important aspects in any manufacturing/production context because it generates the scenarios to gain insight into process performance in reasonable time and cost. With upcoming worldwide applications of Inconel 718 and Glass Fiber Reinforced Polymer (GFRP) composites, machining has become an important issue which needs to be investigated in detail. In turning of hard materials (such as Inconel 718), cutting tool environment features high-localized temperatures (~1000ºC) and high stress (~700 MPa) due to contact between cutting tool and work piece. The tool may experience repeated impact loads during interrupted cuts and the work piece chips may chemically interact with the tool materials. Therefore, the use of coated tool is preferred for turning of Inconel 718. It is observed that performance of machining process is influenced by different machining parameters such as spindle speed, depth of cut and feed rate as in case of turning. Material removal rate (MRR) and flank wear in turning of Inconel 718 using physical vapour deposition (PVD) and chemical vapour deposition (CVD) coated on carbide insert tool are reported. A simulation model based on finite element approach is proposed using DEFORM 3D software. The simulation results are validated with experimental results.

The results indicate that simulation model can be effectively used to predict the flank wear and MRR in turning of Inconel 718. For simultaneous optimization of multiple responses, a fuzzy inference system (FIS) is used to convert multiple responses into a single equivalent response so that uncertainty and fuzziness in data can be addressed in an effective manner. The single response characteristics so generated is known as Multi Performance characteristic Index (MPCI). A non-linear empirical model has been developed using regression analysis between MPCI and process parameters. The optimal process parameters are obtained by a recent population-based optimization method known as imperialistic competitive algorithm (ICA). Analysis of variance (ANOVA) is performed to identify the most influencing factors for all the performance characteristics. The optimal conditions of process parameters during turning of Inconel 718 and GFRP composites are reported. It is observed that flank wear is combatively less when machined with PVD coated tool than CVD coated tool in turning of both Inconel 718 and GFRP composite.

Keywords: Finite element analysis; Fuzzy Inference System; Imperialistic competitive algorithm; Material removal rate; Flank wear

TABLE OF CONTENTS

LIST OF FIGURES

LIST OF TABLES

GLOSSARY OF TERMS

µm	Micro Meter
3D	Three Dimensional
ANN	Artificial Neural Network
ANOVA	Analysis of Variance
CFRP	Carbon Fibre Reinforcement Plastic
CVD	Chemical Vapour Deposition
DOE	Design of Experiment
F value	Fishers Value
FE	Finite Element
FEA	Finite Element Analysis
FEM	Finite Element Method
FIS	Fuzzy Inference System
FRP	Fibre Reinforcement Plastic
GA	Genetic Algorithm
GFRP	Glass Fibre Reinforced Plastic
HB	Higher-the-better
ICA	Imperialist Competitive Algorithm
LB	Lower-the-better
MADM	Multi Attribute Decision Making
MCDM	Multi Criteria Decision Making
mm	Millimeter
MPCI	Multi-Performance Characteristic Index
MRR	Material Removal Rate
PVD	Physical Vapour Deposition
USM	Ultrasonic Machining
WC	Tungsten Carbide

Chapter 1

INTRODUCTION

1.1 Introduction

Recent advances in aerospace and automotive industries find demand of nickel based super alloys and fibre reinforced plastic composites due to their favourable physical and mechanical properties such as high yield strength, excellent fatigue resistance, low thermal conductivity and good corrosion endurance in severe conditions, particularly in making components for jet engines and gas turbines. Therefore, it is essential to analyse the machinability behaviour of these materials to reduce the flank wear, surface roughness and maximize the material removal rate (MRR). Literature in this field highlights various aspects of machining to study process behaviour and parametric influence so that high quality finished parts in terms of dimensional accuracy and surface finish can be produced. The coating of tool is essentially required to reduce the wear while machining hard materials. Coatings of tool act as diffusion fences which prevent the contact between chips formed during the machining and the cutting material itself. Typical constituents of coating are titanium carbide (TiC), titanium nitride (TiN), titanium carbonitride (TiCN) and alumina (Al_2O_3) (Devillez et al., 2007; Amini et al., 2013). Design of experiment (DOE) based on Taguchiôs orthogonal array can be conveniently applied to design the experimental layout so that machinability aspects can be studied to obtain maximum information related to the process with less number of experiments. Simulation of machining process can be used to understand the influence of process parameters on material removal rate, surface roughness and flank wear of tool so that experimental cost, time and effort can be reduced. Simulation model must be validated with experimental results to check the adequacy of the simulation model. Since DOE approach cannot optimize multiple responses in machining processes, attempt has been made to propose a fuzzy inference system coupled with a newly developed technique Imperialist competitive algorithm for simultaneous optimization of multiple performance characteristics.

1.2 Machining of Inconel 718 and GFRP Composites

Super alloys are heat-resistant alloys of nickel, nickel iron and cobalt that exhibit a combination of mechanical strength and resistance to surface degradation generally unmatched by other metallic compounds. The primary uses of these alloys are in (i) aircraft gas turbines e.g. disks, combustion chambers, bolts, castings, shaft exhaust systems, blades, vanes etc. (ii) steam turbine power plants e.g. bolts, blades, stack gas reheaters (iii) reciprocating engines e.g. turbocharger, exhaust valves, hot plugs etc. (iv) metal processing e.g. hot work tool and dies, casting dies (v) medical applications e.g. dentistry uses, prosthetic devices (vi) space vehicles (vii) heat-treating equipment (viii) nuclear power systems (ix) chemical and petrochemical

industries (x) pollution control equipment and (xi) coal gasification and liquefaction systems (Choudhury and Baradie, 1998). Out of commercially available nickel base super-alloys, Inconel 718 is frequently used in aircraft gas turbines, reciprocating engines, space vehicles, nuclear power plants, chemical and petrochemical industries, and heat exchangers (Ezugwu et al., 1998; Choudhury and Baradie, 1998). Hence, it is the essential to analyse the machinability aspects of these components. Super-alloys generally have poor machinability. The characteristics that provide superior high-temperature strength make them difficult to machine. The main characteristics are responsible for its poor machinability;

(i) The high strength of nickel-base super-alloys at cutting temperatures causes high cutting forces generating more heat at the tool tip compared to alloy steel machining, (ii) The low thermal conductivity of these alloys transfers heat produced during machining to the tool, subsequently increasing tool tip temperatures and causing excessive tool wear, which can limit cutting speeds and reduce useful tool life.

(ii) The presence of hard, abrasive intermetallic compounds and carbides in these alloys causes severe abrasive wear at the tool tip.

(iii) The high capacity for work hardening in nickel-based alloys causes depth of cut notching on the tool which leads to burr formation on the work piece.

(iv) The chip produced during machining is tough and continuous requiring chip control geometry.

Inconel 718 is a family of austenitic nickel-chromium based super-alloy. Inconel alloys are oxidation and corrosion resistant materials well suited for service in extreme environments subjected to pressure and heat. When heated, Inconel 718 forms a thick, stable and passivating oxide layer protecting the surface from further attack. As Inconel 718 retains strength over a wide temperature range, it is attractive for high temperature applications where aluminium and steel would succumb to creep as a result of thermally induced crystal vacancies. The properties of Ni-based alloys contributing to poor machinability may be summarised as (i) a major part of their strength is maintained during machining due to their high temperature resistance properties (ii) work hardening occurs rapidly during machining which is a major factor contributing to notch wear at the tool nose and/or depth of cut line (iii) cutting tools suffer from high abrasive wear owing to the presence of hard abrasive carbides in the super-alloy (iv) chemical reaction occurs at high cutting temperatures when machining with commercially available cutting tool materials leading to a high diffusion wear (v) production of a tough and continuous chip which is difficult to control during machining resulting in degradation of the cutting tool by seizure and

cratering (vi) the poor thermal diffusivity of nickel-based alloys often generates high temperature at the tool tip as well as high thermal gradients in the cutting tool; (vii) high yield strength (viii) excellent fatigue resistance; and (ix) good corrosion endurance (Ezugwu et al., 1998).

Fibre-reinforced polymer (FRP) composite materials are defined as materials consisting of two or more constituents (phases) that are combined at the macroscopic level and constituent elements in a composite do not dissolve or merge completely into each other. Fibre-reinforced polymer composites contain a combination of a polymer matrix (either a thermoplastic or thermoset resin such as polyester, isopolyester, vinyl ester, epoxy and phenolic) and reinforcing agent fibres (glass, carbon, aramid or other reinforcing material) in sufficient aspect ratio. Both matrix and fibre maintain their physical and chemical identities. The fibres can be long (continuous) or short (discontinuous) (Teti, 2002). In FRP composites, glass fibre reinforced plastic is the most commonly used composite because of their favourable properties such as high strength to weight ratio, high fracture toughness, excellent corrosion and thermal resistances. It has relatively low stiffness, high elongation, and moderate strength and weight and generally lower cost relative to other FRP composite. It has been used extensively where corrosion resistance is important such as in piping for the chemical industry and in marine applications.

GFRP is inhomogeneous materials that consist of distinctly different phases. The reinforcement fibres are strong and brittle and may have poor thermal conductivity as in the case of glass fibres. Machining of glass fibre composite materials is difficult because of their inert nature, high hardness, and refractoriness. Machining of a composite depends on the properties and relative content of the reinforcement, fibre orientation and the matrix materials as well as on its response to the machining process (Dandekar and Shin, 2012). Oscillating cutting forces are generated because of the intermittent fracture of the fibres during machining. The Glass fibre breaks in brittle manner ahead of the cutting edge. Thus, the surface quality of the machined edge is greatly affected by the glass fibre reinforcement and its orientation. The cutting temperatures are also affected by the thermal properties and orientation of the fibres (Seheikh-Ahmad, 2009). Different thermal expansion coefficients of matrix and fibres lead to thermal stresses which may result in deformation and part damage. High cutting forces in turn result from the use of improper speeds and feeds, improper tool geometry and tool wear. Tool materials in machining composites should be capable of withstanding the abrasiveness of glass fibre and debris resulting from machining. The tool geometry should provide a keen edge capable of

neatly shearing the glass fibres. These two requirements are distinctively different from those expected of a cutting tool in metal machining (Seheikh-Ahmad, 2009).

The demand for cost efficiency in production and the development of new products ranging widely in complexity, material composition, size, and surface finish have forced cutting tool industry to develop new cutting materials and adopt new machining strategies for optimization of the machining process (Wertheim, 1998). Therefore, coated tool have been developed and adopted for cost and performance optimization in high speed machining conditions (HSM), especially high cutting speed and higher feeds (Wertheim, 1998). Coated carbide inserts are a must for working with ferrous materials such as iron, cast iron, steel or stainless steel. When machining super alloys, it is best to use a coated insert most of the time, especially when cutting alloys with medium to high machinability ratings. The use of coated tool is required for machining of titanium alloys, especially when not using high-pressure coolant.

Hence, this work mainly focused on the machinability aspects of Inconel 718 and GFRP composites using coated (PVD and CVD) carbide tool.

1.3 Need for Simulation and Optimization

The finite element analysis can provide a comprehensive and in some cases complementary approach to experimental, mechanistic or analytical approaches to study machining process. It offers capability to predict what could happen during the material removal process and thus it could be possible to design and modify the process input parameters beforehand in order to eliminate problems that may arise during actual machining operations (Davim, 2010). A realistic simulation of the chip formation, related cutting forces and chip temperatures serve to better process understanding. By implementing a material model into the finite element simulation, a realistic description of the material behaviour in terms of strain, strain rate and temperature becomes possible (Uhlmann et al., 2007). The conventional finite element machining simulations are conducted using DEFORM 2D to predict the heat generation and tool tip temperature during the cutting of Ti6Al4V (titanium alloy) using uncoated tool (Pervaiz et al., 2014). FEM machining simulations is carried out using a Lagrangian finite element based machining model to predict the tangential cutting force, temperature distribution at tool tip and effective stress and strain (Ezilarasan et al., 2014).

It has been recognized that conditions during machining such as feed rate, cutting speed and depth of cut should be selected to optimize the economics of machining operations as assessed by productivity, quality, manufacturing cost and time. In multi-objective situation, a suitable parametric condition is explored to simultaneously

optimize more than one objective. Although a large number of optimization methods have been proposed, fuzzy logic coupled with optimization techniques can lead to optimize the process in an uncertain and imprecise situation (Palanikumar et al., 2006). Genetic algorithm coupled with artificial neural network (ANN), an intelligent optimization technique, has been used to optimize parameters in machining of Inconel 718 considering multiple performance measures (Senthilkumaar et al., 2012). Multi-criteria decision making (MCDM) is used for selecting a single solution from non-dominated solutions during multi-objective optimization of high speed machining of Inconel 718 using carbide cutting tool (Thirumalai and Senthilkumaar, 2013). The imperialistic competitive algorithm (ICA) is used for multi-responses optimization of ultrasonic machining (USM) process (Teimouri et al., 2013). Firstly, the USM responses (e.g. MRR, tool wear and surface roughness) are modelled using the adaptive neuro-fuzzy inference system (ANFIS). Then, the developed models are used to define the objective function. Finally the ICA is applied for optimization of USM process.

1.4 Need for research

In modern day engineering, high demands are being placed on components made of Inconel 718 with improved accuracy of machined parts, speed of machining and surface roughness. Inconel 718 is mostly used because of their corrosion resistance and high yield strength (Ezugwu et al., 1998). Therefore, it is essential to study the machinability of Inconel 718. In spite of advantages, a number of key barriers like high heat generation, tool wear in tool insert and decrease in tool life still exist across dry machining of Inconel 718. To overcome this type of difficulties, coated tool (CVD and PVD) have been used to optimize the machining parameters using fuzzy inference system coupled with imperialistic competitive algorithm. A significant performance in tool life can be observed if cryogenic treated tungsten carbide tool is used in high speed turning of Inconel 718 by minimizing work hardening characteristics (Thakur et al., 2012). Simulation modelling is a powerful technique to predict the machining behaviour without incurring high cost of conducting experiments and time. The chip formation process is modelled using finite element (FE) simulation technique during machining of AISI 4340 steel using tungsten carbide tool (Arrazola and Ozel, 2010). A thermo-mechanical finite element model for the simulation of segmented chip formation in metal cutting has also been proposed (Aurich and Bil, 2006). Glass fibre reinforced plastics are used in various fields such as automobile, biomedical and aerospace industries because of their properties like light in weight, high strength, high stiffness, excellent corrosion and thermal resistances. Hence, it is necessary to study the machinability of GFRP

composite. Machining of GFRP composite is very difficult because of its non-homogeneity and mainly glass fibres are responsible for tool wear. The use of coated tool can overcome this type of difficulties. The optimization of machining parameters is also important for obtaining optimal value of process parameters. A utility concept has been used for multi-response optimization in turning of unidirectional glass fibre reinforced plastics composite using Carbide (K10) cutting tool (Kumar et al., 2013).

1.5 Objectives

In this context, the following objectives are made for the present study.

1. To study the effect of process parameters on performance characteristics in turning of Inconel 718 using numerical approach.
2. To validate simulation results obtained for Inconel 718 through experimental analysis.
3. To study machinability of both Inconel 718 and GFRP composite using coated (PVD and CVD) and uncoated tools.
4. To determine optimal parameter setting using multi-response optimization techniques.

1.6 Organization of thesis

The remainder of this thesis is organized as follows:

Chapter 2 Literature Review

The purpose of this chapter on the review of related literature is to provide background information on the issues to be considered in the thesis and emphasize the relevance of the present study.

Chapter 3 Numerical approach for turning of Inconel 718

This chapter describes the numerical approach for turning of Inconel 718. DEFORM 3D has been used for estimating material removal rate and flank wear. In turning of Inconel 718 using CVD coated tool, a three dimensional machining (3D) model is simulated for material removal rate and flank wear using DEFORM 3D. The machining simulation is carried out using Lagrangian approach to predict the flank wear and material removal rate (MRR). Flank wear is calculated using Usui's wear model in the simulation model. The results from simulation model is compared with experimental data generated using Taguchi's L_{16} orthogonal array.

Chapter 4 Multi-response Optimization in Turning of Inconel 718 using FIS embedded with ICA

This chapter covers the effect of machining variables such as spindle speed, feed rate and depth of cut on performance characteristics such as material removal rate, flank wear and surface roughness in the turning of Inconel 718 using chemical vapour deposition (CVD) coated tool and physical vapour deposition (PVD) coated

tool of tungsten carbide (WC). This chapter also covers the detail of coating and reason to use coating. The experiments are planed according to Taguchi's L_{16} orthogonal array. Analysis of variance (ANOVA) is performed to identify the most influencing factors for both the performance characteristics. Fuzzy logic has been used to integrate aforementioned evaluation characteristics into a single response i.e. MPCI (Multi Performance characteristic Index). An empirical model has also been derived for MPCI by using nonlinear regression analysis. Finally, imperialistic competitive algorithm (ICA) has been used to generate the optimal machining combination.

Chapter 5 Experimental Investigation on Performance of Coating of Cutting Tools in Turning of Glass Fibre Reinforced Plastic (GFRP) Composite

This chapter presents the application of fuzzy inference system with imperialistic competitive algorithm approach to obtain the optimal combination in turning of GFRP composite. The process parameters such as spindle speed, feed rate and depth of cut, coating of tool material and volume fraction of fibre has been taken into consideration to assess their effect on evaluation characteristics viz., material removal rate, flank wear and surface roughness. A mixed level L_{18} orthogonal array has been chosen for experimentation. The machining evaluation characteristics are converted into a single response by using fuzzy inference system. Non-linear regression analysis has been used to derive an empirical model which is treated as objective function for ICA. Finally, ICA has been implemented to generate the optimal parametric combination.

Chapter 6 Executive summary and conclusions

The present work emphasizes on improvement the machinability of Inconel 718 and GFRP composite.

Chapter 2

LITERATURE REVIEW

2.1 Introduction

The purpose of literature review is to provide background information on the issues to be considered in this thesis and emphasize the relevance of the present study. This dissertation holds various aspects during machining of Inconel 718 and GFRP composite. The study also explores the advantages of numerical modelling (finite element analysis) and multi-objective optimization methods. The topics include brief review:

- On numerical modelling (FEM modelling) of turning of Inconel 718 using chemical vapor deposition (CVD) coated tool.
- On experimental investigations of Inconel 718 and GFRP composite.
- On flank wear analysis of cutting tool using numerical and experimental approach.
- On multi-objective optimization of process parameters during machining of both Inconel 718 and GFRP composite.

2.2 Finite element analysis (FEA)

Many industries and academic centres are looking for an alternative that can help them to understand the metal cutting process with view to improve the manufacturing quality, machining process performance, optimum cutting conditions and cost reduction. One of these alternatives is the finite element analysis. Many researchers have studied application of finite element method to analyse the chip separation, tool wear, cutting forces, temperature and residual stresses for improving machining environment. Zebala and Slodki (2013) have applied finite element modelling (FEM) to analyse the effect of chip breakers during turning of Inconel 718. Uhlmann et al. (2007) have studied the formation of chips during high speed turning of Inconel 718 using different software such as DEFORM and ABAQUS. Vaz Jr. et al. (2007) have explained the complex physical phenomenon involved in chip formation using numerical modelling. Lorentzon and Jarvstrat (2008) have developed an empirical model through a finite element simulation to predict tool wear in machining of Inconel 718. It has been shown that advanced friction model is necessary than Coulomb friction for accurate prediction of wear. Lorentzon et al. (2009) have examined the effect of different fracture criteria on chip formation, particularly formation of segmented chips by a finite element model considering Inconel 718 as work piece. It has been noticed that produced chips are long and continuous at low cutting speeds (below 50 m/min) whereas chips are segmented at high cutting speeds (above 100 m/min). Yue et al. (2009) have proposed a finite element model to estimate tool wear in turning of hardened steel with polycrystalline cubic boron nitride (PCBN) tool. The

study implements Usui's tool wear model to study the relationship between tool life and cutting parameters. Attanasio et al. (2010) have developed a tool wear model in turning of AISI 1045 steel bars with ISO P40 uncoated tools using finite element analysis. The study highlights influence of rake angle and tool stresses on tool. Li (2012) presents a FEM simulation approaches for predicting tool wear and tool life in orthogonal cutting. Ceretti et al. (2000) have used DEFORM 3D to simulate cutting operations, particularly orthogonal cutting and oblique cutting operation. Yen et al. (2004) have developed a methodology to forecast the tool wear and tool life of uncoated carbide tool in orthogonal cutting of carbon steel using FEM simulation. Pittala and Monno (2010) have used DEFORM 3D to predict cutting forces in milling of aluminium alloy by coated tungsten carbide (WC)-Cobalt (Co) tool insert. Inta et al. (2010) have presented modelling of progressive tool wear in turning operation by integrating programming language MATLAB code with commercial FEM code DEFORM 2D Machining. Tanase et al. (2012) have predicted cutting edge temperature considering appropriate friction model at the tool-chip interface using DEFORM 3D software package. Tamizharasan and Kumar (2012) have studied the effect of tool geometry on flank wear, surface roughness and cutting forces while machining of AISI 1045 with uncoated carbide inserts. It is reported that wear depth and cutting force decrease as nose radius increases. Bhoyar and Kamble (2013) have proposed a model to predict cutting forces, specific cutting energy and temperatures occurring at different points of chip/tool contact region and coating/substrate boundary for a wide range of tool materials using DEFORM 3D. Ezilarasan et al. (2014) have explored the simulated turning of Nimonic C-263 super alloy with cemented carbide cutting tool using DEFORM 3D. Arrazola et al. (2014) have compared experimental residual stresses with 3D finite element based simulation in machining of nickel-based alloy IN718.

2.3 Tool Wear Model

Usui et al. (1984) have developed an analytical model for crater and flank wear of tungsten carbide tool insert. Wear characteristics equation is first derived theoretically and verified experimentally. Zhao et al. (2002) have examined the effect of internal cooling on the flank wear of cutting tool in orthogonal cutting. The study has also presented a flank wear model for a cutting tool based on wear models considering the normal stress and thermal softening. Arsecularatne and Zhang (2006) have studied wear mechanisms of cutting tools made of tungsten-carbide (WC), polycrystalline cubic boron nitride (PCBN) and polycrystalline diamond (PCD) considering tool life and tool tip temperature. The study reveals that dominant tool wear mechanism for WC is diffusion wear whereas chemical wear for PCBN.

2.4 Turning of Inconel 718

Extensive research has been carried out using experimental, analytical and computational approaches in an effort to understand the effects of various process parameters during machining. Thakur et al. (2009) have examined the behaviour of cutting parameters in machining of super-alloy Inconel 718 by cemented tungsten carbide (K20) insert tool. Thakur et al. (2009) have demonstrated correlation between cutting speed, feed, and depth of cut with cutting force, cutting temperature, and tool life in high speed turning of Inconel 718 using cemented tungsten carbide tool in an effort to identify the optimum combination of cutting parameters. Thakur et al. (2010) have attempted to enhance the machinability characteristics in high speed turning of super-alloy Inconel 718 using quantity of lubricant, delivery pressure at the nozzle, frequency of pulses, direction of application of cutting fluid, cutting speed, and feed rate as the process parameters. It has been concluded that use of optimized minimum quantity lubrication parameters under pulsed jet mode leads to lower cutting force, cutting temperature, and flank wear. Bhatt et al. (2010) have conducted experimental investigation to study the wear mechanisms of uncoated tungsten carbide (WC), PVD and CVD tools in oblique finish turning of Inconel 718. Khidhir and Mohamed (2010) have studied the effect of cutting speed on surface roughness and chip formation when machining nickel-based alloy. The study has also explored the types of wear caused due to cutting speed on coated and uncoated carbide inserts. Pawade and Joshi (2011) have proposed a multi-objective optimization approach for simultaneous optimization of surface roughness and cutting forces in high-speed turning of Inconel 718 using Taguchi grey relational analysis (TGRA). The study reveals that depth of cut has most significant effect on performance characteristics. Zhou et al. (2012) have studied on surface quality generated under high speed finish turning conditions of age-hardened Inconel 718. The study also focusses on surface roughness, metallographic analysis of surface layer and surface damages produced by machining with coated and uncoated cubic boron nitride (CBN) tools. Olovsjo et al. (2012) have developed a model to examine the effect of parameters such as composition, grain size, hardness, heat treatment, temperature and strain rate on ductility, strain hardening and yield strength in machining of Inconel 718. Thakur et al. (2012) have established the relationship among degree of work hardening and tool life as a function of cutting parameters like cutting speed, feed, depth of cut, untreated tungsten carbide and post-cryogenic-treated tool in machining of Inconel 718. Zhu et al. (2013) have emphasized on study of tool wear in the machining of nickel-based super alloys. This study reveals the existing gaps in the knowledge on equilibrium thermodynamic condition, thermal-mechanical

coupling, tool nose radius and thermal diffusion layer in coated tools in machining of nickel-based super alloys.

Cantero et al. (2013) have analysed tool wear mechanisms in finish turning of Inconel 718 both in wet and dry condition using cemented carbides, ceramics and CBN tools. Fahad et al. (2012) have investigated the cutting performance of tungsten carbide tools with multilayer CVD (chemical vapour deposition) coatings in dry turning of low carbon alloy steel (AISI/SAE-4140) over a wide range of cutting speeds (between 200 and 879 m/min). The study reveals that coating layouts and cutting tool edge geometry significantly influence heat distribution in the cutting tool. Devillez et al. (2007) have studied the behaviour of coated carbide tools at high cutting speeds in dry machining during orthogonal cutting. Cutting and feed forces are measured and tool wear mechanisms analysed for various cutting conditions. The performance of coated tool are compared and classified in order to select the tool and optimal cutting conditions. Arunachalam et al. (2004) have developed a set of guidelines, which will assist the selection of the appropriate cutting tools and conditions for generating favourable compressive residual stresses. They have specially dealt with residual stresses and surface integrity when machining (facing) age hardened Inconel 718 using two grades of coated carbide cutting tools specifically developed for machining heat resistant super alloys (HRSA). The effect of insert shape, cutting edge preparation, type of insert and nose radius of insert on both residual stresses and surface finish is studied at optimum cutting condition. Umbrello (2013) has investigated the effect of cutting speed and feed on the surface integrity during dry machining of Inconel 718 alloy using coated tools. In particular, the influence of the cutting conditions on surface roughness, affected layer, micro hardness, grain size, and microstructural alteration are investigated. Costes et al. (2007) have conducted the investigation to find the wear mechanisms and optimal tool grade during finishing operations of Inconel 718. They have found good result in a low CBN content with a ceramic binder and small grains. They have also checked wear mechanisms on the rake and flank faces. Fan et al. (2013) have studied the effect of tool material, tool shape and cutting parameters on the surface quality. Furthermore, they have also observed the tool wear and machined surface morphology, the effect of built-up edge (BUE), chip side flow and tool wear on surface quality in dry machining Inconel 718. Thakur et al. (2009) have attempted to study and analyse the machining characteristics considering the relationship between cutting force, tool-chip contact length, cutting temperature and its relationship with thermal loading, chip microstructural study and tool life during turning of Inconel 718 using tungsten carbide (K20) insert. Homami et al. (2014) have studied to understand the

complicated relationships between the cutting conditions and the process parameters in turning from both the modelling and optimization points of view. They carried out statistical analysis for identifying the significant factors of the cutting process, artificial neural networks (ANNs) for modelling the system and genetic algorithm (GA) for optimization of the cutting parameters. Pusavec et al. (2011) have examined the surface integrity characteristics of machined surface for different combinations of cooling/lubrication during turning of Inconel 718. The residual stresses on the machined surface and sub-surface, surface hardness and surface roughness among the significant characteristics are also studied. Jafarian et al. (2013) have developed the optimal machining parameters including cutting speed, feed rate and depth of cut for improving surface integrity in terms of residual stress and surface roughness in finish turning of Inconel 718. The process was modelled by ANN and GA. Then, the Genetically Optimized Neural Network System (GONNS) technique is used to find optimal machining parameters for minimizing the tensile residual stress. Amini et al. (2013) have investigated the effect of cutting speed, feed rate and depth of cut on surface roughness and tangential cutting force during high speed turning Inconel 718 by ceramic and carbide cutting tools.

2.5 Turning of GFRP composites

Palanikumar et al. (2009) have focused on the multiple performance optimization on machining characteristics of glass fibre reinforced plastic (GFRP) composites. They have examined the effect of cutting speed, depth of cut and feed on responses like material removal rate, flank wear and average surface roughness. The Non-dominated Sorting Genetic Algorithm (NSGA-II) is used to optimize the cutting conditions. Kumar et al. (2011) have presented an effective approach for the optimization of turning parameters based on the Taugchiôs experimental design approach with regression analysis. They have also discussed the use of Taugchiôs technique for minimizing the surface roughness and maximizing the material removal rate in machining unidirectional glass fiber reinforced plastics (UD-GFRP) composite with a polycrystalline diamond (PCD) tool. Palanikumar (2006) have discussed the application of the Taguchi method with fuzzy logic to optimize the machining parameters for machining of GFRP composites with multiple characteristics. A multi-response performance index (MRPI) is used for optimization. Kumar (2013) has presented a utility concept for multi-response optimization in turning unidirectional glass fibre reinforced plastics composite using carbide (K10) cutting tool. The process parameters such as tool nose radius, tool rake angle, feed rate, cutting speed, depth of cut and cutting environment are selected for this study. Statistically significant parameters are found to simultaneously minimize surface roughness and

maximize the material removal rate. The results are further verified by confirmation experiments. Khan et al. (2011) have examined the machinability of glass fibre reinforced plastic (GFRP) composite material. They have fabricated GFRP composite material using E-glass fibre with unsaturated polyester resin using a filament winding process. Machining process are carried out using two different alumina cutting tools namely a Ti [C, N] mixed alumina cutting tool (CC650) and a SiC whisker reinforced alumina cutting tool (CC670). The machining process is performed at different cutting speeds at constant feed rate and depth of cut. The performance of the alumina cutting tools is evaluated by measuring the flank wear and surface roughness of the machined GFRP composite material. Kini et al. (2010) have studied the effect of machining parameters on surface roughness and material removal rate (MRR) in turning of ±30° filament wound glass fibre reinforced polymers (GFRP) using coated tungsten carbide inserts under dry cutting conditions. They have developed second order empirical models for turning of GFRP utilising factorial experiments. Sait et al. (2009) have presented a new approach for optimizing the machining parameters in turning of glass fibre reinforced plastic (GFRP) pipes. Optimisation of machining parameters is carried out using desirability function analysis. The turning experiments are conducted for filament wound and hand layup GFRP pipes using K20 grade cemented carbide cutting tool. The machining parameters such as cutting velocity, feed rate and depth of cut are optimized by multi-response considerations namely surface roughness, flank wear, crater wear and machining force. Hussain et al. (2011) have studied the machinability of GFRP composite tubes of different fibre orientation angle varying from 30° to 90°. Machining studies are carried out on geared lathe using three different cutting tools such as carbide (K-20), cubic boron nitride (CBN) and polycrystalline diamond (PCD). The cutting parameters considered are cutting speed, feed, depth of cut and fibre orientation. The performance of the cutting tools is evaluated by measuring surface roughness (Ra) and cutting force (F_z). Chang (2006) has examined the chip formation in turning of high strength glass fibre reinforced plastic materials in turning with chamfered main cutting edge of P and K type carbide tools. Chip formation mechanisms have been obtained with respect to tip's geometries and nose radii of cutting tools. Palanikumar (2008) has discussed the use of Taguchi method and response surface methodologies for minimizing the surface roughness in machining glass fibre reinforced (GFRP) plastics with a polycrystalline diamond (PCD) tool.

Davim and Mata (2007) have investigated the machinability of glass ýbre reinforced plastics (GFRPs) manufactured by hand lay-up in turning. Statistical techniques using orthogonal arrays and analysis of variance (ANOVA) have been

employed to assess the inþuence of cutting parameters on specific cutting pressure and surface roughness. Mkaddem et al. (2013) have discussed the performance of multilayer coatings in dry cutting of fibre reinforced polymers. The cutting tests are performed on unidirectional carbon/epoxy and glass/epoxy specimens with 45° fibre orientation using both Chemical Vapour Deposited (CVD) and Physical Vapour Deposited (PVD) multilayer coatings with neatly different composition, grain size and substrate-to-coating adherence. SEM inspections are performed on the flank face in order to characterize the wear patterns. The released particles of both the coating layers and composite phases are found to govern the wear progression and friction over the flank face. Teti (2002) has discussed about various issues involved in conventional machining of the major types of composite materials. Seheikh-Ahmad (2009) has explored various characteristics during machining of polymer composites using various machining operations. Dandekar and Shin (2012) have presented a comprehensive review on modelling of machining of composite materials with a focus on the process of turning. Also discussed modelling of both fibre reinforced and particle reinforced composites. Modelling studies include molecular dynamic simulations, 2-D and 3-D finite element models and the emerging field of multi-scale modelling.

2.6 Imperialistic competitive algorithm (ICA)

Atashpaz-Gargari and Lucas (2007) have proposed a novel population based optimization algorithm for optimization inspired by the imperialistic competition. This algorithm also starts with an initial population like other evolutionary algorithms. Population individuals called countries are of two types i.e. colonies and imperialists and that all together form some empires. Teimouri et al. (2013) have used the imperialistic competitive algorithm (ICA) for multi-responses optimization of ultrasonic machining (USM) process using neuro-fuzzy inference system (ANFIS) coupled with ICA. Lian et al. (2012) have applied ICA in process planning. Yousefi et al. (2012) have used imperialist competitive algorithm (ICA) for optimization of a cross-flow plate fin heat exchanger with main objectives of minimization of total weight and total annual cost. Further, numerical results of ICA are compared with genetic algorithm results. Enayatifar et al. (2013) have developed a new evolutionary algorithm for multi-objectives based on imperialist competitive algorithm (ICA). Bashiri and Bagheri (2013) have proposed a new multi-response imperialist competitive algorithm (MRICA) in machining applications and compared with multi-objective genetic algorithm (MOGA). Niknam et al. (2011) have presented an efficient hybrid evolutionary optimization algorithm based on combined modified imperialist competitive algorithm (MICA) and K-means (K) known as K-MICA for clustering of

data. K-MICA algorithm is tested on several data sets and its performance is compared with ant colony optimization (ACO), particle swarm optimization (PSO), simulated annealing (SA), genetic algorithm, tabu search (TS), honey bee mating optimization (HBMO). Sabour et al. (2011) have proposed an imperialist competitive ant colony optimization (ICACO) for optimizing the truss structures. It is observed that ICACO is able to accelerate the convergence rate effectively compared to other algorithms. Talatahari et al. (2012) have established superiority of a novel chaotic improved imperialist competitive algorithm (CICA) over other algorithms at least for the benchmark functions. Ahmadi et al. (2013) have presented a new ICA-ANN model for oil rate prediction of wells. Duan and Huang (2014) have applied ICA in optimal path planning of unmanned combat aerial vehicle (UCAV). Idoumghar et al. (2013) have proposed a new hybrid imperialist competitive algorithm (ICA)-particle swarm optimization (PSO) algorithm to solve single objective and multi-objective problems.

2.7 Fuzzy Inference System (FIS)

Bose et al. (2013) have applied fuzzy logic based Taguchi analysis to optimize the performance parameters such as brake specific energy consumption, volumetric efficiency and brake thermal efficiency in hydrogen injection system for diesel engine. Shabgard et al. (2013) have applied a fuzzy-based algorithm for prediction of material removal rate (MRR), tool wear ratio (TWR), and surface roughness (R_z, R_k) in electrical discharge machining (EDM) and ultrasonic-assisted EDM (US/EDM) processes. Krishnamoorthy et al. (2012) have used grey fuzzy optimization method to optimize the drilling parameters for multiple output performance characteristics such as thrust force, torque, entry delamination, exit delamination and eccentricity of the holes during drilling of carbon fibre reinforced plastic (CFRP) composites. Analysis of variance (ANOVA) is used to find the most influential factor in drilling of CFRP composites. Majumder (2013) has described the application of a hybrid approach using fuzzy logic and particle swarm optimization (PSO) for optimizing the process parameters such as pulse current, pulse-on-time and pulse-off-time for output responses like material removal rate and electrode wear ratio (EWR) during the electric discharge machining of AISI 316LN stainless steel. Abhishek et al. (2013) have studied the effect of process parameters such as cutting speed, feed and depth of cut on MRR and surface roughness in turining of Nylon 6 using high speed steel cutting tool. Hanafi et al. (2013) have applied fuzzy models to optimize process parameters (cutting speed, feed rate and depth of cut) for multiple performance measures (cutting force, cutting power and specific cutting pressure) during turning of

reinforced poly ether ether ketone (PEEK) composite using titanium nitrite (TiN) coated cutting tools.

2.8 Multi-objective optimization

Thirumalai and Senthilkumaar (2013) have applied technique for order preference by similarity to ideal solution (TOPSIS) for selecting best parameter setting out of a large number of non-dominated solutions during high-speed machining of Inconel 718 using carbide cutting tool for reduce the uncertainty in choosing the best solution. Sardinas et al. (2006) have presented a multi-objective optimization technique based on genetic algorithms to optimize the cutting parameters such as cutting depth, feed and speed for two conflicting objectives like tool life and operation time in turning process. Yang and Natarajan (2010) have attempted to solve multi-objective optimization problem (minimization of tool wear and maximization of metal removal rate) subjected to the temperature and surface roughness constraints using multi-objective differential evolution (MODE) algorithm and non-dominated sorting genetic algorithm (NSGA-II) in turning of EN24 steel using tungsten carbide tool. Karpat and Ozel (2007) have presented dynamic-neighbourhood particle swarm optimization (DN-PSO) methodology for multi-objective optimization in turning process. Ranganathan and Senthilvelan (2011) have used grey relational analysis based on Taguchi technique for optimization of multiple response characteristics (surface roughness, tool life and metal removal rate) in hot turning of stainless steel (type 316) using tungsten carbide tool. Umer et al. (2014) have used multi-objective genetic algorithm (MOGA-II) optimization for oblique turning operations while machining AISI H13 tool steel using polycrystalline cubic boron nitride cutting tool. Bharti et al. (2012) have used non-dominated sorting genetic algorithm to optimize electric discharge machining (EDM) process using Inconel 718 as work piece and copper as tool electrode. Khamel et al. (2012) have investigated the effect of process parameters (cutting speed, feed rate and depth of cut) on performance characteristics (tool life, surface roughness and cutting forces) in finish hard turning of AISI 52100 bearing steel with cubic boron nitride (CBN) tool using composite desirability function associated with the response surface methodology quadratic models. Senthilkumaar et al. (2012) have proposed the genetic algorithm coupled with artificial neural network (ANN) to optimize the machining parameters in turning of Inconel 718. Ezugwu et al. (2005) have developed a prediction methodology based on artificial neural network during high speed turning of Inconel 718 with PVD-coated carbide (K 10) inserts.

One of the current challenges faced by manufacturing industries is the reduction of machining time and cost of experiments during machining of Inconel 718 and glass fibre reinforced plastic (GFRP) composites. In this direction, the current chapter highlights the development and problems associated with various aspects of dry turning of Inconel 718 and GFRP composites. The present literature survey begins with papers published after 1984 with maximum attention paid to last ten years. Table 2.1 presents the source and number of citations from each source. The majority of the citations are found in journals (93.88%). Journals viz., International Journal of Advanced Manufacturing Technology, Journal of Materials Processing Technology, Journal of Mechanical Science and Technology and International Journal of Machine Tools and Manufacture are most citied journals in this literature survey.

Table 2.1 Summary of publications referred

Source	Citation
Academic Journal of Manufacturing Engineering	1
Annals of the CIRP	1
Applied Soft Computing	1
Applied Mathematics and Computation	2
Arabian Journal for Science and Engineering	1
Archives of Computational Methods in Engineering	1
Communications in Nonlinear Science and Numerical Simulation	1
CIRP Annals-Manufacturing Technology	2
Energy	1
Engineering Applications of Artificial Intelligence	2
International Journal of Advanced Manufacturing Technology	21
International Journal of Machine Tools and Manufacture	7
International Journal of Refractory Metals and Hard Materials	1
International Journal of Simulation Modelling	1
International Journal of Research in Engineering and Technology	1
International Journal of Heat and Mass Transfer	1
International Journal of Industrial Engineering and Production Research	1
International Journal of Engineering, Science and Technology	2
Journal of Intelligent Manufacturing	1
Journal of Mechanical Science and Technology	7
Journal of Materials Sciences	1
Journal of Materials Processing Technology	6
Journal of Manufacturing Systems	1

Journal of Manufacturing Technology Management	1
Materials and Manufacturing Processes	1
Metals and Materials International	2
Materials and Design	3
Measurement	2
Neurocomputing	1
Procedia CIRP	1
Proceedings in Manufacturing Systems	1
Proceedings of the Institution of Mechanical Engineers	1
Simulation Modelling Practice and Theory	2
Surface and Coatings Technology	1
Tribology international	1
Wear	7
World Applied Sciences Journal	1
Conference papers	3
Book	5
Manual (DEFROM 3D)	1
Total	98

The surveyed literature is classified into a variety of sections dealing with specific issues related with machining of Inconel 718 and GFRP, finite element analysis, tool wear model, turning of Inconel 718, turning of GFRP, ICA, FIS and multi-objective optimization. Figure 2.1 shows the percentage of citations in each section discussed above.

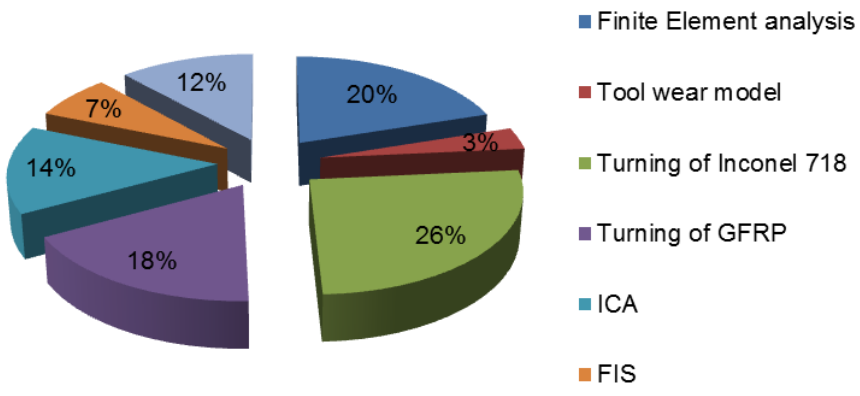

Figure 2.1 Percentage of paper surveyed

2.9. Conclusions

This chapter highlights to understand the machinability aspects of Inconel 718 and GFRP carried out by the researchers. The literature mainly focus on understanding the effect of machining variables such as cutting speed, feed rate and depth of cut on different performance evaluation characteristics in machining of these materials. Literatures also highlight the different methods of optimization techniques to evaluate the optimal parametric combination but less extent of work has been carried out using evolutionary techniques. The present work attempts to explain the effect of process variables in machining of Inconel 718 and GFRP. Attempt has been made for simultaneous optimization of multiple performance characteristics using fuzzy inference system coupled with a newly developed technique Imperialist competitive algorithm.

Chapter 3

A NUMERICAL APPROACH FOR TURNING OF INCONEL 718

3.1 Introduction

Nickel-based super alloys are widely used in aerospace industry particularly in making components for jet engines and gas turbines because of their high yield strength, excellent fatigue resistance, and good corrosion resistance in severe conditions. Out of commercially available nickel based super-alloys, Inconel 718 is frequently used in aircraft gas turbines, reciprocating engines, space vehicles, nuclear power plants, chemical and petrochemical industries, and heat exchangers. Hence, it is essential to analyse the machinability aspects of this alloy. Metal cutting of hard materials (super-alloys) is a challenging task for tool engineers. In machining process, material is removed from the surface of the work piece by a cutting tool forming unwanted material as chip. The complexities arise due to large deformation and high strain-rate in the primary shear zone and frictional contact between the cutting tool and chip along the secondary shear zone. Experimental analysis of metal machining process is normally expensive and time consuming. Alternative approach to get insight into machining process is computational methods such as boundary element, finite difference, finite element, and analytical methods. Amongst these methods, finite element modelling (FEM) is popular among the practitioners and researchers (Uhlmann et al., 2007; Vaz et al., 2007; Zebala et al., 2013). Finite element analysis was first applied to study metal cutting in the early 1970s when Tay et al. (Tay et al., 1974) developed a two-dimensional (2D) finite element model for orthogonal turning of steel in order to determine the temperature distribution in the chip and cutting tool (Ceretti et al., 2000; Aurich and Bil, 2006; Arrazola and Ozel, 2010; Attanasio et al., 2010; Pittala and Monno, 2010; Inta et al., 2010; Tanase et al., 2012; Bhoyar and Kamble, 2013; Arrazola et al., 2014; Pervaiz et al., 2014).

The present work attempts to study the effect of machining variables such as spindle speed, feed rate and depth of cut on performance characteristics such as material removal rate and tool wear in turning of Inconel 718 using chemical vapour deposition (CVD) coated tool of tungsten carbide (WC). The work aims at developing a three dimensional machining model for simulation of material removal rate and tool wear using DEFORM 3D. The machining simulation is carried out using Lagrangian approach to predict the flank wear and material removal rate (MRR). Flank wear is calculated using Usuiôs wear model in simulation model (Usui et al., 1984). The Johnson-Cook constitutive equation is implemented in the finite element model to study the deformation behaviour of Inconel 718 during the machining process and the constant coulomb friction model is employed in the finite element model to incorporate the friction characteristics of Inconel 718 alloy during machining (friction

developed at the interface of cutting tool and work piece). The results from simulation model are compared with experimental data.

3.2 Simulation Modeling

Finite element method has been proved to be an effective technique for analysing chip formation process and predicting machining performance characteristics such as temperatures, forces, stresses etc. (Fagan, 1992; Lorentzon and Jarvstrat, 2008; Lorentzon et al., 2009; Yue et al., 2009;). In this work, finite element method is used to simulate turning of Inconel 718 using CVD coated tungsten carbide tool. DEFORM 3D software is used for finite element analysis. DEFORM 3D software is based on an implicit Lagrangian computational approach (DEFROM 3D manual, 2007). For evaluation of flank wear and MRR, it is necessary to determine the output tool-chip interface pressure, tool-chip interface temperature, sliding velocity and volume change in work piece material (Yen et al., 2004). At initial stage of simulation, the process parameters for work piece and tool insert have to be defined. During simulation an initial temperature of 20°C, shear friction factor of 0.6, heat transfer coefficient of 45 N/sec/mm/°C and no coolant is set. The size ratio for tool insert is considered as 4. Similarly, the size ratio for work piece is 7. Tetrahedral element type for both work and tool insert with relative mesh size of 20000 is considered. Here, the work piece is considered as plastic material whereas the tool insert is treated as rigid material. In the simulation process, cutting length for work piece has been taken as 60 mm. The simulation steps are 5000. Figures 3.1 (A) to 3.1 (C) show the work piece at different steps of simulation. The physical and mechanical properties of Inconel 718 are as: density 8.2 g/cm^3, modulus of elasticity 205 GPa shear modulus 78 GPa specific heat capacity 435 J/kg°C, thermal conductivity 11.4 W/m/K, melting range 1260°C-1335°C, yield strength 1185 MPa, ultimate tensile strength 1435 MPa and thermal expansion 0.000012 m/m/°C at temperature 93°C. A three layered CVD coated (TiN, Al_2O_3 and TiCN) tungsten carbide tool is used due to its excellent build-up edge resistance, high hardness capable of cutting hard materials, high stability at high speeds and temperature and good wear resistance characteristics (Upadhyaya, 2001; Nouari and Ginting, 2007). The thermal barrier effect of the coating, especially Al_2O_3 layer, appears to significantly resist tool deformation at initial stage of cutting of hard materials. Vickerôs hardness of TiN coating is 2200 as compared to 1580 of tungsten carbide. Similarly, melting point of TiCN coating is 3070°C in comparison to 2785°C of tungsten carbide.

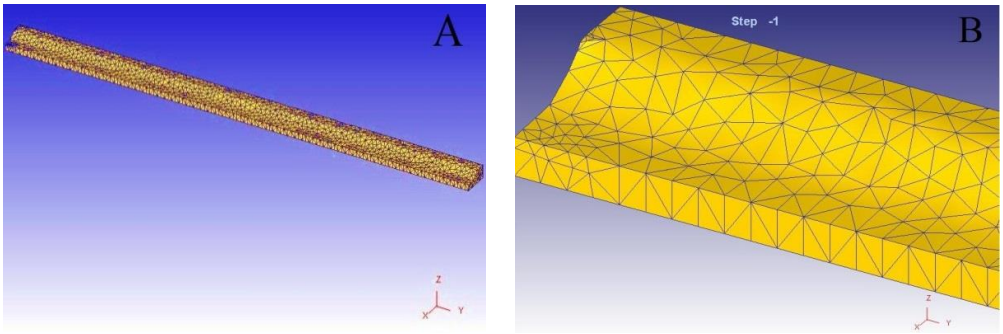

Figure 3.1 (A) Simplified model for work piece with mesh before turning
Figure 3.1 (B) Work piece at step 1

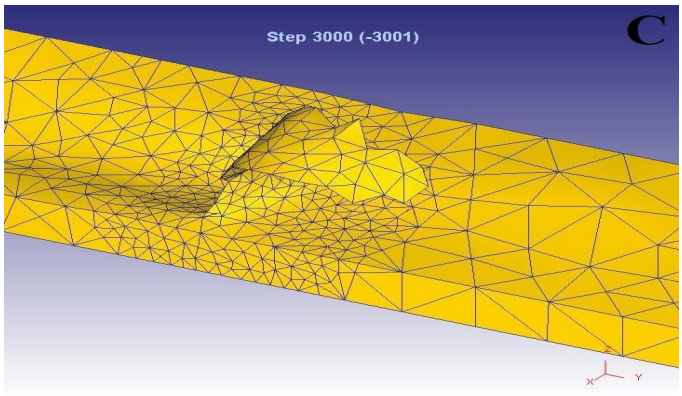

Figure 3.1 (C) Work piece in deformed shape at Step 3000

Johnson-cook model is suitable for modelling material because high strain, strain rate, strain hardening and non-linear material properties are involved in turning process (Uhlmann et al., 2007; Ezilarasan et al., 2014). The material model is given in equation 3.1. It is defined in DEFORM 3D material library. The constant of Johnson-cook model is shown in Table 3.1.

$$\bar{\sigma} = \left[A + B\bar{\varepsilon}^{n}\right] * \left[1 + C \ln\left(\frac{\dot{\bar{\varepsilon}}}{\dot{\bar{\varepsilon}}_0}\right)\right] * \left[1 - \left(\frac{T - T_r}{T_m - T_r}\right)^{m}\right] \quad (3.1)$$

where,

$\bar{\sigma}$ = Flow stress

A = Yield stress constant

B = Strain hardening coefficient

n = Strain hardening exponent

C = Strain rate dependence coefficient

m = Temperature dependence coefficient

$\bar{\varepsilon}$ = Equivalent plastic strain

$\dot{\bar{\varepsilon}}$ = Strain rate

$\dot{\bar{\varepsilon}}_0$ = Reference strain rate

T = Temperature

T_r = Room temperature

T_m = Melting temperature

Table 3.1 Johnson-Cook model constants for Inconel 718 (Uhlmann et al., 2007)

A (MPa)	B (MPa)	n	C	m	$\dot{\varepsilon}_0$ (1/s)	T_r (°C)	T_m (°C)
450	1700	0.65	0.017	1.3	0.001	20	1297

During machining process, friction plays an important role along cutting tool and work piece contact. Friction affects chip geometry, built edge formation, cutting temperature and tool wear. The friction force is defined by Coulombôs law shown in equation 3.2. The shear friction factor of 0.6 is considered in this work (Ezilarasan et al., 2014).

$$f_s = \varepsilon \sigma_t \tag{3.2}$$

where, f_s = Fictional stress, μ = Shear friction factor, $\mathring{u}_t =$ Interface pressure.

The tool insert is defined from DEFORM 3D library. The meshed tool insert is shown in Figure 3.2. During turning simulation, +Y axis is the cutting direction, -X axis is the feed direction and +Z axis is the depth of cut direction.

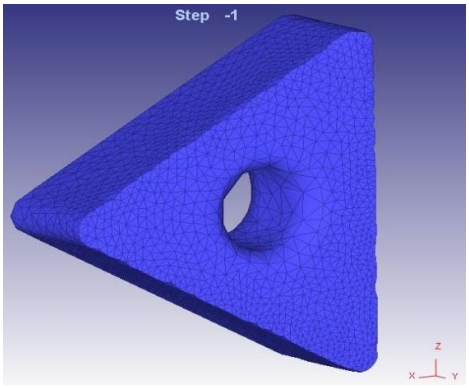

Figure 3.2 The meshed tool insert

After simulation, Usui model is used for calculation of flank wear (equation 3.3). The parameters such as interface pressure, interface temperature and sliding velocity are noted down from each simulation run (Usui et al., 1984).

$$\frac{dw}{dt} = A\, \mathring{u}_t V \exp\left(-\frac{B}{d'}\right) \tag{3.3}$$

where $w =$ Flank wear, $\mathring{u}_t =$ Interface pressure, $V =$ Sliding velocity, $d' =$ Interface temperature.

3.3 Experimental Details

A series of experiment has been carried out in CNC lathe (Model No. Sprint 16 TC manufactured by Batliboi Ltd. India) to assess the behaviour of machining parameters (spindle speed, feed rate and depth of cut) on the material removal rate and tool wear. A bar of Inconel 718 having diameter 30 mm, length 150 mm and

tensile strength of 1100 MPa has been used as work piece material. The composition of the work piece in mass percentage of 50-55 Ni, 17-21 Cr, 2.8-3.3 Mo, 4.75-5.5 Nb, 0.35 Mn, 0.2-0.8 Cu, 0.65-1.15 Al, 1 Co, 0.3 Ti, 0.35 Si, 0.08 C, 0.015 S, 0.015 P, 0.006 B and balance Fe. Here, chemical vapour deposition (CVD) coated tool of TNMA 332_KC9025 manufactured by Kennametal (three coatings: TiN-1µm, Al2O3-9.5µm and TiCN-4µm) is used as tool material having tool signature (10-10-7-7-5-5-0.8). Base material of coated tool is tungsten carbide (WC). DTGNL tool holder is used for this tool insert. Figure 3.3 shows the dimensions of tool TNMA 332: IC = 9.52 mm, T = 4.76 mm, R = 0.8 mm, B = 13.49 mm and H = 3.81 mm where IC = theoretical diameter of the insert inscribed circle, T = thickness of the tool insert, R = nose radius of tool insert, B = cutting edge length and H = inner hole diameter.

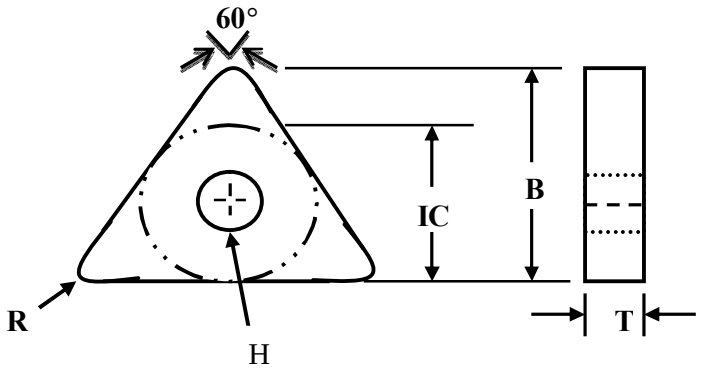

Figure 3.3 Tool Insert dimensions

A schematic layout for experimentation is highly required for reduction of experimental time and cost. Therefore, Taguchi method is adopted to design the experimental layout to examine the effect of the machining parameters with less number of experimental runs. In the present study, three process parameters have been varied at four different levels. Therefore, the possible combination of experiments is 4^3 (64). Using Taguchiôs orthogonal array concept, the number of experiments can be reduced to 16 for obtaining process related information in an effective manner. Table 3.2 presents different levels of process parameters such as spindle speed, feed rate and depth of cut. L_{16} orthogonal array used for conducting experiments is shown in Table 3.3. For experimentation, work piece is cut for a length of 60 mm during machining.

Table 3.2. Domain of experimentation

Sl. No.	Factors	Symbols	Unit	Level 1	Level 2	Level 3	Level 4
1	Spindle speed	N	RPM	421	605	787	1020
2	Depth of cut	d	mm	0.4	0.6	0.8	1
3	Feed rate	f	mm/rev	0.08	0.12	0.16	0.20

Tool wear is caused due to relative motion between the cutting tool and the work piece or the cutting tool and chip on machining area during turning. Tool wear is measured experimentally by optical microscope (SteREO Discovery V20 manufactured by Carl Zeiss MicroImaging Inc. having eyepiece magnification: 10X and objective magnification: 2.5X to 100X) as shown in Figure 3.4 (a) and Figure 3.4 (b). Maximum damage length of flank face has been considered for assessing the flank wear of tool insert. Experimental data of material removal rate and tool wear are listed in Table 3.2.

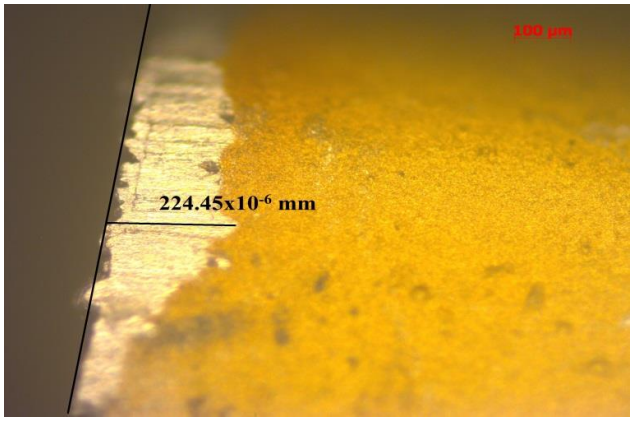

Figure 3.4 (a) Flank wear for CVD coated tool for spindle Speed 421 RPM, depth of cut 0.6 mm, feed rate 0.12 mm/rev

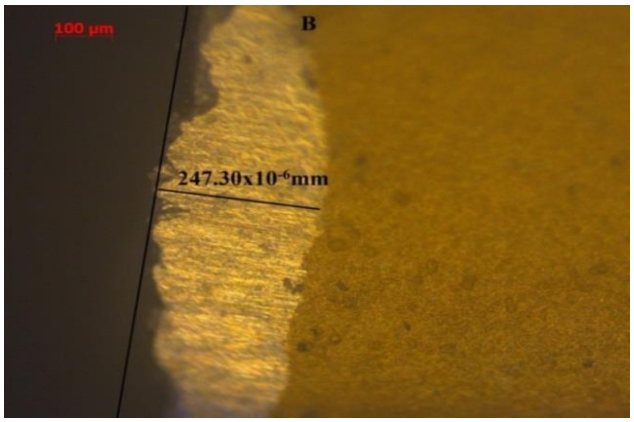

Figure 3.4 (b) Flank wear for CVD coated tool for spindle Speed 600 RPM, depth of cut 0.6mm, feed rate 0.08 mm/rev

As material removal rate (MRR) and tool wear have dominant effect on economics of the machining operations, estimation of these machining

characteristics is important and necessary in metal cutting for maintaining both productivity and quality. Material removal rate is defined as volume of work piece material that can be removed per time unit.

$$MRR = \frac{(V_i - V_f)}{t_m} \tag{3.4}$$

where, V_i = initial volume of work-piece, V_f = final volume of work-piece and t_m = machining time.

Table 3.3 Experimental data

Sl. No.	Levels of factors			Experimental Responses	
	N	d	f	Flank wear (μm)	MRR (mm^3/sec)
1	421	0.4	0.08	211.25	23.91
2	421	0.6	0.12	224.45	30.81
3	421	0.8	0.16	241.82	34.24
4	421	1	0.2	288.18	46.22
5	605	0.4	0.12	231.94	28.45
6	605	0.6	0.08	247.3	33.71
7	605	0.8	0.2	257.46	34.78
8	605	1	0.16	317.43	48.78
9	787	0.4	0.16	232.46	38.36
10	787	0.6	0.2	246.41	43.91
11	787	0.8	0.08	255.67	52.04
12	787	1	0.12	320.27	68.63
13	1020	0.4	0.2	280.37	42.96
14	1020	0.6	0.16	312.57	51.05
15	1020	0.8	0.12	337.53	64.84
16	1020	1	0.08	350.76	73.02

3.4 Results and discussions

Simulations of turning process for all experimental runs shown in Table 3.2 are carried out using DEFORM 3D. Usui's tool wear model has been used to evaluate flank wear. During simulation, the length of work piece that is machined is kept constant as 60 mm. In Usui's tool wear model, the flank wear is a function of interface pressure, relative velocity and absolute temperature. The constants of the wear model are taken as A = 0.0000000078 and B = 5302 (Yen et al., 2004; Tamizharasan et al., 2012; Li, 2012). In order to determine flank wear, it is necessary to observe tool tip temperature. The tool tip temperature arises due to interface friction between the tool tip and work piece. It has been noticed that temperature may vary from 950°C to 1100°C in turning simulation of Inconel 718. Figure 3.5 (a), 3.5 (b) and 3.5 (c) exhibit tool interface temperature, tool interface pressure and tool sliding velocity respectively for assessing the flank wear.

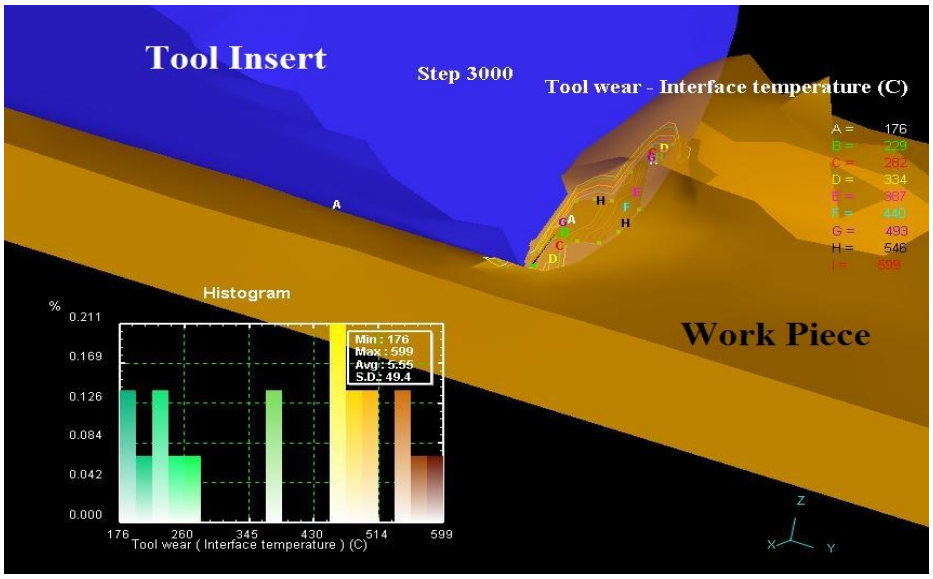

Figure 3.5 (a) Tool interface temperature in machining of Inconel 718 at spindle speed 605 RPM, depth of cut 0.4 mm, and feed rate 0.12 mm/rev

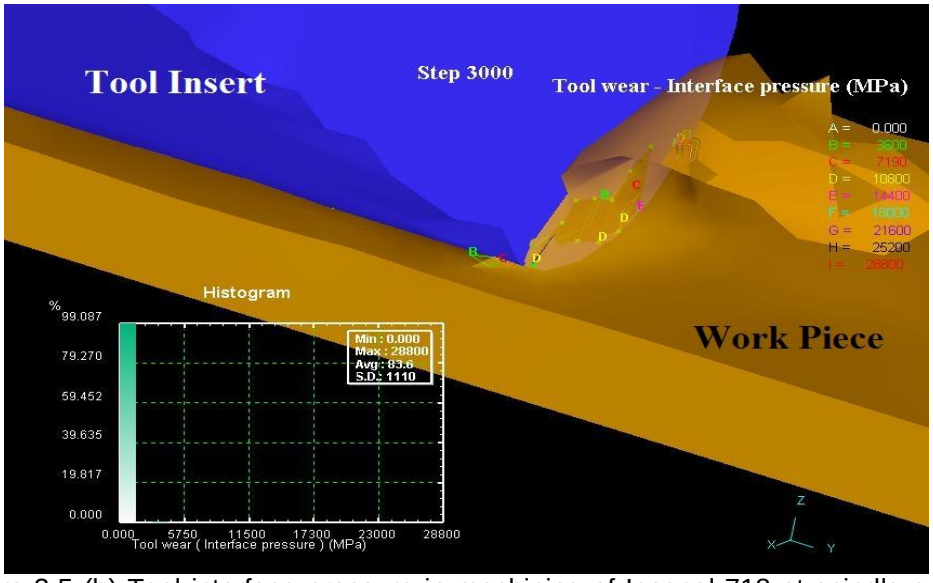

Figure 3.5 (b) Tool interface pressure in machining of Inconel 718 at spindle speed 605 RPM, depth of cut 0.4 mm and feed rate 0.12 mm/rev

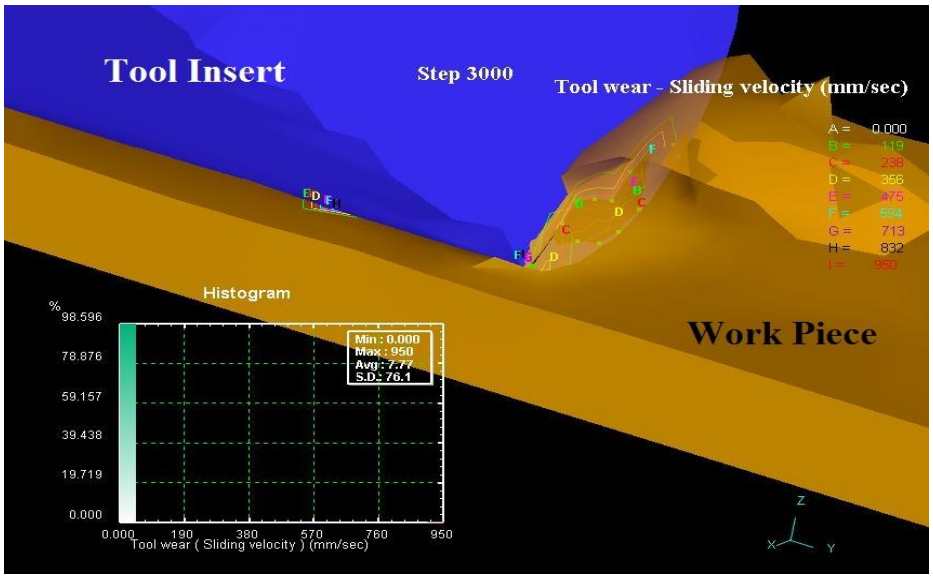

Figure 3.5 (c) Tool sliding velocity in machining of Inconel 718 at spindle speed 605 RPM, depth of cut 0.4 mm and feed rate 0.12 mm/rev

Material removal rate is evaluated using the values of change in volume obtained after the simulation through DEFORM 3D. The relation for calculation of MRR is shown in equation 3.4. Figure 3.6 shows the change in volume for a specific experimental run.

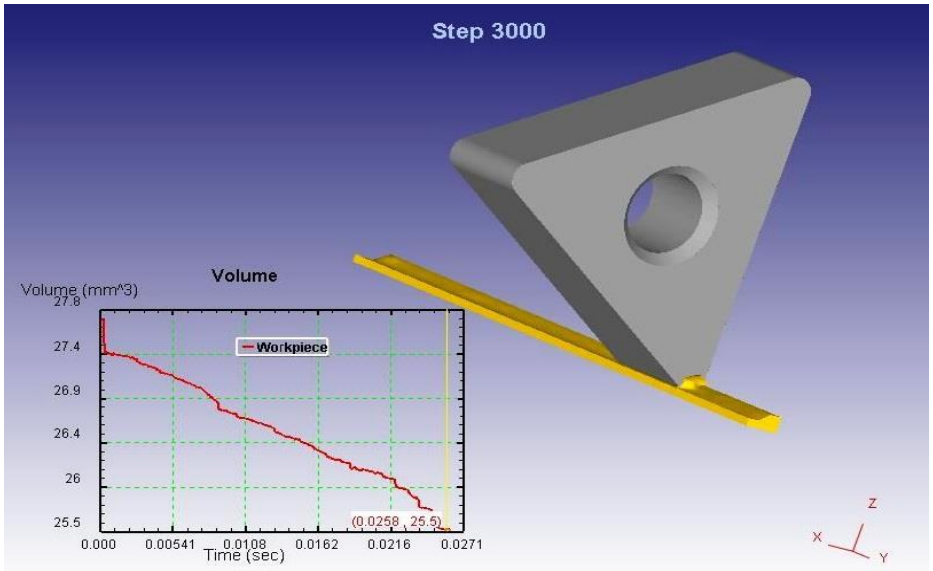

Figure 3.6 Change in volume in machining of Inconel 718 at spindle speed 605 RPM, depth of cut 0.4 mm and feed rate 0.12 mm/rev

Experimental data are collected as per experimental plan of Taguchi's L_{16} orthogonal array. Lower-the-better (LB) criterion is used for flank wear whereas higher-the-better (HB) criterion is used for MRR. Analysis of variance (ANOVA) is a method of partitioning observed variance into components of different explanatory variables to identify significance of each parameter (Thakur et al., 2009; Senthilkumaar et al., 2012). Table 3.4 and 3.5 present the ANOVA tables for flank wear and material removal rate respectively. It is to be noted that spindle speed and depth of cut are significant factors influencing on flank wear at significance level 0.05. Similarly, the factors like spindle speed, depth of cut and feed rate are significant factors influencing on MRR at significance level 0.05. The optimal parametric setting can be obtained from the factorial plots. Figure 3.7 (a) reveals that spindle speed, depth of cut and feed rate should be maintained at 421 RPM, 0.4 mm and 0.08 mm/rev respectively to minimize flank wear. Similarly, Figure 3.7 (b) indicates that spindle speed, depth of cut and feed rate should be maintained at 1020 RPM, 1 mm and 0.12 mm/rev respectively to maximize MRR.

Table 3.4 ANOVA for flank wear

Source	Degree of freedom	Sum of squares	Adjusted S S	Adjusted M S	F-Value	P-Value
Spindle speed	3	13635.0	13635.0	4545.01	54.36	0.000
Depth of cut	3	14075.0	14075.0	4691.66	56.11	0.000
Feed rate	3	430.0	430.0	143.32	1.71	0.263
Residual Error	6	501.7	501.7	83.61		
Total	15	28641.7				

Table 3.5 ANOVA for MRR

Source	Degree of freedom	Sum of Squares	Adjusted S S	Adjusted M S	F-Value	P-Value
Spindle speed	3	1599.02	1599.02	533.008	260.28	0.000
Depth of cut	3	1451.51	1451.51	483.837	236.27	0.000
Feed rate	3	92.27	92.27	30.756	15.02	0.003
Residual Error	6	12.29	12.29	2.048		
Total	15	3155.09				

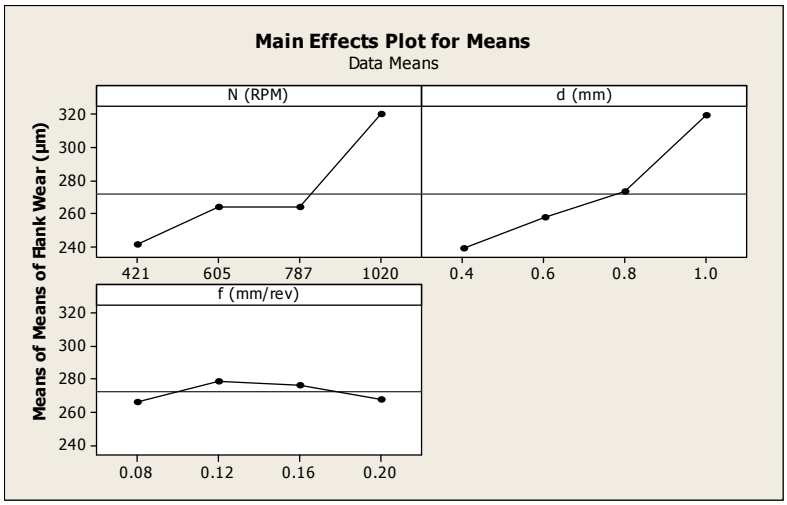

Figure 3.7 (a) Main effect plot for flank wear

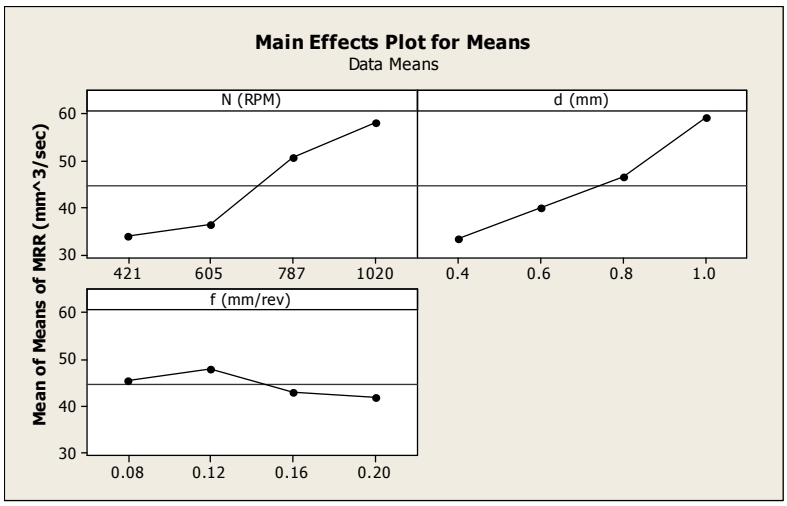

Figure 3.7 (b) Main effect plot for MRR

Figure 3.8 (a), 3.8 (b) and 3.8 (c) show the micrographs of the tool after turning at spindle speed of 421 RPM, feed rate of 0.20mm/rev and depth of cut of 1mm obtained from scanning electron microscope (JEOL JSM 6480LV). Flank wear is the main wear in the turning operation. The high flank wear is observed when spindle speed = 1020 RPM, depth of cut = 1 mm and feed rate = 0.08 mm.

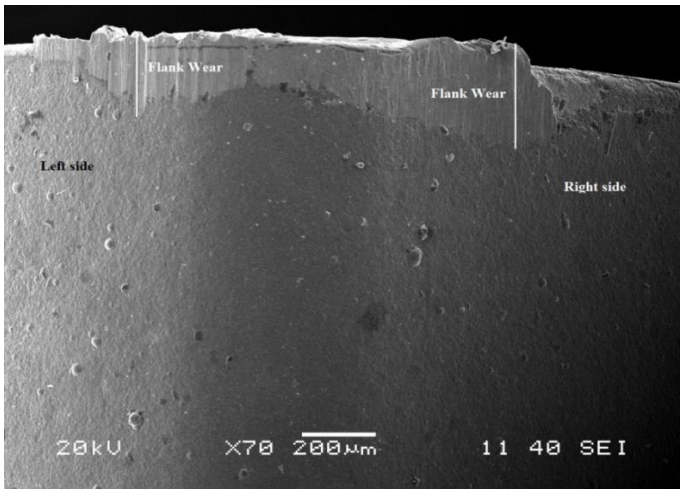

Figure 3.8 (a) Flank wear of CVD coated WC insert spindle speed of 421 RPM, depth of cut of 1 mm and feed rate of 0.20 mm

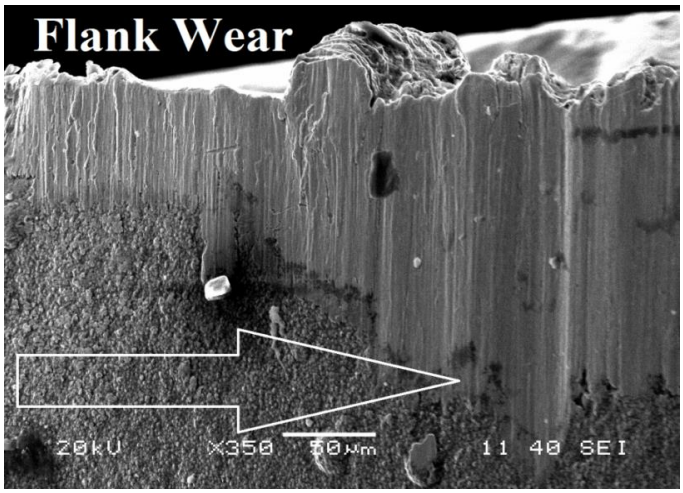

Figure 3.8 (b) Flank wear of CVD coated WC insert at spindle speed of 421 RPM, depth of cut of 1 mm and feed rate of 0.20 mm on left side of tool tip

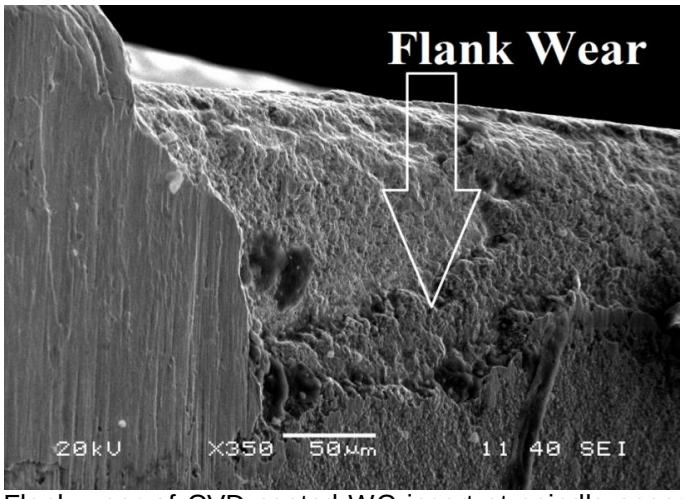

Figure 3.8 (c) Flank wear of CVD coated WC insert at spindle speed of 421 RPM, depth of cut of 1 mm and feed rate of 0.20 mm on right side of tool tip

The results obtained from the experimental and simulation runs need to be compared for checking the accuracy of the model by determining relative percentage error using equation 3.5.

$$\text{Relative Error } (\%) = \frac{|M_i - Y_i|}{Y_i} \times 100 \quad (3.5)$$

where M_i and Y_i are the simulation and experimental response value for i^{th} run.

Table 3.6 shows the relative error (%) for flank wear and MRR. Figures 3.9 and 3.10 show the comparison between the results obtained from simulation approach and experimental for flank wear and material removal rate respectively (Tamizharasan and Kumar, 2012; Ezilarasan et al. 2014). The average relative error (%) for flank wear and MRR have been found as 4.18% and 6.68% respectively. Therefore, it can be concluded that simulation of turning process results in good agreement with experimental outputs.

Table 3.6 Simulation results and corresponding relative error

Sl. No.	Simulation results		Experimental results		Relative error in %	
	Flank Wear (μm)	MRR (mm^3/sec)	Flank Wear (μm)	MRR (mm^3/sec)	Flank Wear	MRR
1	219.25	25.85	211.25	23.91	3.79	8.11
2	230.84	32.78	224.45	30.81	2.85	6.39
3	236.09	36.68	241.82	34.24	2.37	7.13
4	294.00	48.18	288.18	46.22	2.02	4.24
5	225.17	31.14	231.94	28.45	2.92	9.46
6	233.95	36.15	247.3	33.71	5.40	7.24
7	260.68	37.43	257.46	34.78	1.25	7.62
8	294.31	52.02	317.43	48.78	7.28	6.64
9	253.97	36.44	232.46	38.36	9.25	5.01
10	250.57	47.21	246.41	43.91	1.69	7.52
11	243.65	56.51	255.67	52.04	4.72	8.59
12	332.96	66.86	320.27	68.63	3.96	2.58
13	273.89	39.36	280.37	42.96	2.31	8.38
14	299.73	55.23	312.57	51.05	4.12	8.19
15	307.56	65.55	337.53	64.84	8.88	1.1
16	365.32	79.43	350.76	73.02	4.15	8.78
Average relative error					4.18	6.68

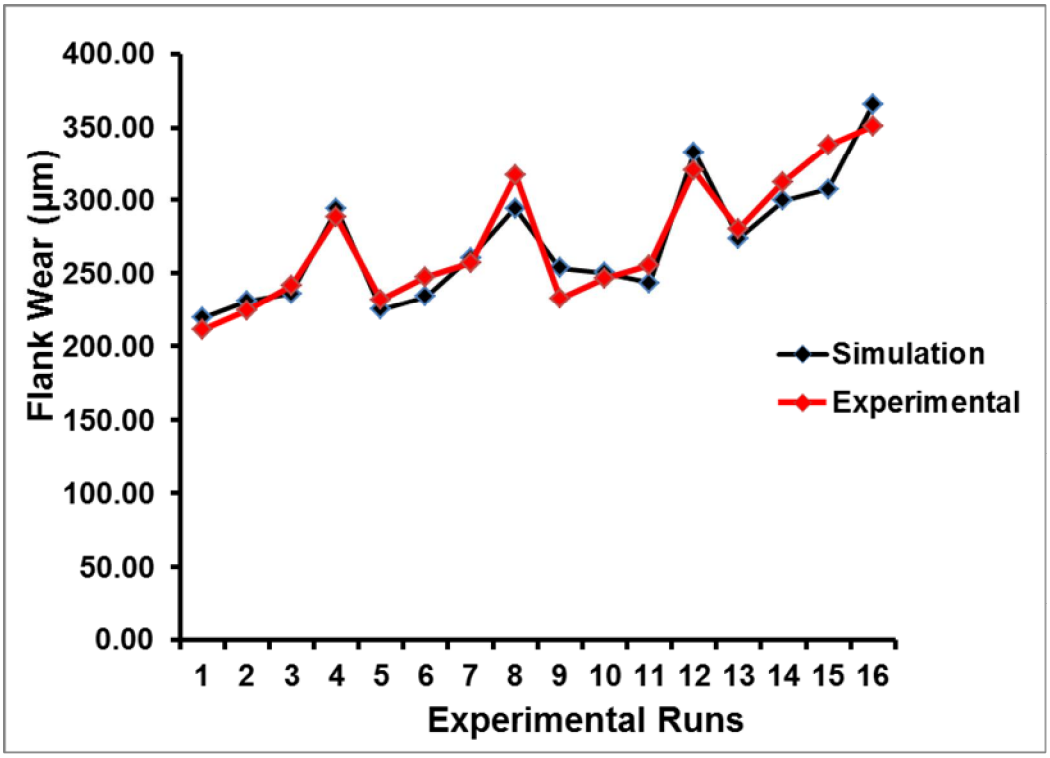

Figure 3.9 Comparison between experimental and simulation results for flank wear

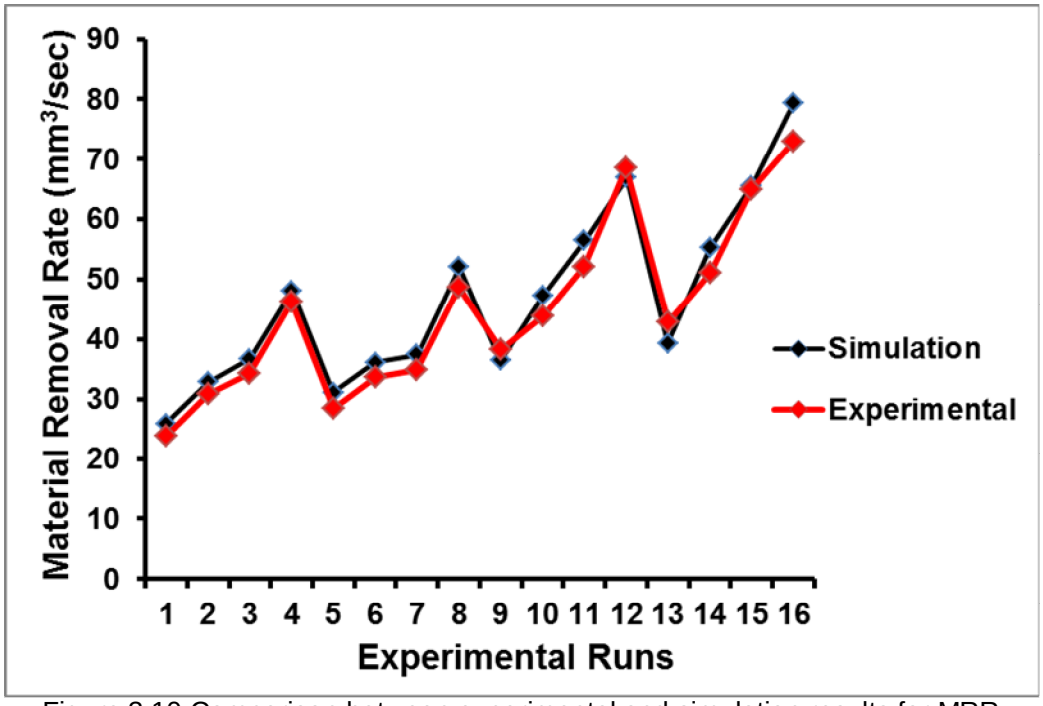

Figure 3.10 Comparison between experimental and simulation results for MRR

3.5 Conclusions

This work presents numerical simulation of tool wear and material removal rate in turning of Inconel 718 and validation by experimental data. Effect of process variables on tool wear and material removal rate have been examined using a statistical design of experiment approach for experimental data collection. The simulation approach enables to predict the tool wear and material removal rate at any given cutting time as cutting tool geometry is constantly updated in FEM simulation through DEFORM 3D. Comparison of simulation data for tool wear and material removal rate with experimental data shows that both are in good agreement. Thus, it can be concluded that simulation of machining process using DEFORM 3D can predict the performance characteristics with reasonable accuracy quickly and appreciably save the time for running additional set of experiments. The following conclusions are drawn from the study:

1. Simulation modelling is one of the convenient means to predict the machining performance characteristics without restoring to costly experimentation.
2. The simulation approach enables to predict the tool wear and material removal rate at any given cutting time as cutting tool geometry is constantly updated in FEM simulation through DEFORM 3D.
3. In case of CVD coated tool, the percentage relative error between experimental and simulation predicted value of flank wear and MRR is below 7% (Tamizharasan and Kumar, 2012; Ezilarasan et al., 2014). In most instances, simulation predicts higher value for flank wear and MRR than experimental values. However, simulation can appreciably save costly experimental time, cost, and resources.
4. This study confirms the ability of the DEFORM 3D simulation model to predict the flank wear and MRR in case of CVD coated tool.
5. During turning process, the maximum temperature at tool tip-work piece interface is 1100°C at spindle speed of 1020 RPM, depth of cut of 1mm and feed rate of 0.08mm/rev.
6. In experiments, the value of flank wear varies from 211.25 µm to 350.76 µm whereas it varies from 219.25 µm to 365.32 µm in simulation.
7. Analysis of variance suggests that the most influencing factors are spindle speed, depth of cut and feed rate in case of MRR whereas spindle speed and depth of cut are the most influencing factors in case of flank wear.

Chapter 4

MULTI-RESPONSE OPTIMIZATION IN TURNING OF INCONEL 718 USING FIS EMBEDDED WITH ICA

4.1 Introduction

Inconel 718 is one of the important alloys among the nickel-based alloys. Inconel 718 has been found in various applications in many industries owing to its unique properties such as high yield strength, excellent fatigue resistance, high oxidation resistance, corrosion resistance even at very high temperatures and retains a high mechanical strength under these conditions as well. Inconel 718 is widely used in aircraft engine parts, reciprocating engines, chemical processing, pressure vessels, steam turbine power plants, space vehicles, medical applications, marine applications, pollution control equipment and automotive sector. Due to special characteristics such as low thermal conductivity, high work hardening, presence of abrasive carbide particles, high hardness, high heat generation during machining, and high affinity to react with tool material, it is difficult to machine Inconel 718. Hence, it is classified as ódifficult-to-cut materialsò. Cost effective machining with generation of good surface finish on the Inconel 718 components during turning operation is a challenge to the manufacturing engineers (Thakur et al., 2009). Therefore, many studies use coated tool (such as CVD coated tool, PVD coated tool and ceramic tools) for cutting such type of materials (Arunachalam et al., 2004; Costes et al., 2007; Thakur et al., 2009; Umbrello, 2013; Fan et al. 2013). Out of many conventional machining methods, turning operation is most commonly performed to modify shape, dimension and surface of a work piece (Thakur et al., 2010; Khidhir and Mohamed, 2010; bhatt et al., 2010; Pawade and Joshi, 2011; Thakur et al. 2012).

Although many works related to machinability studies of Inconel 718 have been carried out recently using experimental, statistical, and numerical approaches, optimization of machining parameters has not been adequately addressed. The present chapter proposes an experimental approach to estimate influence of machining parameters such as spindle speed, feed and depth of cut on material removal rate, flank wear and surface roughness using Taguchiôs L_{16} experimental strategy. The effect of CVD and PVD coated tools on machining of Inconel 718 is also explained in this chapter. The effect of machining parameters on the flank wear is examined through SEM micrographs. Analysis of variance is conducted to identify significant process parameters.

4.2 Coating Methods

4.2.1 Coating

Machining efficiency is improved by reducing the machining time with high speed machining. When machining process is performed on ferrous materials such as iron, cast iron, steel or stainless steel and super alloys, very high temperature is

generated and chemical reactions do occur on tool material causing reduction in cutting speed affecting productivity of the process. Therefore, it is necessary for tool materials to possess high temperature resistance and sufficient inactivity.

Many ceramic materials such as TiC, Al_2O_3 and TiN possess high strength at elevated temperature and low fracture toughness than that of conventional tool materials such as high speed steels and cemented tungsten carbides. Machining of hard and chemically reactive materials at high cutting speed can be attained by depositing single and multi-layer coatings on conventional tool materials to combine the beneficial properties of ceramics and traditional tool materials (Chinchanikar and Choudhury, 2013). The effect of coatings generally aims at (Schintlmeister et al. 1989):

- Reduction in friction, heat generation and cutting force.
- Reduction in the diffusion between the chip and the surface of the tool, especially at higher speeds (the coating acts as a diffusion barrier).
- Reduction in tool wear.

In order to increase the tool life and reduce the tool wear, hard coating is deposited on cutting tools. The majority of cutting tools use chemical vapour deposition (CVD) or physical vapour deposition (PVD) for hard coatings which improves tool life and machining performance of cutting tool.

CVD (Chemical Vapour Deposition)

CVD is the chemical reaction process in which the constituents of a vapour phase diluted with inert gases chemically react near the heated substrate to form a solid thin film on the substrate (Groover, 2002; Madou, 1997). The entire process takes place in an enclosed reaction chamber maintained at temperature ranging from 900 to 1100°C. The CVD coating is formed through the chemical reactions of different gases used to obtain the required coating on substrate e.g. titanium carbide is formed through the reactions of titanium chloride and methane in hydrogen gas at 1000°C. The entire CVD process follows: (1) vapour phase of required coating, (2) gaseous compound driven to the deposition zone using appropriate temperature and energy source and (3) finally the chemical reaction of the constituents to form the required solid coating on the substrate (Madou, 1997).

PVD (Physical Vapour Deposition)

PVD method deposits thin films on the cutting tools through physical techniques, mainly sputtering and evaporation. PVD process is a low temperature process and is carried out in a vacuum chamber. The process of PVD consists of two basic steps; (1) the vaporization of the required coating material and (2) condensation of the

vapour phase to a thin film on the substrate (Groover, 2002). PVD processes are typically performed at temperature around 200 to 500°C. The PVD process deposits a much dense coating on the substrate and provides a much sharper edge compared to the CVD process. Some of the typical coating materials deposited using a PVD processes are TiN, TiC, TiCN and TiAlN.

Coating materials

The majority of inserts presently used in various metal cutting operations are cemented carbide tools coated with a material consisting of nitrides (TiN, CrN), carbides (TiC, CrC, W_2C, WC/C), oxides (alumina) or combinations of these and nano composite materials. Coating cemented carbide with TiC, TiN and Al_2O_3 dramatically reduces the rate of flank wear.

4.3 Optimization process parameters through ICA

4.3.1 Fuzzy Inference System

The ordinary set define exact boundary condition whereas fuzzy set does not allows sharply defined boundary due to the generalization of characteristics function to a membership function. The main idea of the fuzzy set theory is quite intuitive and natural. This technique, being part of knowledge based decisional systems (Knowledge Based Processing), is widely applied in the ýeld of manufacturing systems (Krishnamoorthy et al., 2012; Bose et al., 2013; Shabgard et al., 2013; Majumder, 2013; Abhishek et al., 2013; Hanafi et al., 2013).

Fuzzy inference is the process of formulating the mapping from a given input to an output using fuzzy logic. The mapping then provides a basis from which decisions can be made. The process of fuzzy inference involves fuzzification of crisp input by defining membership function, fuzzy logic operators, and if-then rules. Block diagram of a typical fuzzy logic system is presented in Figure 4.1. As outlined in Figure 4.1, a fuzzy rule based system consists of four parts: fuzzifier, knowledge base, inference engine, and defuzzifier. These four parts are described below:

- Fuzzifier: The real world input to the fuzzy system is applied to the fuzzzifier. In fuzzy literature, this input is called crisp input since it contains precise information about the specific information about the parameter. The fuzzifier converts this precise quantity to the form of imprecise quantity like 'low', 'medium', 'high' etc. with a degree of belongingness to it. Typically, the value ranges from 0 to 1.
- Knowledge base: The main part of the fuzzy system is the knowledge base in which both rule base and database are jointly referred. The database defines the membership functions of the fuzzy sets used in the fuzzy rules whereas the rule base contains a number of fuzzy if-then rules.

- Inference engine: The inference system or the decision-making unit performs the inference operations on the rules. It handles the way in which the rules are combined.
- Defuzzifier: The output generated by the inference block is always fuzzy in nature. A real world system will always require the output of the fuzzy system to the crisp or in the form of real world input. The job of the defuzzifier is to receive the fuzzy input and provide real world output. In operation, it works opposite to the input block.

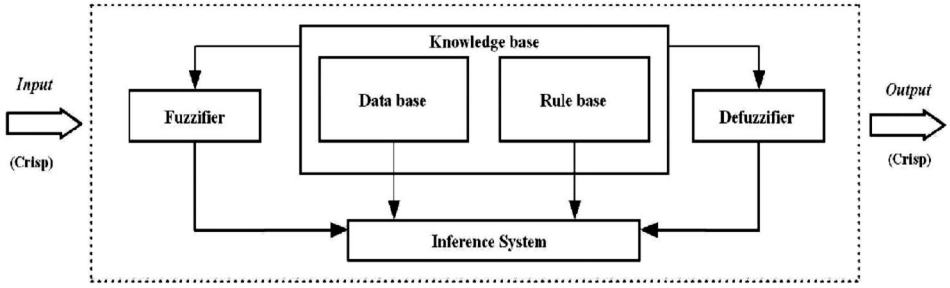

Figure 4.1 Fuzzy Inference System

In general, two most popular fuzzy inference systems are available: Mamdani fuzzy model and Sugeno fuzzy model. The selection depends on the fuzzy reasoning and formulation of fuzzy IF-THEN rules. Mamdani fuzzy model is based on the collections of IF-THEN rules with both fuzzy antecedent and consequent predicts. The benefit of this model is that the rule base is generally provided by an expert and hence to a certain degree, it is translucent to explanation and study. Because of its ease, Mamdani model is still most commonly used technique for solving many real world problems.

A fuzzy set A is represented by trapezoidal fuzzy number which is defined by the quadruplet (a, b, c, d). Membership function $\mu_A(x)$ is defined as:

$$\mu_A(x) \begin{cases} = 0, & x < a, \\ = \dfrac{(x-a)}{(b-a)}, & a \le x \le b \\ = 1, & b \le x \le c \\ = \dfrac{(d-x)}{(d-c)}, & c \le x \le d \\ = 1, & x > d \end{cases} \qquad (4.1)$$

If b=c, the function is called triangular membership function. The triangular fuzzy number is used because of mathematical convenience.

The Mamdani implication method is employed for the rules definition.

For a rule R_i : If x_1 is A_{1i} and x_2 is A_{2i}é é x_s is A_{si} then y_i is C_i, i=1,2,é .,M

where M is total number of fuzzy rule, x_j (j=1,2,é ,s) are input variables, y_i are the output variables, and A_{ji} and C_i are fuzzy sets modeled by membership functions $\mu_{A_{ji}}(x_j)$ and $\mu_{C_i}(y_i)$ respectively. The aggregated output for the M rules is:

$$\mu_{C_i}(y_i)=\max[\min\{\mu_{A_{1i}}(x_1),\mu_{A_{1i}}(x_2),.....,\mu_{A_{1i}}(x_S)\}],\ i=1,2,.....,M \quad (4.2)$$

Using a defuzzification method, fuzzy values can be combined into one single crisp output value. The center of gravity, one of the most popular methods for defuzzifying fuzzy output functions, is employed. The formula to find the centroid of the combined outputs $\hat{y}_i$ is given by:

$$\hat{y}_i = \frac{\int y_i \mu_{C_i}(y_i)\,dy}{\int \mu_{C_i}(y_i)\,dy} \quad (4.3)$$

4.3.2 Imperialist Competitive Algorithm (ICA)

The recently introduced ICA uses the socio-political process of imperialism and imperialistic competition as a source of inspiration (Atashpaz-Gargari and Lucas, 2007). ICA is meta-heuristic algorithm that initiates with a random number of populations namely countries, some of which are selected to be the imperialists and the remaining countries are colonized by these imperialists who collectively form an empire (Niknam et al., 2011; Sabour et al., 2011; Bashiri and Bagheri, 2013; Talatahari et al., 2013; Ahmadi et al., 2013; Duan and Huang, 2014; Idoumghar et al., 2013).

The representatives of this algorithm are called ócountriesõ There are two types of countries; some of the best countries are selected to be the óimperialistõ states and the remaining countries form the ócoloniesõ of these imperialists. All the colonies of initial countries are divided among the imperialists based on their ópowerõ The power of each country is inversely proportional to its cost. The imperialist states together with their colonies form some óempiresõ

After initial formation of empires, the colonies in each empire start moving toward their relevant imperialist country. This movement is a simple model of assimilation policy which was followed by some of the imperialist states. The total power of an empire depends on both the power of the imperialist country and the power of its

colonies. This fact is modelled by defining the total power of an empire as the power of the imperialist country plus a percentage of mean power of its colonies.

Then, the imperialistic competition begins among all the empires. Any empire that is unable to succeed in this competition or cannot increase its power (or at least prevent losing its power) will be eliminated from the competition. The imperialistic competition will gradually result in an increase in the power of the powerful empires and a decrease in the power of weaker ones. Weak empires will lose their power and ultimately they will collapse. The movement of colonies toward their relevant imperialist states along with competition among empires and also the collapse mechanism will cause all the countries to converge to a state in which there exists just one empire in the world and all the other countries are colonies of that empire. In this ideal new world, colonies will have the same position and power as the imperialist.

Procedures Involved in ICA

Each country is formed of an array of variable values and the related cost of a country is found by assessment of the cost function f_{cost} of the corresponding variables considering the related objective function. Total number of initial countries is set to $N_{country}$ and the number of the most powerful countries to form the empires is taken as N_{imp}. The remaining N_{col} of the initial countries will be the colonies each of which belongs to an empire. To form the initial empires, the colonies are divided among imperialists based on their power. To fulfil this aim, the normalized cost of an imperialist is defined as follows:

$$C_n = f_{cost}^{(imp,n)} - \max_i \{f_{cost}^{(imp,i)}\} \tag{4.4}$$

where $f_{cost}^{(imp,n)}$ cost is the cost of the n^{th} imperialist and C_n is its normalized cost. The initial colonies are divided among empires based on their power or normalized cost and for the n^{th} empire it will be as follows:

$$N.C_n = \text{Round}\left|\frac{C_n}{\sum_{i=1}^{N_{imp}} C_i}\right| . N_{col} \tag{4.5}$$

where $N.C_n$ is the initial number of the colonies associated to the n^{th} empire which are selected randomly among the colonies. These colonies along with the n^{th} imperialist form the n^{th} empire.

In the ICA, the assimilation policy is modelled by moving all the colonies toward the imperialist. This movement is shown in Figure 4.2 in which a colony moves toward the imperialist by a random value that is uniformly distributed between 0 and $\beta \times d$.

$$\{x\}_{new} = \{x\}_{old} + U(0, \beta \times d) \times \{V_1\} \quad (4.6)$$

where β is a assimilation coefficient (taken as 2) and d is the distance between colony and imperialist. $\{V_1\}$ is a vector which its start point is the previous location of the colony and its direction is toward the imperialist locations. The length of this vector is set to unity.

In ICA, to increase the searching around the imperialist, a random amount of deviation is added to the direction of movement. Figure 4.2 presents the new direction which is obtained by deviating the previous location of the country as great as θ which is a random number with uniform distribution.

If the new position of a colony is better than that of the corresponding imperialist (considering the cost function), the imperialist and the colony change their positions and the new location with the lower cost becomes the imperialist.

Imperialistic competition is another strategy utilized in the ICA methodology. All empires try to take the possession of colonies of other empires and control them. The imperialistic competition gradually reduces the power of weaker empires and increases the power of more powerful ones. The imperialistic competition is modelled by just picking some of the weakest colonies of the weakest empires and making a competition among all empires to possess these colonies. Based on their total power, in this competition, each of empires will have a possibility of taking possession of the mentioned colonies.

Total power of an empire is affected by the power of imperialist country and the colonies of an empire as

$$TC_n = f_{cost}^{(imp,n)} + \xi . \frac{\sum_{i=1}^{N.C_n} f_{cost}^{(col,i)}}{N.C_n} \quad (4.7)$$

where TC_n is the total cost of the n^{th} empire and ξ is a positive number (taken as 0.1).

Similar to equation 4.4, the normalized total cost is defined as:

$$NTC_n = TC_n - \max_i \{TC_i\} \quad (4.8)$$

where NTC_n is the normalized total cost of the n^{th} empire. Having the normalized total cost, the possession probability of each empire is evaluated by

$$p_n = \left| \frac{NTC_n}{\sum_{i=1}^{N_{imp}} NTC_i} \right| \tag{4.9}$$

When an empire loses all its colonies, it is assumed to be collapsed. In this model implementation where the powerless empires collapse in the imperialistic competition, the corresponding colonies will be divided among the other empires.

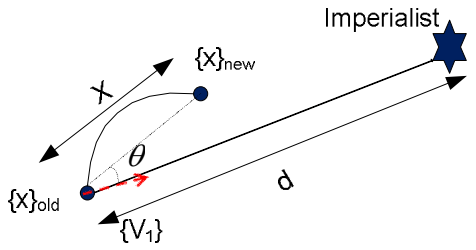

Figure 4.2 Movement of colonies to its new location

Moving colonies toward imperialists are continued and imperialistic competition and implementations are performed during the search process. When the number of iterations reaches a pre-defined value, the search process is stopped.

4.4 Experimental details

A series of experiments has been carried out in CNC lathe (Model No. Sprint 16 TC manufactured by: Batliboi Ltd. Surat, India) as shown in Figure 4.3 to assess the behaviour of machining parameters (spindle speed, feed rate and depth of cut) on the material removal rate and tool wear. The details of lathe specifications are shown in Table 4.1. A bar of Inconel 718 having diameter 30 mm, length 150 mm and tensile strength of 1100 MPa has been used as work piece material possessing composition in mass percentage of 50-55 Ni, 17-21 Cr, 2.8-3.3 Mo, 4.75-5.5 Nb, 0.35 Mn, 0.2-0.8 Cu, 0.65-1.15 Al, 1 Co, 0.3 Ti, 0.35 Si, 0.08 C, 0.015 S, 0.015 P, 0.006 B, and balance Fe (Figure 4.4). Here, first chemical vapour deposition (CVD) coated tool of CNMG 431_KC9225 manufactured by Kennametal (four coatings: TiN, TiCN, Al_2O_3, TiN) having tool signature (10-10-7-7-5-5-0.4) and second PVD coated CNMG 431_KC5010 manufactured by Kennametal (single coating: AlTiN) having tool signature (6-6-0-0-5-5-0.4) are used as tool materials (Figure 4.5). Base material of both coated tool is tungsten carbide (WC). PCLNL2525M12 tool holder is used for both tool insert (Figure 4.6).

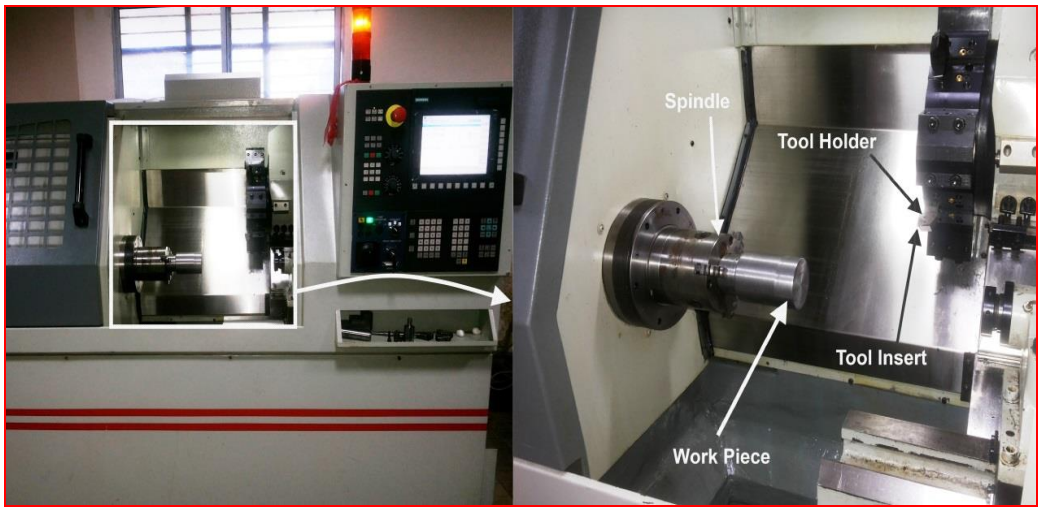

Figure 4.3 CNC lathe

Table 4.1 Details of CNC Turning Lathe

Details	Unit	Description
Swing over Bed	mm	400
Turning Diameter	mm	225
Turning Length	mm	300
Spindle speed	RPM	50-5000
Spindle Motor	KW	5.5/7.5
Z axis stroke	mm	325
X axis stroke	mm	125
Maximum no. Tools In Turret	NOs.	8
Rapid Transverse	m/min.	20

Figure 4.4 Work Piece (Inconel 718 rod)

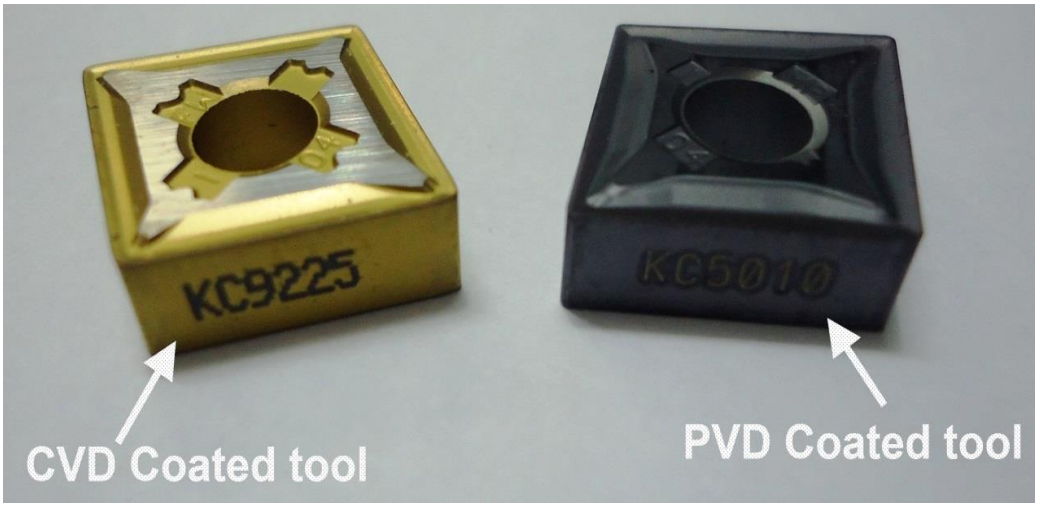

Figure 4.5 Tool Inserts

Figure 4.6 Tool Holder

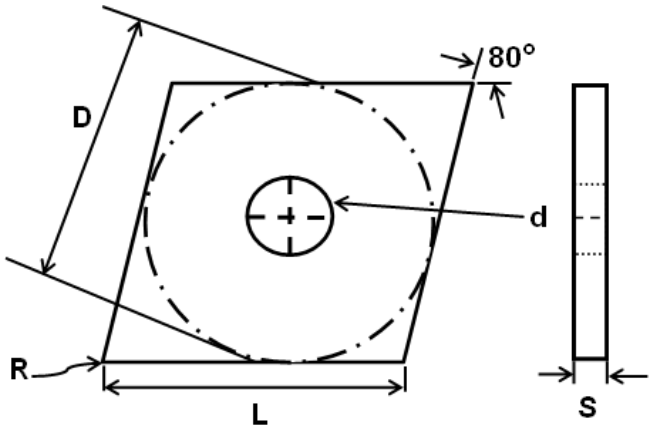

Figure 4.7 Tool Insert dimensions

Figure 4.7 shows the dimensions of both tool CNMG 431: D = 12.70 mm, S = 4.76 mm, R = 0.4 mm, L = 12.90 mm, d = 5.16 mm. where, D = Theoretical diameter

of the insert inscribed circle, S = Thickness of the tool insert, R = Nose radius of tool insert, L = Cutting edge length, d = Inner hole diameter.

Table 4.2 presents different levels of process parameters such as spindle speed, feed rate and depth of cut for turning of Inconel 718. A schematic layout for experimentation is highly required for reduction of experimental time and cost. Therefore, Taguchi method is used to design the experimental layout to examine the effect of the machining parameters with less number of experimental runs. In the present study, three process parameters have been varied into four different levels. So, the possible combination of experiments is 4^3 (64). Hence, Taguchi method is adopted to reduce the number of experiments by utilizing the orthogonal array concept. Therefore, L_{16} orthogonal array has been chosen for experimentation shown in Table 4.3. During experimentation, work piece is cut for a length of 60 mm in each run.

Table 4.2 Process parameters and their levels (both CVD and PVD coated tool)

Sl. No.	Factors	Symbols	Unit	Level 1	Level 2	Level 3	Level 4
1	Spindle speed	N	RPM	400	600	800	1000
2	Depth of cut	d	mm	0.4	0.6	0.8	1
3	Feed rate	f	mm/rev	0.08	0.12	0.16	0.20

Tool wear is caused due to relative motion between the cutting tool and the work piece or the cutting tool and chip on machining area during turning. Tool wear is measured experimentally by optical microscope (SteREO Discovery V20 manufactured by Carl Zeiss MicroImaging Inc. having eyepiece magnification: 10X and objective magnification: 2.5X to 100X, Figure 4.8) as shown in Figure 4.9 (a), Figure 4.9 (b) Figure 4.9 (c) and Figure 4.9 (d). Maximum damage length of flank face has been considered for assessing the flank wear of tool insert. Experimental data of material removal rate, flank wear and surface roughness for CVD and PVD coated tool are listed in Table 4.3 and Table 4.4 respectively.

Figure 4.8 Optical microscope

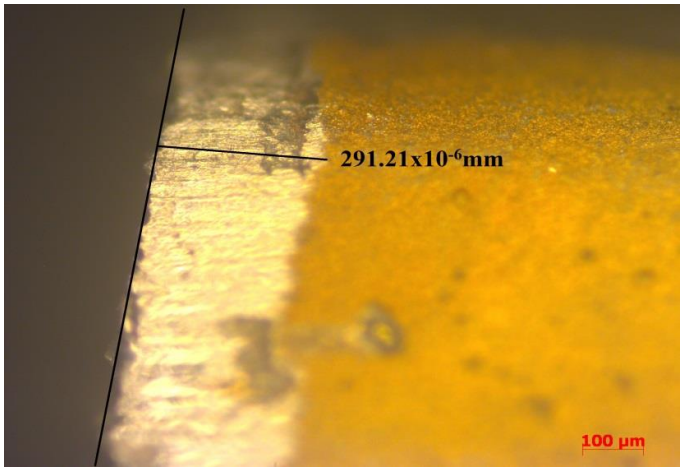

Figure 4.9 (a) Flank wear for CVD coated tool for spindle Speed 400 RPM, depth of cut 1 mm, feed rate 0.2 mm/rev

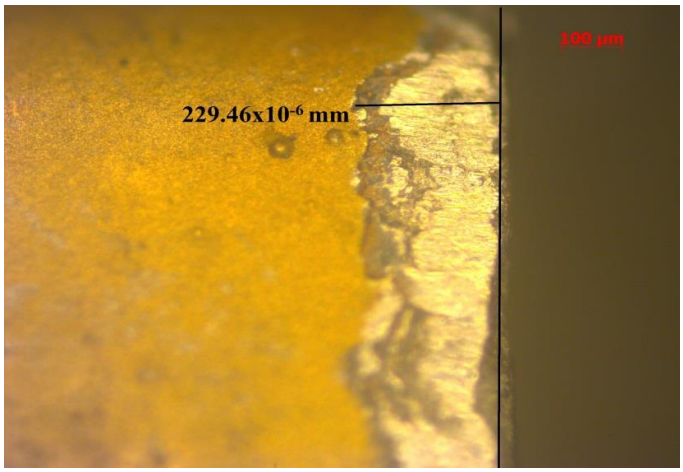

Figure 4.9 (b) Flank wear for CVD coated tool for spindle Speed 600 RPM, depth of cut 0.4 mm, feed rate 0.12 mm/rev

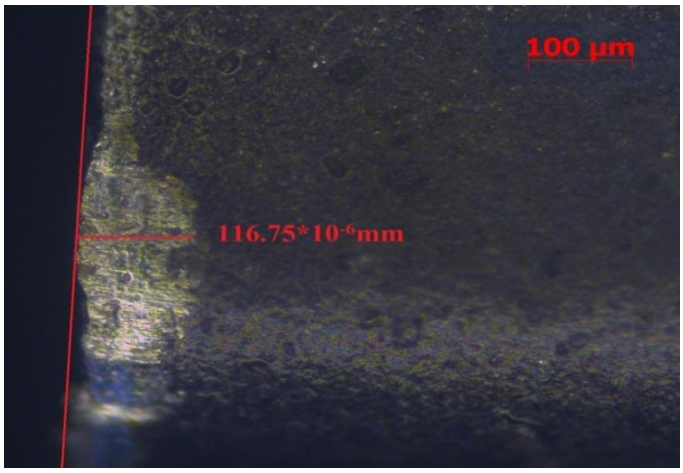

Figure 4.9 (c) Flank wear for PVD coated tool for Spindle Speed 400 RPM, depth of cut 0.8 mm, feed rate 0.16 mm/rev

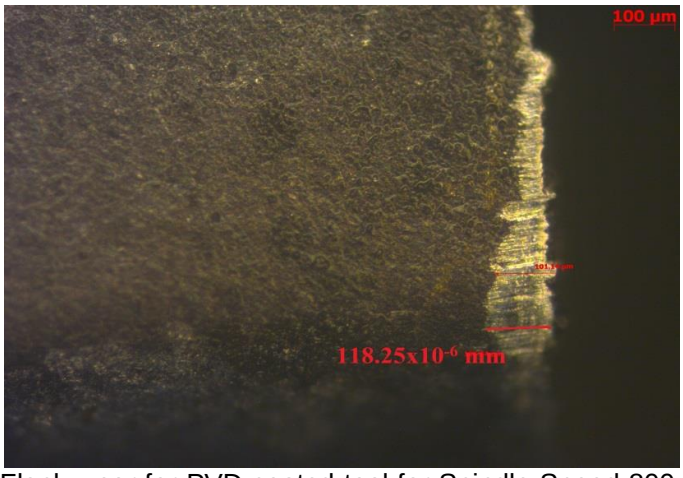

Figure 4.9 (d) Flank wear for PVD coated tool for Spindle Speed 800 RPM, depth of cut 0.8 mm, feed rate 0.08 mm/rev

As material removal rate (MRR) and tool wear have dominant effect on economics of the machining operations, estimation of these machining characteristics is important and necessary in metal cutting for maintaining both productivity and quality. Material removal rate is defined as volume of work piece material that can be removed per time unit.

$$MRR = \frac{(V_i - V_f)}{t_m} \tag{4.10}$$

where V_i = initial volume of work-piece, V_f = final volume of work-piece and t_m = machining time.

Surface roughness is another important index which is caused to action of cutting tool on work-piece. Surface roughness tester SJ-210 (Make: Mitutoyo) having a stylus which skids over machined surface to measure the roughness (Figure 4.10).

Figure 4.10 Surface roughness tester SJ-210 (Make: Mitutoyo)

Table 4.3 Experimental data (with CVD coated tool)

Sl. No.	Process Parameters			Experimental Results		
	N	d	f	MRR (mm^3/sec)	Flank wear (µm)	Surface Roughness (µm)
1	400	0.4	0.08	22.31	206.12	1.23
2	400	0.6	0.12	28.71	222.34	1.34
3	400	0.8	0.16	32.32	246.43	1.37
4	400	1	0.2	37.33	291.21	1.42
5	600	0.4	0.12	27.89	229.46	1.67
6	600	0.6	0.08	34.63	245.62	1.58
7	600	0.8	0.2	38.89	270.25	1.73
8	600	1	0.16	49.56	309.54	1.87
9	800	0.4	0.16	38.86	238.68	1.66
10	800	0.6	0.2	45.62	254.61	1.56
11	800	0.8	0.08	54.83	280.23	1.732
12	800	1	0.12	67.75	315.92	1.92
13	1000	0.4	0.2	41.82	290.85	1.87
14	1000	0.6	0.16	53.67	323.49	1.96
15	1000	0.8	0.12	63.41	345.63	2.07
16	1000	1	0.08	76.56	370.76	2.19

Table 4.4 Experimental data (with PVD coated tool)

Sl. No.	Process Parameters			Experimental Results		
	N	d	f	MRR (mm^3/sec)	Flank wear (µm)	Surface Roughness (µm)
1	400	0.4	0.08	17.65	101.130	1.597
2	400	0.6	0.12	22.65	105.745	1.256
3	400	0.8	0.16	47.03	116.750	1.519
4	400	1	0.2	47.64	98.3350	1.815
5	600	0.4	0.12	18.34	96.2200	1.022
6	600	0.6	0.08	16.67	108.470	1.758
7	600	0.8	0.2	58.82	102.285	1.542
8	600	1	0.16	48.02	101.975	1.554
9	800	0.4	0.16	30.96	99.7430	1.227
10	800	0.6	0.2	37.95	96.9850	1.874
11	800	0.8	0.08	33.14	118.250	1.635
12	800	1	0.12	35.29	101.860	1.224
13	1000	0.4	0.2	45.25	99.420	1.315
14	1000	0.6	0.16	42.74	115.570	1.385
15	1000	0.8	0.12	41.47	116.360	1.078
16	1000	1	0.08	36.11	106.840	1.469

4.5 Results and discussions

4.5.1 CVD Coated tool

Experimental data are collected as per experimental plan of Taguchi's L_{16} orthogonal array. Lower-the-better (LB) criterion is used for flank wear and surface roughness whereas higher-the-better (HB) criterion is used for MRR. Analysis of variance (ANOVA) is a method of partitioning observed variance into components of different explanatory variables to identify significance of each parameter. Table 4.5, Table 4.6 and Table 4.7 present the ANOVA table for material removal rate, flank wear and surface roughness respectively. It is to be noted that spindle speed and depth of cut are significant factors influencing on flank wear at significance level 0.05. Similarly, the factors like spindle speed, depth of cut and feed rate are significant factors influencing on MRR at significance level 0.05. For surface roughness, spindle speed, depth of cut and feed rate are significant factors at the significant level 0.05. The optimal parametric setting can be obtained from the factorial plots. Figure 4.11 (a) indicates that spindle speed, depth of cut and feed rate should be maintained at 1000 RPM, 1 mm and 0.08 mm/rev respectively to maximize MRR. Similarly, Figure 4.11 (b) reveals that spindle speed, depth of cut and feed rate should be maintained at 400 RPM, 0.4 mm and 0.08 mm/rev respectively to minimize the flank wear and Figure 4.11 (c) indicates that spindle speed, depth of cut and feed rate should be maintained at 400 RPM, 0.4 mm and 0.20 mm/rev respectively to minimize surface roughness.

Table 4.5 ANOVA for material removal rate (R-square 99.2%)

Source	Degree of freedom	Sum of squares	Adjusted S S	Adjusted M S	F-Value	P-Value
N	3	2040.58	2040.58	680.193	140.61	0.000
d	3	1354.18	1354.18	451.392	93.31	0.000
f	3	104.83	104.83	34.944	7.22	0.020
Residual Error	6	29.03	29.03	4.838		
Total	15	3528.61				

Table 4.6 ANOVA for flank wear (R-square 99.5%)

Source	Degree of freedom	Sum of squares	Adjusted S S	Adjusted M S	F-Value	P-Value
N	3	18222.7	18222.7	6074.22	204.40	0.000
d	3	14405.3	14405.3	4801.78	161.58	0.000
f	3	34.9	34.9	11.62	0.39	0.764
Residual Error	6	178.3	178.3	29.72		
Total	15	32841.2				

Table 4.7 ANOVA for surface roughness (R-square 99.3%)

Source	Degree of freedom	Sum of squares	Adjusted S S	Adjusted M S	F-Value	P-Value
N	3	0.93630	0.93630	0.312099	253.26	0.000
d	3	0.15918	0.15918	0.053059	43.06	0.000
f	3	0.02411	0.02411	0.008036	6.52	0.026
Residual Error	6	0.00739	0.00739	0.001232		
Total	15	1.12698				

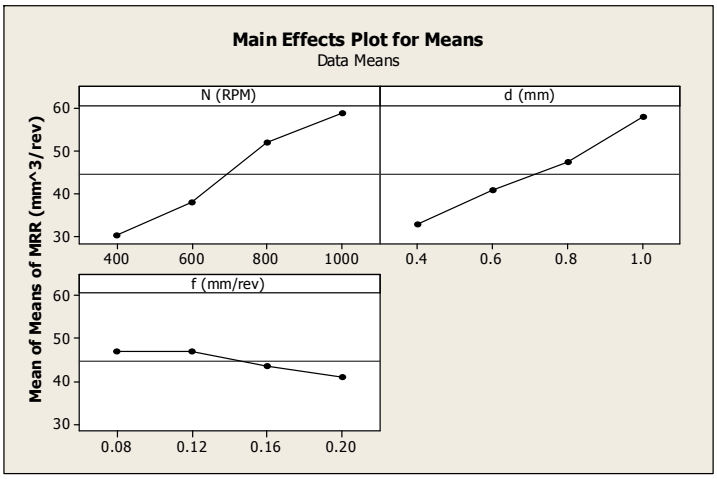

Figure 4.11 (a) Main effect plot for MRR

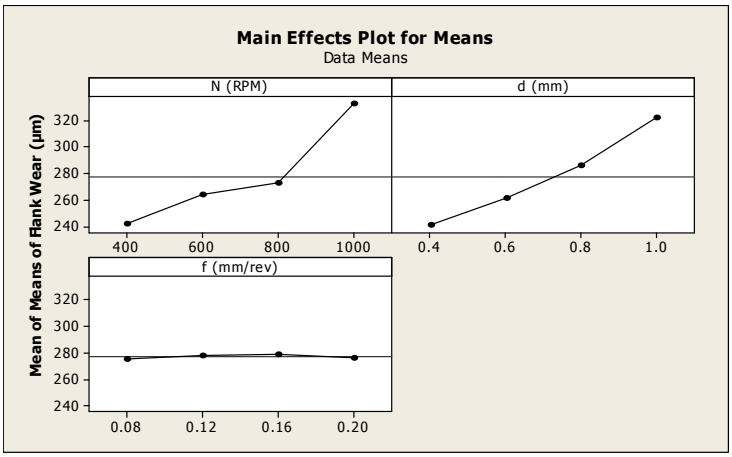

Figure 4.11 (b) Main effect plot for flank wear

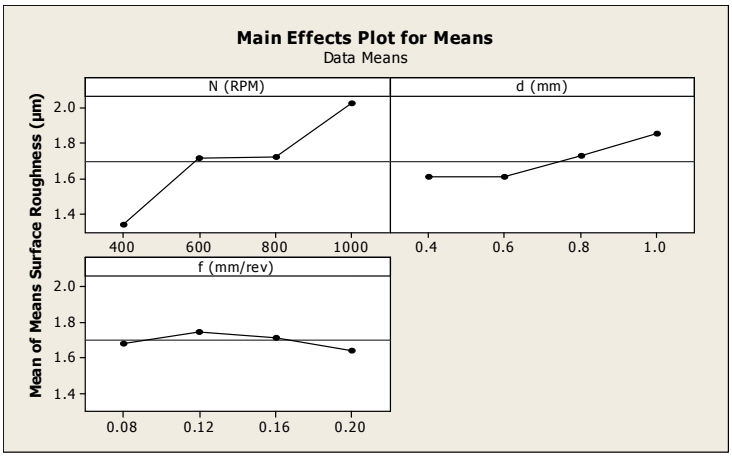

Figure 4.11 (c) Main effect plot for Surface roughness

4.5.2 PVD coated tool

Experimental data are collected as per experimental plan of Taguchiôs L_{16} orthogonal array. Lower-the-better (LB) criterion is used for flank wear and surface roughness whereas higher-the-better (HB) criterion is used for MRR. Table 4.8, Table 4.9 and Table 4.10 present the ANOVA table for MRR, flank wear and surface roughness respectively. It is to be noted that spindle speed, depth of cut and feed rate are significant factors influencing on MRR at significance level 0.05. For flank wear and surface roughness, all the factors (spindle speed, depth of cut and feed rate) are significant. The optimal parametric setting can be obtained from the factorial plots. Figure 4.12 (a) reveals that spindle speed, depth of cut and feed rate should be maintained at 1000 RPM, 0.8 mm and 0.20 mm/rev respectively to maximize MRR. Similarly, Figure 4.12 (b) indicates that spindle speed, depth of cut and feed rate should be maintained at 600 RPM, 0.4 mm and 0.20 mm/rev respectively to minimize flank wear and Figure 4.12 (c) indicates that spindle speed, depth of cut and feed

rate should be maintained at 1000 RPM, 0.4 mm and 0.12 mm/rev respectively to minimize surface roughness.

Table 4.8 Analysis of Variance for Means MRR (R-square 97.5%)

Source	Degree of freedom	Sum of squares	Adjusted SS	Adjusted MS	F- Value	P-Value
N	3	148.08	148.08	49.359	5.17	0.042
d	3	861.09	861.09	287.031	30.09	0.001
f	3	1254.39	1254.39	418.131	43.84	0.000
Residual Error	6	57.23	57.23	9.539		
Total	15	2320.79				

Table 4.9 Analysis of Variance for Means Flank Wear (R-square 94.6%)

Source	Degree of freedom	Sum of squares	Adjusted SS	Adjusted MS	F- Value	P-Value
N	3	114.50	114.50	38.167	4.95	0.046
d	3	460.36	460.36	153.452	19.92	0.002
f	3	232.98	232.98	77.661	10.08	0.009
Residual Error	6	46.22	46.22	7.703		
Total	15	854.06				

Table 4.10 Analysis of Variance for Means Surface Roughness (R-square 94.7%)

Source	Degree of freedom	Sum of squares	Adjusted SS	Adjusted MS	F- Value	P-Value
N	3	0.12143	0.12143	0.040477	4.76	0.040
d	3	0.17504	0.17504	0.058345	6.87	0.023
f	3	0.62280	0.62280	0.207600	24.43	0.001
Residual Error	6	0.05099	0.05099	0.008498		
Total	15	0.97025				

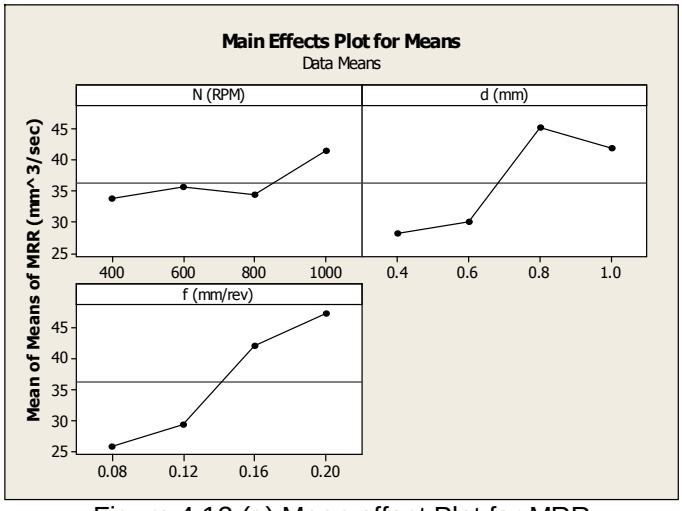

Figure 4.12 (a) Mean effect Plot for MRR

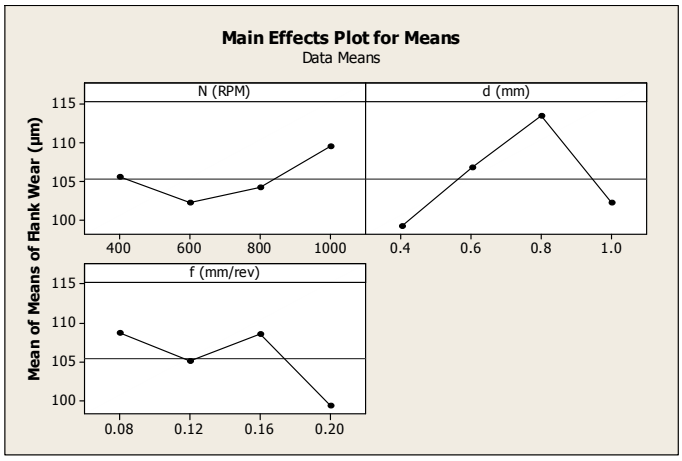

Figure 4.12 (b) Mean effect plot for Flank Wear

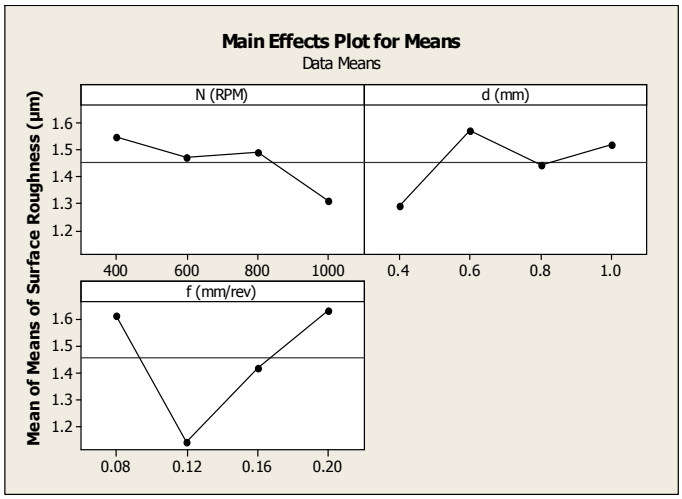

Figure 4.12 (c) Mean effect plot for Surface roughness

Micrographs of the tool after turning with CVD and PVD coated tool are observed in scanning electron microscope (JEOL JSM 6480LV Figure 4.13). The micrographs are shown for process parameters setting of spindle speed of 600 RPM, depth of cut of 1mm and feed rate of 0.16 mm/rev for CVD coated tool and spindle speed of 400 RPM, depth of cut of 0.4 mm and feed rate of 0.08 mm/rev for PVD coated tool in Figure 4.14 (a) and Figure 4.14 (b) respectively. Flank wear is the main wear in the turning operation. The high flank wear is observed when spindle speed = 1000 RPM, depth of cut = 1 mm and feed rate = 0.08 mm in turning with CVD coated tool but in case of PVD coated tool high flank wear is observed when spindle speed = 800 RPM, depth of cut = 0.8 mm and feed rate = 0.08 mm.

Figure 4.13 Scanning electron microscope (JEOL JSM 6480LV)

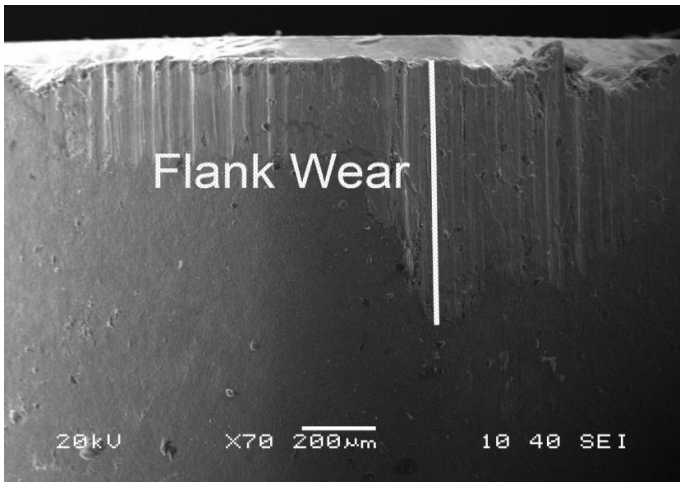

Figure 4.14 (a) Flank wear of CVD coated WC insert spindle speed of 600 RPM, depth of cut of 1 mm and feed rate of 0.16 mm

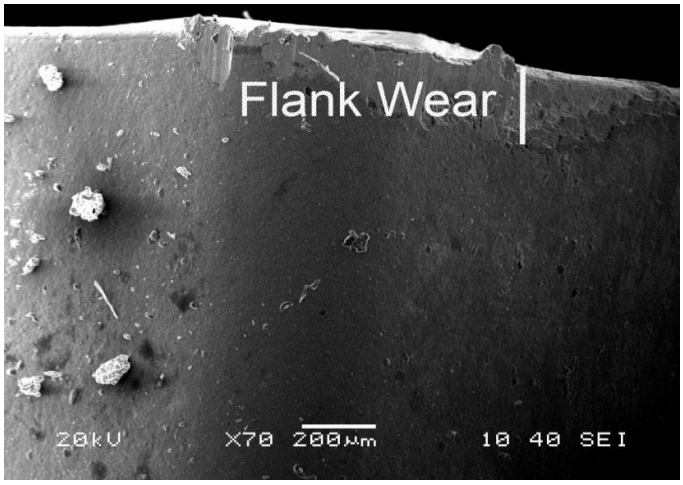

Figure 4.14 (b) Flank wear of PVD coated WC insert at spindle speed of 400 RPM, depth of cut of 0.4 mm and feed rate of 0.08 mm

4.5.3 Optimization with Fuzzy Inference System coupled with ICA

The methodology used for the optimization is fuzzy inference system coupled with imperialistic competitive algorithm (ICA). Fuzzy inference system has been utilized to convert multiple performance characteristics (MRR, flank wear and surface roughness) into single objective characteristics i.e. Multi Performance Characteristic Index (MPCI). Then, non-linear mathematical model has been developed as function of process parameters. Finally, this model has been fed as objective function for ICA to generate the optimal machining condition. The basic flowchart of proposed methodology has been illustrated in Figure 4.15.

Initially, all the output responses (i.e. MRR, Flank wear and surface roughness) have been normalized within the range 0 to 1 (where 0 denotes as worst value and 1 denotes best value) (Table 4.11 and Table 4.12). The formulae for normalization are given as followsa (Abhishek et al., 2013):

For surface roughness and flank wear (Smaller-the-better criterion):

$$y_{ij} = \frac{x_{ij} - \max x_{ij}}{\min x_{ij} - \max x_{ij}} \tag{4.11}$$

For, MRR (Higher-the-better criterion):

$$y_{ij} = \frac{x_{ij} - \min x_{ij}}{\max x_{ij} - \min x_{ij}} \tag{4.12}$$

where x_{ij} is experimental value, $\max x_{ij}$ is the maximum value and $\min x_{ij}$ is minimum observed value.

In fuzzy inference system (Figure 4.16), individual normalized values of each response (for MRR, flank wear and average surface roughness) have been served as input variable. Aforementioned input responses has been expressed using three linguistic variables viz. ñsmallò, ñmediumò ñlargeò as presented in Figures 4.17 (a)-4.17 (c) whereas output factor (MPCI) has been expressed using five linguistic variables viz. ñvery smallò, ñsmallò, ñmediumò, ñlargeò, ñvery largeò as shown in Figure 4.18.

In this work, the fuzzy set comprises for each input variable and output variable as a symmetric triangular membership function. Twenty seven fuzzy rules (Table 4.13) have been explored for fuzzy reasoning (Figure 4.19 (a), Figure 4.19 (b)). Fuzzy logic converts linguistic inputs into linguistic output. Linguistic output is again converted to numeric values (MPCI) by defuzzification method. Numeric values of MPCIs have been tabulated in Table 4.11 and 4.12.

Nonlinear regression is a mathematical method for finding a nonlinear model of the relationship between dependent and independent variables. The proposed mathematical model between the independent parameters and dependent variable is presented in the following form.

$$MPCI = C \times N^{x_1} \times d^{x_2} \times f^{x_3} \quad (4.13)$$

where C indicates a constant, N is the spindle speed, d is the depth of cut and f is the feed. x_1, x_2, and x_3 are estimated exponents of the regression model. Statistical software (SYSTAT 7.0) is used to estimate the parameters in nonlinear models using the Gauss-Newton nonlinear least-squares algorithm. The empirical relations between the multi performance characteristics index (MPCI) and the machining parameters are given below (equation 4.14 and equation 4.15).

MPCI empirical model for CVD coated tool (R-Square = 98.9%)

$$MPCI = 0.687 \times N^{(-0.081)} \times d^{(0.164)} \times f^{(-0.102)} \quad (4.14)$$

MPCI empirical model for PVD coated tool (R-Square = 97.4%)

$$MPCI = 0.226 \times N^{(0.297)} \times d^{(0.257)} \times f^{(0.561)} \quad (4.15)$$

Aforesaid mathematical model are treated as objective function for ICA. Initial parameters setting for ICA as follows:

Set up parameters for implementation of ICA

1. Initial point [0, 0, 0]
2. Initial population
    a. Number of countries 80
    b. Number of imperialist 8
3. Assimilation coefficient, $\beta = 2$
4. A coefficient used to calculate total cost of empire, $\xi = 0.1$
5. Number of decades as stop condition = 1000

Finally, ICA has been implemented to find global optimal which are tabulated in Table 4.14 and the convergence plots are shown in Figure 4.20 (a) and Figure 4.20 (b).

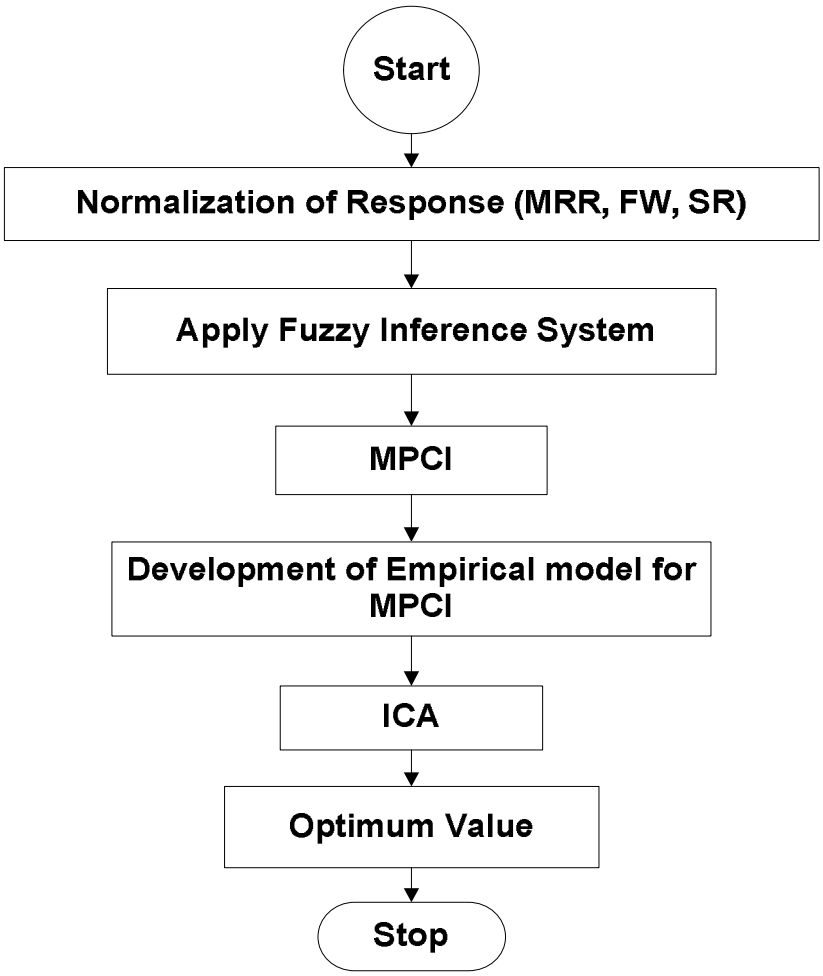

Figure 4.15 Flow Chart of Proposed Methodology

Table 4.11 Normalize value of responses and MPCI (CVD Coated tool)

Sl. No.	N-MRR	N-FW	N-SR	MPCI
1	0	1	1	0.5
2	0.117972	0.901482	0.885417	0.502
3	0.184516	0.755163	0.854167	0.516
4	0.276866	0.483175	0.802083	0.525
5	0.102857	0.858236	0.541667	0.352
6	0.227097	0.760083	0.635417	0.454
7	0.305622	0.610483	0.479167	0.397
8	0.502304	0.371842	0.333333	0.411
9	0.305069	0.802235	0.552083	0.433
10	0.429677	0.705479	0.65625	0.543
11	0.599447	0.549866	0.477083	0.544
12	0.837604	0.33309	0.28125	0.54
13	0.359631	0.485362	0.333333	0.395
14	0.578065	0.287111	0.239583	0.425
15	0.757604	0.152636	0.125	0.456
16	1	0	0	0.5

Table 4.12 Normalize value of responses and MPCI (PVD coated tool)

Sl No.	Nr-MRR	Nr-FW	Nr-SR	MPCI
1	0.02325	0.777122	0.325117	0.252
2	0.141874	0.567635	0.725352	0.453
3	0.720285	0.068089	0.416667	0.558
4	0.734757	0.903995	0.069249	0.556
5	0.03962	1	1	0.527
6	0	0.44394	0.13615	0.178
7	1	0.724694	0.389671	0.675
8	0.743772	0.738765	0.375587	0.545
9	0.339027	0.840082	0.75939	0.534
10	0.504864	0.965275	0	0.48
11	0.390747	0	0.280516	0.379
12	0.441756	0.743985	0.762911	0.587
13	0.678055	0.854744	0.656103	0.612
14	0.618505	0.121652	0.573944	0.574
15	0.588375	0.085792	0.934272	0.712
16	0.46121	0.51793	0.475352	0.473

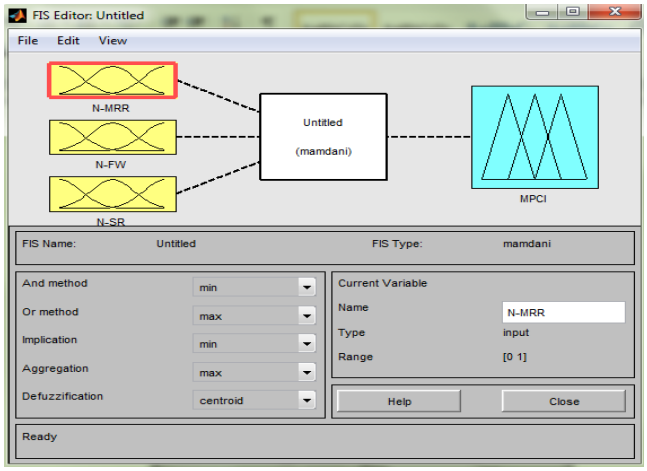

Figure 4.16 Schematic diagram of fuzzy model

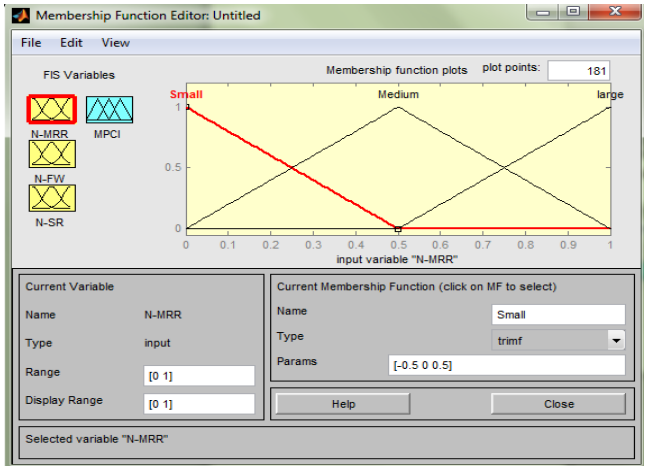

Figure 4.17 (a) Membership function for N-MRR

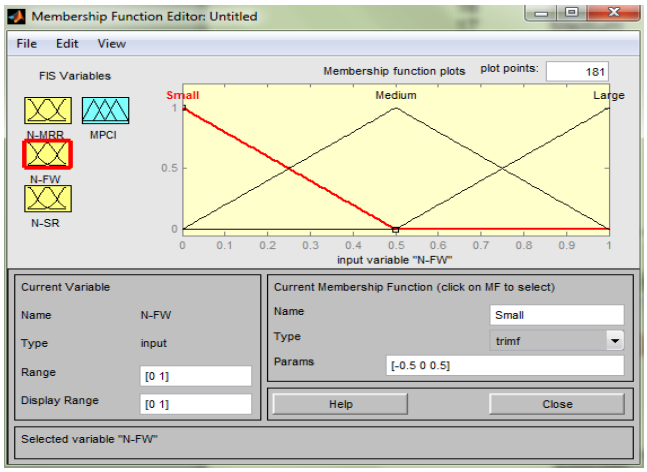

Figure 4.17 (b) Membership function for N-FW (Flank Wear)

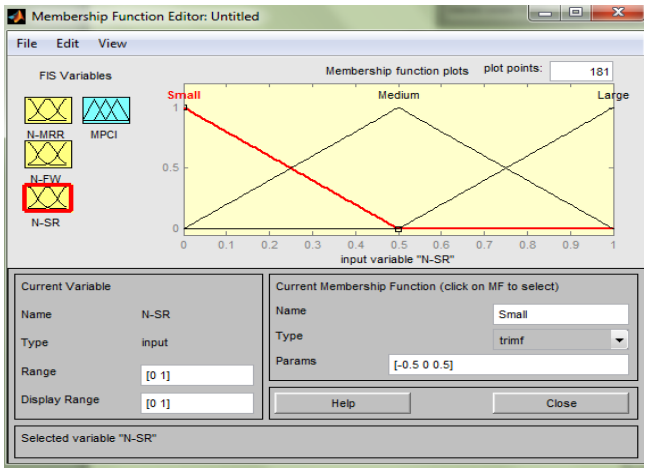

Figure 4.17 (c) Membership function for N-SR (Surface Roughness)

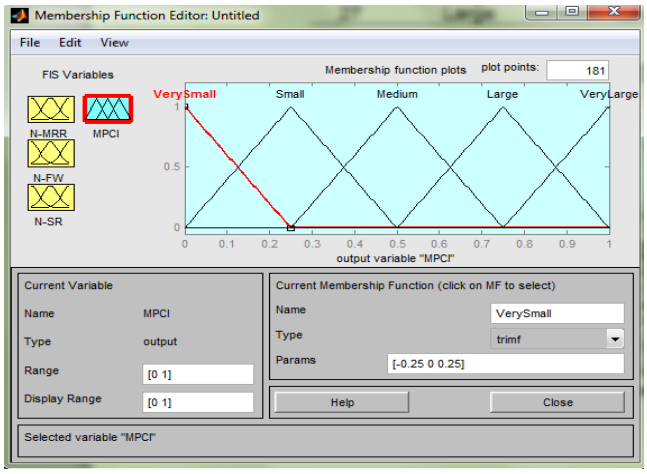

Figure 4.18 Membership function for MPCI

Table 4.13 Fuzzy Rule

Sl. No.	MRR	Flank Wear	Sourface Roughness	MPCI
1	Small	Small	Small	Very small
2	Small	Small	Medium	Small
3	Small	Small	Large	Medium
4	Small	Medium	Small	Very small
5	Small	Medium	Medium	Small
6	Small	Medium	Large	Medium
7	Small	Large	Small	Small
8	Small	Large	Medium	Small
9	Small	Large	Large	Medium
10	Medium	Small	Small	Small
11	Medium	Small	Medium	Medium
12	Medium	Small	Large	Large
13	Medium	Medium	Small	Small
14	Medium	Medium	Medium	Medium
15	Medium	Medium	Large	Large
16	Medium	Large	Small	Medium
17	Medium	Large	Medium	Medium
18	Medium	Large	Large	Large
19	Large	Small	Small	Medium
20	Large	Small	Medium	Large
21	Large	Small	Large	Very large
22	Large	Medium	Small	Medium
23	Large	Medium	Medium	Large
24	Large	Medium	Large	Very large
25	Large	Large	Small	Large
26	Large	Large	Medium	Large
27	Large	Large	Large	Very large

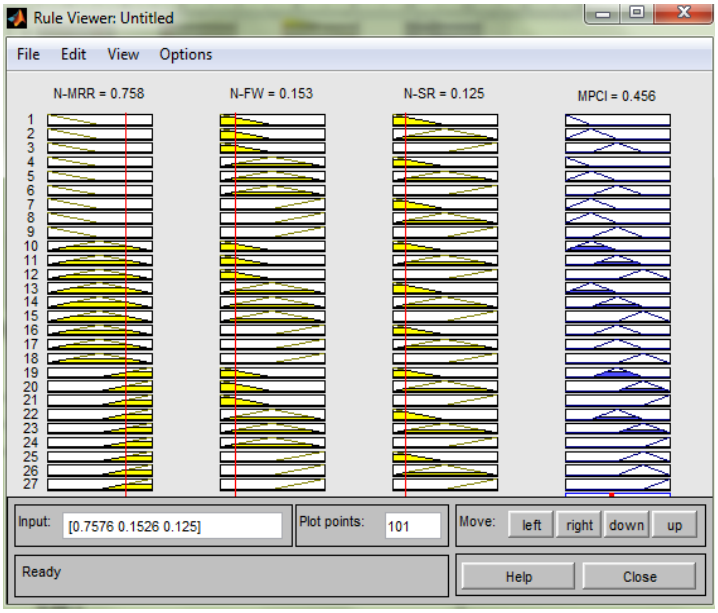

Figure 4.19 (a) Evaluation of MPCI with Fuzzy Rule Base (CVD coated tool)

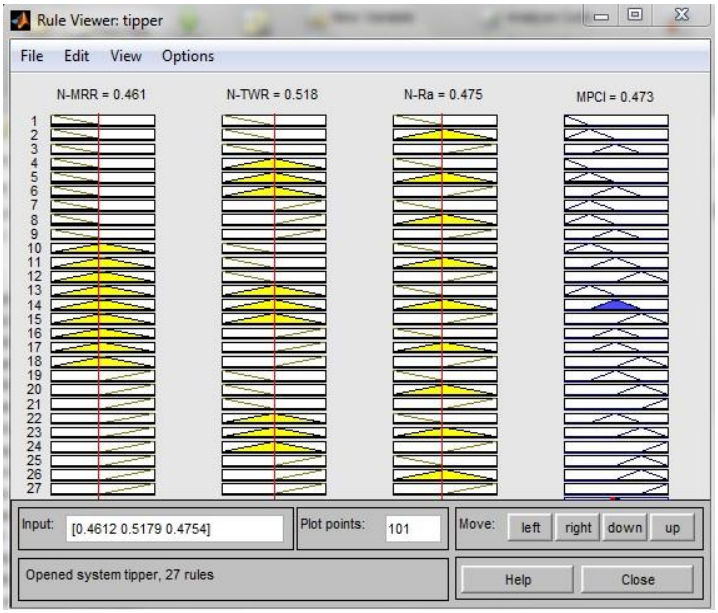

Figure 4.19 (b) Evaluation of MPCI with Fuzzy Rule Base (PVD coated tool)

Table 4.14 Optimal value of MPCI

Sl. No.	Tool coating	Spidle speed (RPM)	Depth of cut (mm)	Feed (mm/rev)	Fitness Value
1	CVD	400	1	0.08	0.5471
2	PVD	1000	1	0.2	0.7664

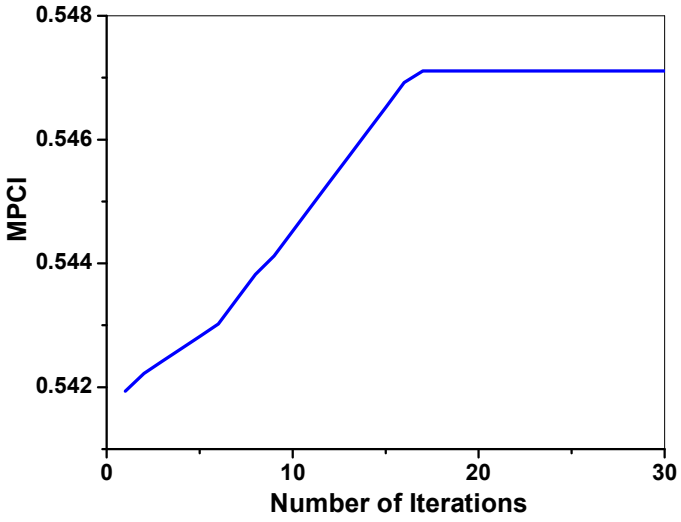

Figure 4.20 (a) Convergence Curve for MPCI (CVD coated tool)

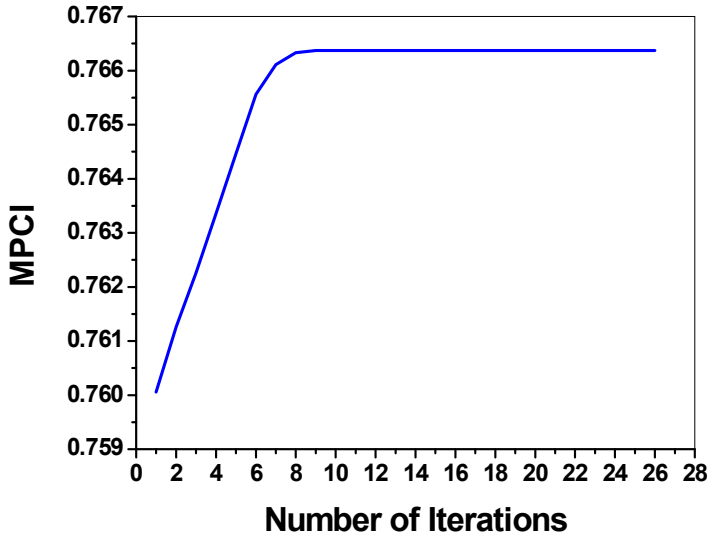

Figure 4.20 (b) Convergece curve for MPCI (PVD coated tool)

4.6 Comparison between CVD and PVD coated tool

Performance of PVD and CVD coated tool is shown in Figure 4.21 (a) to Figure 4.21 (c). From the below figures, it is observed that performance of PVD coated tool in case of flank wear and surface roughness is more efficient than CVD coated tool whereas in case of MRR CVD coated tool provides better result. The minimum value of flank wear for PVD coated tool and CVD coated tool is 96.22 µm and 206.12 µm respectively, the minimum value of surface roughness for PVD and CVD coated tool is 1.022 µm and 1.2 µm respectively and maximum value of MRR for PVD and CVD coated tool is 58.82 and 76.56 respectively. The results indicate that turning of Inconel 718 using PVD coated tool possess good surface finish with less flank wear. The result indicates that the performance of single layered (AlTiN) PVD coated tool is better than multi layered (TiN, Al_2O_3, TiCN, TiN) CVD coated tool (Chinchanikar and Choudhury, 2013).

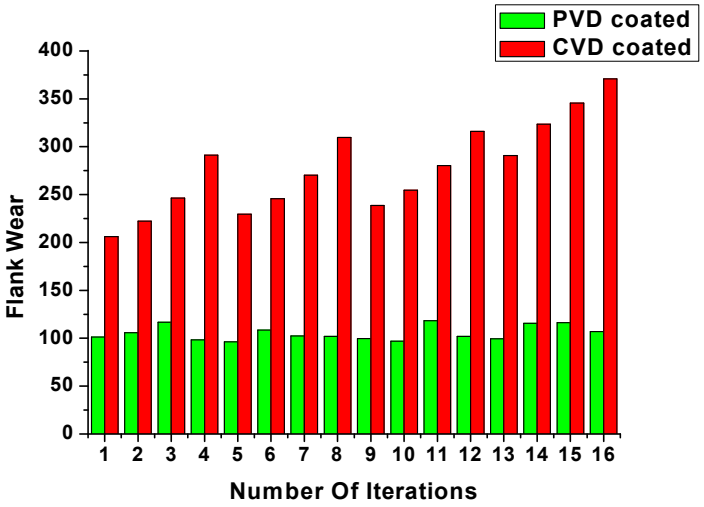

Figure 4.21 (a) Comparison Graph for Flank Wear

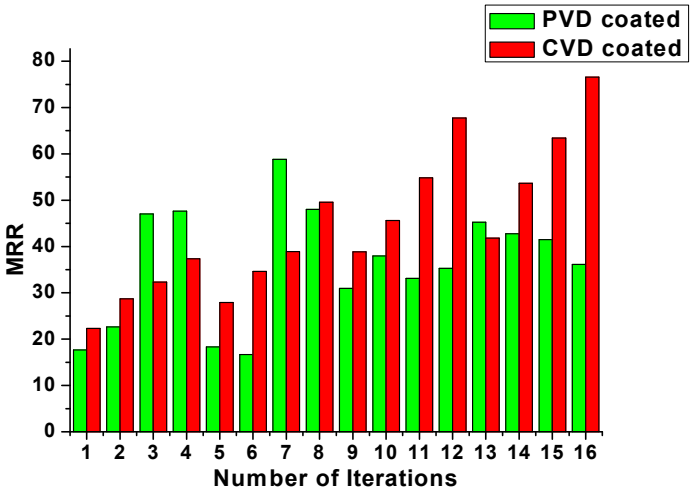

Figure 4.21 (b) Comparison Graph for MRR

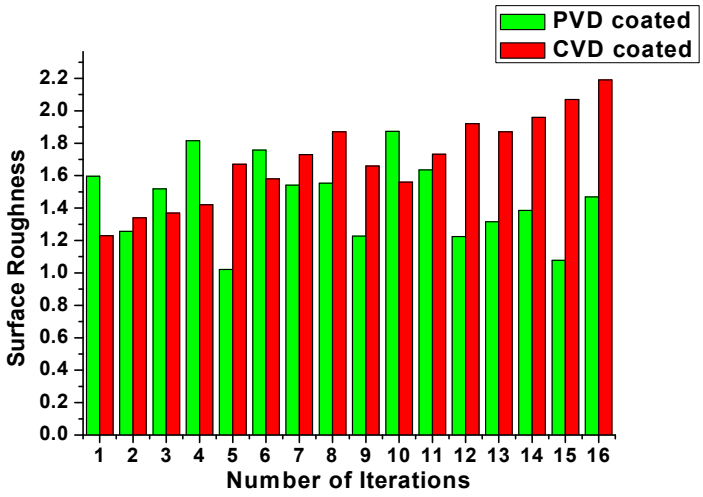

Figure 4.21 (c) Comparison Graph for Surface Roughness

4.7 Conclusions

In this study, Inconel 718 has been machined under dry condition using PVD coated and CVD coated cutting tools. Fuzzy inference system coupled with ICA is used to obtain optimal process parameters. The work also highlighted to compare the performance characteristics such as MRR, Flank wear and surface roughness using PVD coated tool and CVD coated tool. The following conclusions can be drawn from this study.

1. PVD (single layer coating: AlTiN) coated tool is more efficient than CVD (four layers coating: TiN, Al_2O_3, TiCN, TiN) coated tool in case of flank wear.
2. Fuzzy inference system (FIS) coupled with ICA is suitable to obtain the optimal process parameters.
3. The optimal parametric combination for CVD coated tool is spindle speed 400 RPM, depth of cut 1mm and feed rate 0.08 mm/rev and for PVD coated tool is spindle speed 1000 RPM, depth of cut 1 mm and feed rate 0.2 mm/rev.

Chapter 5

EXPERIMENTAL INVESTIGATION ON PERFORMANCE OF COATING OF CUTTING TOOLS IN TURNING OF GLASS FIBRE REINFORCED PLASTIC (GFRP) COMPOSITES

5.1 Introduction

With the increasing use of fibre reinforced plastics (FRPs) in defence, space, aerospace and manufacturing industries, the studies on machining of these materials are important from practical point of view. Composite material are increasingly used in various fields of science and engineering due to their unique properties such as high stiffness, lightweight, good corrosive resistance, low thermal expansion, etc. (Khan and Kumar, 2011). Although most of fibre reinforced composite (FRP) material parts are processed to a near net shape, machining is often necessary for finishing, trimming, drilling and grinding. Due to these reasons, conventional machining on the FRP composite has gained importance to meet the required dimensional accuracy and good surface finish. In FRP family, glass fibre reinforced plastic (GFRP) composite is used in most applications as compared to other FRP composites. With increasing applications of GFRP composites; machining and machinability aspects of composites are very important and need to be studied in detail (Teti, 2002; Palanikumar et al., 2006; Chang, 2006; Davim and mata, 2007; Palanikumar et al., 2009; Sait et al., 2009; Kini and Chincholkar, 2010; Kumar et al., 2011; Hussain et al., 2011; Kumar et al. 2013; Mkaddem et al., 2013).

This chapter demonstrate the experimental investigations on the influence of important process parameters such as spindle speed (N), feed rate (f) and depth of cut (d) on responses like material removal rate (MRR), flank wear and surface roughness, during turning of GFRP composite. Taguchi's parameter design is adopted to understand effect of process parameters on responses. Conventional Taguchi method can effectively establish optimal parameter settings for a single objective characteristic. When multiple objectives under consideration are conflicting in nature, the approach becomes unsuitable. The multiple objectives measures considered in this work are MRR, flank wear and surface roughness. All these responses can be combined together into an equivalent response when MRR should be maximized and flank wear and surface roughness should be minimized. Fuzzy inference system (FIS) has the ability to combine all the responses simultaneously, to result in an equivalent response called multi performance characteristics index (MPCI). A regression equation between process parameters and MPCI is developed and validated. Imperialistic competitive algorithm (ICA) has been used to obtain optimal setting of process parameters.

5.2 Experimental Details

Experimentation has been done on CNC lathe (Model No. Sprint 16 TC manufactured by: BATLIBOI LTD. SURAT) as shown in Figure 4.6 (Chapter 4). Table 4.1 (Chapter 4) describes the brief descriptions of CNC turning lathe. In this work,

the work piece material has been taken as a bar of randomly oriented fibre of glass fibre reinforced plastic (GFRP) having dimensions 30×150 mm (Figure 5.1). GFRP rods having 10%, 20% and 30% fibres in volume percentage are used in this experimentation (Table 5.1). Figures 5.2 and 5.3 are present the micrographs of GFRP before turning of GFRP. Here, two coated tool insert such as chemical vapor deposition (CVD) and physical vapor deposition (PVD) of tungsten carbide (WC) are used. Table 5.1 shows the specifications of GFRP whereas Table 5.2 shows the specification of cutting tool and dimension of the cutting tool which are discussed earlier in chapter 4 (section 4.4). The machining variables such as spindle speed, feed rate and depth of cut have been taken into consideration to examine their effect on the material removal rate, tool wear and surface roughness.

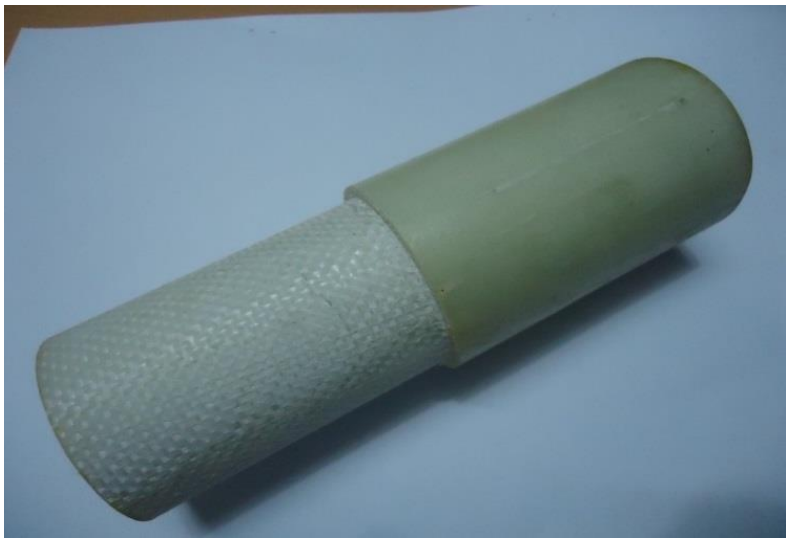

Figure 5.1 GFRP composite rod (30mm×150mm)

Table 5.1 Specifications of GFRP composite

Resin used	Polyester resin
Fiber orientation	Random
Method of preparation	Hand molding method
Reinforcement percentage	10%, 20%, 30%
Density	2.6 gm/cm^3

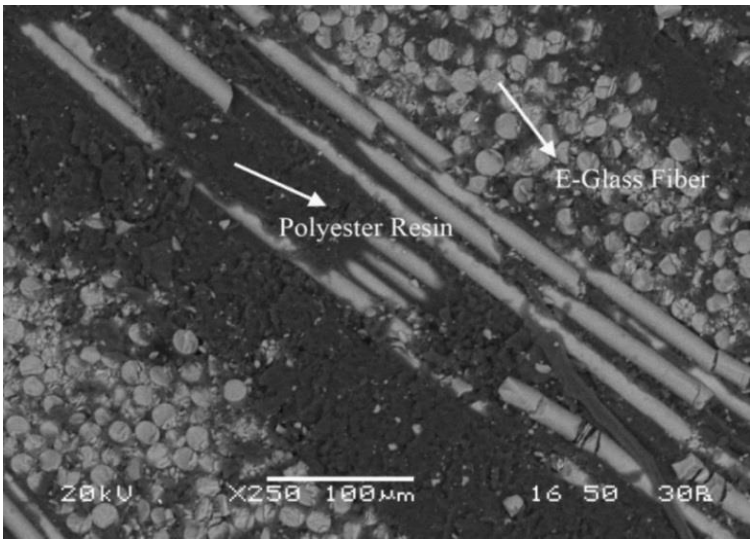

Figure 5.2 10% reinforcement of randomly oriented glass fibre GFRP composite SEM (scanning electron microscope) picture

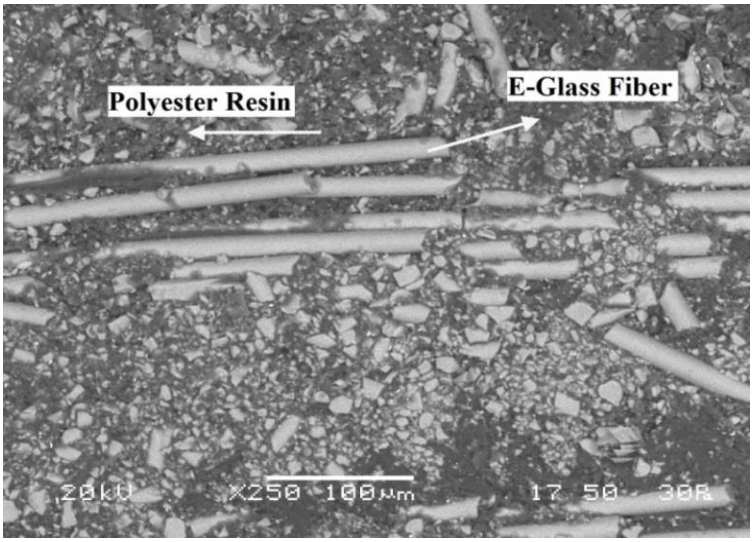

Figure 5.3 30% reinforcement of randomly oriented glass fibre GFRP composite SEM picture

Table 5.2 Tool Specifications

Coating	CVD coated tool	PVD coated tool
Tool signature	(10-10-7-7-5-5-0.4)	(6-6-0-0-5-5-0.4)
Coatings material	TiN, TiCN, Al_2O_3, TiN	AlTiN
Grade	CNMG 431 FW_KC9225	CNMG 431 MP_KC5010
Tool Holder	Grade PCLNL2525M12	

Table 5.3 presents different levels of process parameters such as coating of tool material, spindle speed, feed rate, depth of cut and volume fraction of fibre for turning of GFRP composite. A schematic layout for experimentation is highly required for

reduction of experimental time and cost. Therefore, Taguchi's philosophy is used to design the experimental layout to examine the effect of the machining parameters with less number of experimental runs. In the present chapter, five process parameters have been taken, one parameter being coating varied in two different levels and other four process parameters are varied in three different levels. So, the possible combination of experiments is $2^1 \times 3^4$. Hence, Taguchi method is adopted to reduce the number of experiments by utilizing the orthogonal array concept. Thereby, mixed level L_{18} orthogonal array has been chosen for experimentation shown in Table 5.4. For experimentation, work piece is cut for a length of 60 mm in each run.

Table 5.3 Process parameters and their levels

Sl. No.	Parameters	Symbols	Level 1	Level 2	Level 3
1	Coating	C	KC 5010 (PVD)	KC 9225 (CVD)	-
2	Spindle Speed (RPM)	N	860	1400	2000
3	Feed (mm/rev)	f	0.210	0.298	0.396
4	Depth of Cut (mm)	d	0.5	1.0	1.5
5	Volume Fraction of fibre (%)	v	10	20	30

In turning of GFRP, material removal rate (MRR), flank wear and surface roughness are important responses which is decides the machinability of GFRP composite. Hence, it is necessary to evaluate these responses characteristics to maintain the quality of finish part. These performance characteristics are evaluated as same procedures which are illustrated in chapter 4 (section 4.4). The responses MRR, flank wear and surface roughness are calculated and listed in Table 5.4. Figure 5.4 (a) and Figure 5.4 (b) show the flank wear on PVD and CVD coated tool respectively.

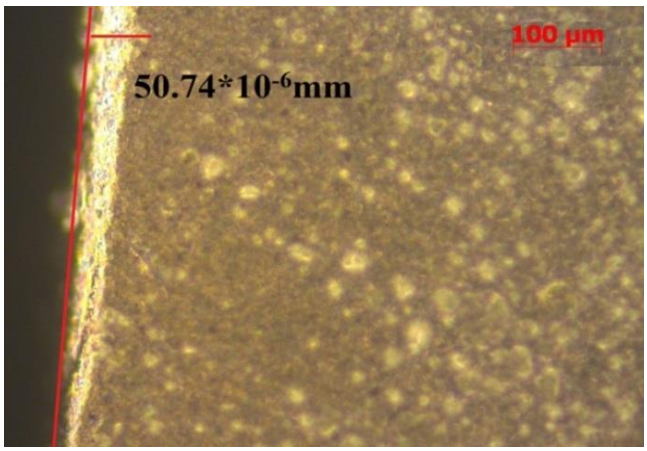

Figure 5.4 (a) Flank Wear of setting PVD coated tool, Spindle Speed 860 RPM, Feed 0.210 mm and Volume Fraction of fibre 10%

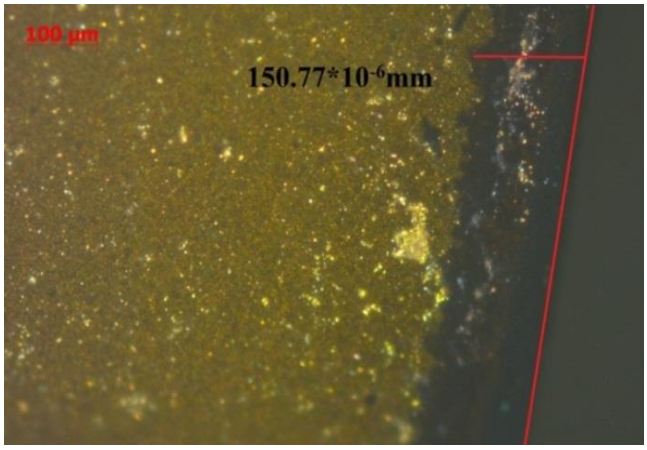

Figure 5.4 (b) Flank Wear of setting CVD coated tool, Spindle Speed 2000 RPM, Feed 0.210 mm and Volume Fraction of fibre 20%

Table 5.4 Experimental Results

Sl. No.	Process Parameters					Experimental Results		
	C	N	f	d	v	MRR (mm^3/sec)	Flank Wear (µm)	Surface Roughness (µm)
1	1	1	1	1	1	35.78	50.74	8.66
2	1	1	2	2	2	48.97	57.87	5.712
3	1	1	3	3	3	32.35	58.59	4.7
4	1	2	1	1	2	18.91	65.1	8.417
5	1	2	2	2	3	23.33	70.91	6.842
6	1	2	3	3	1	37.18	85.17	8.86
7	1	3	1	2	1	32.56	93.87	9.64
8	1	3	2	3	2	42.31	70.13	6.4
9	1	3	3	1	3	18.46	65.54	4.463
10	2	1	1	3	3	28.43	120.81	4.9
11	2	1	2	1	1	26.59	93.32	7.36
12	2	1	3	2	2	20.14	108.98	4.252
13	2	2	1	2	3	10.93	156.68	6.1
14	2	2	2	3	1	41.67	162.33	9.28
15	2	2	3	1	2	13.14	146	5.12
16	2	3	1	3	2	32.69	150.77	8.302
17	2	3	2	1	3	11.54	130.21	5.72
18	2	3	3	2	1	31.54	148.87	7.254

5.3 Results and discussions

Experimental data are collected as per experimental plan of Taguchiôs L_{18} orthogonal array. Lower-the-better (LB) criterion is used for flank wear and surface roughness whereas higher-the-better (HB) criterion is used for MRR. Analysis of variance (ANOVA) is a method of partitioning observed variance into components of different explanatory variables to identify significance of each parameter. Table 5.6, Table 5.7 and Table 5.8 present the ANOVA for material removal rate (MRR), flank wear and surface roughness respectively. It is to be noted that coating of tool insert,

depth of cut and volume fraction of fibre are significant factors influencing on MRR at significance level 0.05 (Table 5.5). Similarly, the factors like coating of tool insert, spindle speed and depth of cut are significant factors influencing on flank wear at significance level 0.05 (Table 5.6). For surface roughness, the factors like spindle speed, feed rate and volume fraction of fibre are significant influencing factors at significance level 0.05 (Table 5.7). The optimal parametric setting can be obtained from the factorial plots. Figure 5.5 (a) reveals that coating of tool material, spindle speed, feed rate, depth of cut and volume fraction of fibre should be maintained at PVD coated tool, spindle speed 860 RPM, feed 0.298 mm/rev, depth of cut 1.5 mm and volume fraction of fibre 10% respectively to maximize MRR. Similarly, Figure 5.5 (b) indicates that PVD coated tool, spindle speed 860 RPM, feed 0.298 mm/rev, depth of cut 0.5 mm and volume fraction of fibre 30% to minimize flank wear and surface roughness Figure 5.5 (c) shows that CVD coated tool, spindle speed 860 RPM, feed rate 0.396 mm/rev, depth of cut 0.5 mm and volume fraction of fibre 30% to minimize surface roughness.

Table 5.5 Analysis of Variance for Means MRR (R-square 89.8%)

Source	DF	Seq SS	Adj SS	Adj MS	F-value	P-value	% Contribution
C	1	297.5	297.5	297.5	11.11	0.010	14.22
N	2	184.9	184.9	92.44	3.45	0.083	8.84
f	2	167.0	167.0	83.48	3.12	0.100	7.98
d	2	678.6	678.6	339.31	12.68	0.003	32.43
v	2	550.5	550.5	275.23	10.28	0.006	26.31
Residual Error	8	214.2	214.2	26.77			10.24
Total	17	2092.6					

Table 5.6 Analysis of Variance for Means Flank Wear (R-square 96.8%)

Source	DF	Seq SS	Adj SS	Adj MS	F-value	P-value	% Contribution
C	1	20003.3	20003.3	20003.3	192.78	0.000	77.24
N	2	3759.7	3759.7	1879.9	18.12	0.001	14.52
f	2	236.2	236.2	118.1	1.14	0.367	0.91
d	2	941.3	941.3	470.6	4.54	0.048	3.63
v	2	126.0	126.0	63.0	0.61	0.568	0.49
Residual Error	8	830.1	830.1	103.8			3.21
Total	17	25896.6					

Table 5.7 Analysis of Variance for Means Surface Roughness (R-square 94.0%)

Source	DF	Seq SS	Adj SS	Adj MS	F-value	P-value	% Contribution
C	1	1.6236	1.6236	1.6236	4.08	0.078	3.06
N	2	7.1153	7.1153	3.5576	8.95	0.009	13.40
f	2	10.8798	10.8798	5.4399	13.69	0.003	20.49
d	2	0.7936	0.7936	0.3968	1.00	0.410	1.49
v	2	29.5061	29.5061	14.7530	37.12	0.000	55.57
Residual Error	8	3.1798	3.1798	0.3975			5.99
Total	17	53.0981					

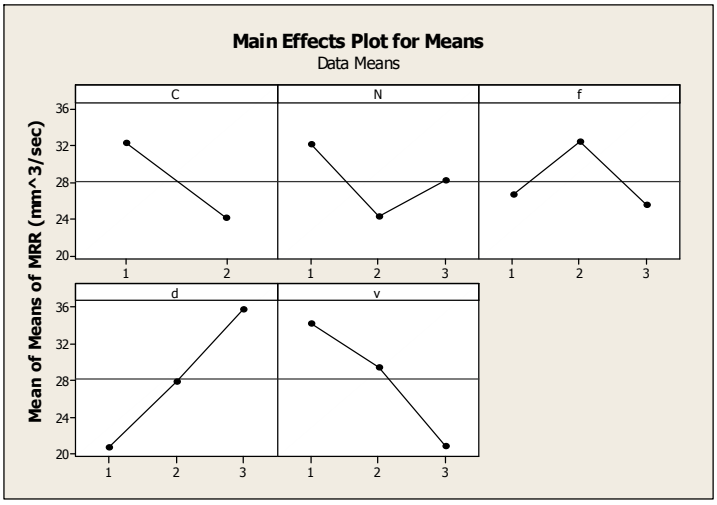

Figure 5.5 (a) Mean effect plot for MRR

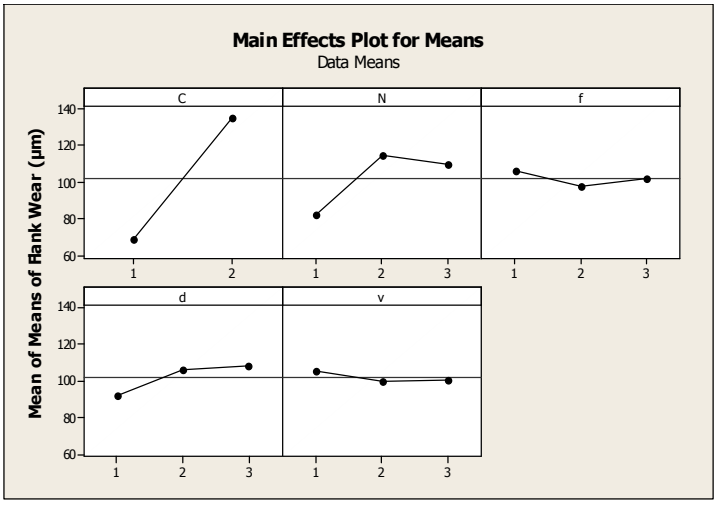

Figure 5.5 (b) Mean effect plot for Flank wear

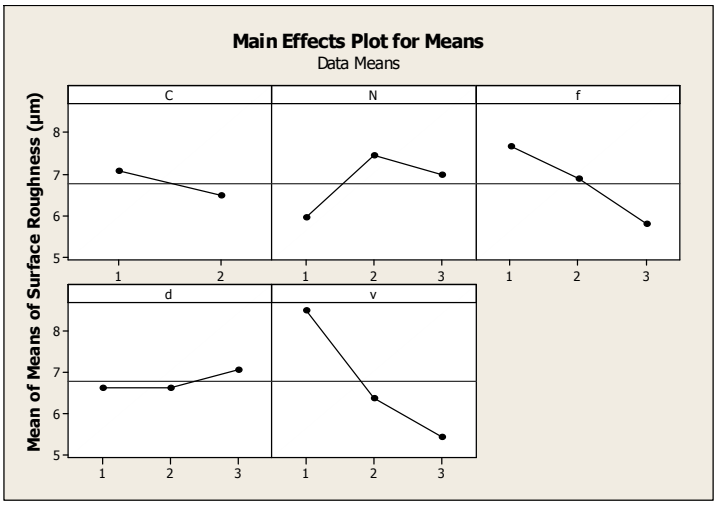

Figure 5.5 (c) Mean effect plot for Surface roughness

5.4 Mathematical model development

Nonlinear regression is a mathematical method for finding a nonlinear model of the relationship between dependent and independent variables. The proposed mathematical model between the independent parameters and dependent variable is presented in the following form (Thirumalai and Senthilkumaar, 2013).

$$Y = Z \times C^{X_1} \times N^{X_2} \times f^{X_3} \times d^{X_4} \times v^{X_5} \quad (5.2)$$

where Z indicates a constant, C is the coating of tool material, N is the cutting speed, f is the feed, d is the depth of cut, v is the volume fraction of fiber, x_1, x_2, x_3, x_4, x_5 are estimated exponents of the regression model. Statistical software (SYSTAT 7.0) is used to estimate the parameters in nonlinear models using the Gauss-Newton nonlinear least-squares algorithm. The empirical relations between the multi performance characteristics index (MPCI) and the machining parameters are given in equation 5.2.

5.5 Optimization with Fuzzy Inference System coupled with ICA

For optimization of multiple responses, a fuzzy inference system (FIS) is used to convert multiple responses into a single equivalent response so that uncertainty and fuzziness in data can be addressed in an effective manner. The single response characteristics, so generated are known as Multi Performance characteristic Index (MPCI). A non-linear empirical model has been developed using regression analysis between MPCI and process parameters. The optimal process parameters are obtained by a recent population-based optimization method known as imperialistic competitive algorithm (ICA).

It is necessary to normalize the output responses (such as; MRR, flank wear and surface roughness) in a common scale i.e. 0 to 1 (0 is considered as worst value

whereas 1 considered as best value) in order to eliminate the dimensional effect. Initially machining evaluation characteristics are normalized by using formulas given below:

For MRR (Higher-is better):

$$\frac{X_{ij} - X_{min}}{X_{max} - X_{min}} \tag{5.4}$$

For surface roughness and cutting force (Lower-is better):

$$\frac{X_{max} - X_{ij}}{X_{max} - X_{min}} \tag{5.5}$$

The normalized value for each aforementioned characteristic (Table 5.8) is treated as input variable and the MPCI has been considered as output variable (Figure 5.6). In calculating MPCI, three membership functions {Figure 5.7 (a) to Figure 5.7 (c)} have been assigned to each of the input variables viz. (i) Normalized value of MRR (ii) Normalized value of flank wear (FW) (iii) Normalized value of surface roughness (SR). The selected membership functions for individual input variables are: ñsmallò, ñMediumò, and ñLargeò, whereas for MPCI, five membership functions have been assigned: ñVery Smallò, ñSmallò, ñMediumò, ñLargeò, and ñVery Largeò (Figure 5.7 (d)). A set of 27 rules are formed which converts linguistic inputs into linguistic output (Figure 5.8). Linguistic output is again converted to numeric values (MPCI) (Figure 5.9) by de-fuzzification method (Table 5.8) by using centre of gravity method.

By using non-linear regression analysis, a mathematical model derived for MPCI is given as follows:

$$MPCI = 0.503 \times C^{(-0.184)} \times N^{(0.282)} \times f^{(0.142)} \times d^{(0.135)} \times v^{(0.081)} \tag{5.3}$$

R-Square value 97.6%

Finally, the developed mathematical model is act as an objective function in ICA. The optimal setting for maximizing MPCI appears as (C=1 N=1 f=3, d=3 and v= 3) also shown in Table 5.9. The fitness function value (predicted MPCI) for ICA appears as 0.7528 as shown in Figure 5.10.

Table 5.8 Normalize Value for Responses

Sl No.	Nr-MRR	Nr-FW	Nr-SR	MPCI
1	0.65326	1	0.181886	0.588
2	1	0.936105	0.729027	0.734
3	0.563091	0.929653	0.916852	0.701
4	0.209779	0.871315	0.226986	0.351
5	0.325973	0.819249	0.519302	0.42
6	0.690063	0.69146	0.144766	0.463
7	0.568612	0.613496	0	0.373
8	0.824921	0.826239	0.601336	0.662
9	0.19795	0.867372	0.960839	0.576
10	0.460042	0.372076	0.879733	0.645
11	0.411672	0.618425	0.423163	0.439
12	0.242114	0.478089	1	0.622
13	0	0.050632	0.657016	0.337
14	0.808097	0	0.066815	0.443
15	0.058097	0.146339	0.838901	0.451
16	0.572029	0.103594	0.24833	0.424
17	0.016036	0.287839	0.727543	0.379
18	0.541798	0.12062	0.442836	0.491

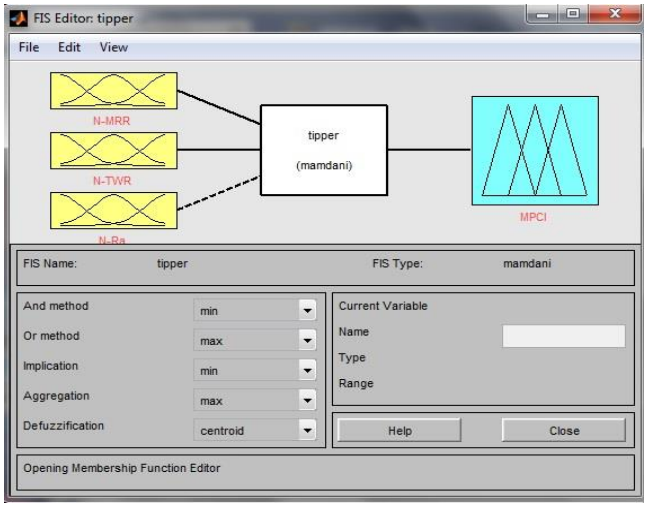

Figure 5.6 Schematic diagram of fuzzy model

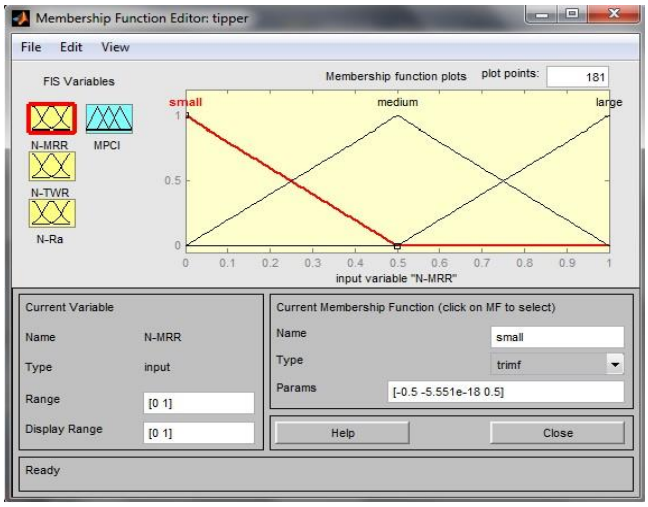

Figure 5.7 (a) Membership function for N-MRR

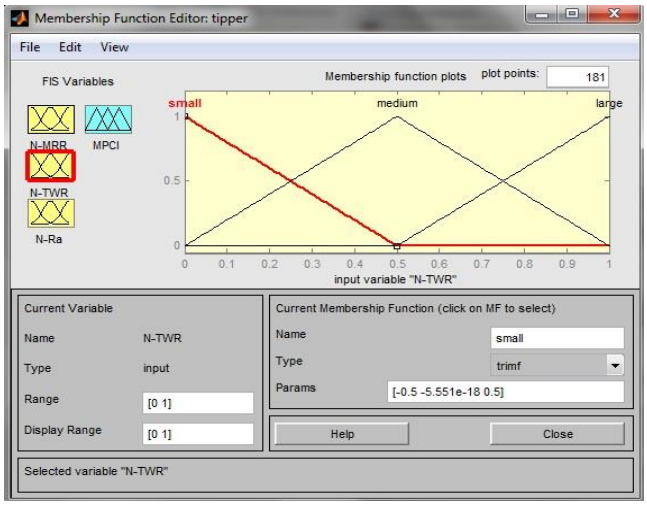

Figure 5.7 (b) Membership function for N-FW (flank wear)

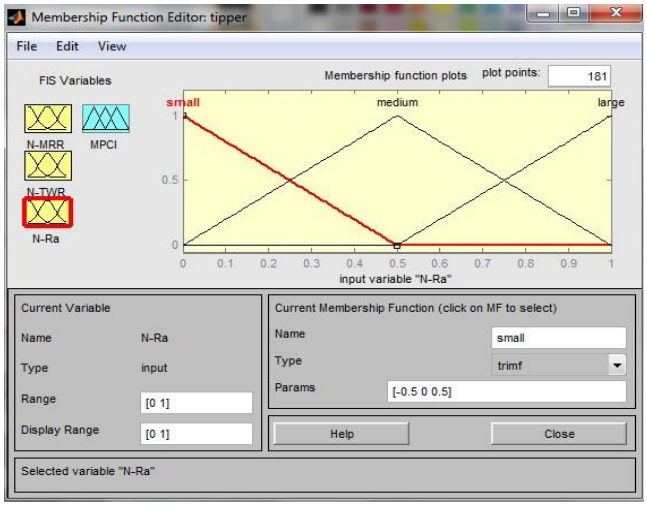

Figure 5.7 (c) Membership function for N-SR (surface roughness)

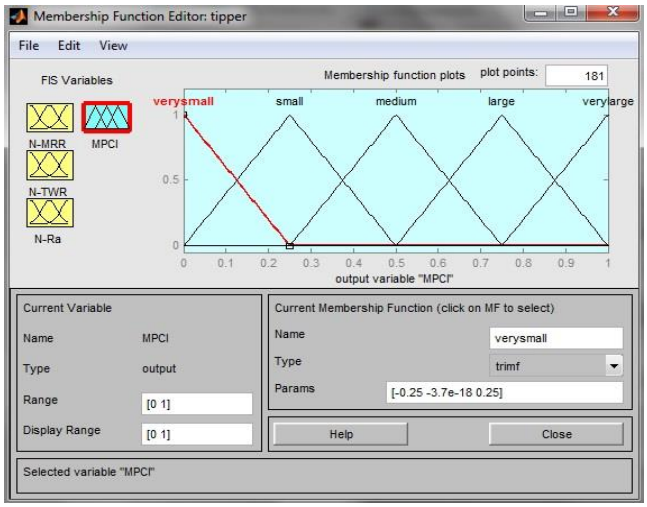

Figure 5.7 (d) Membership function for MPCI

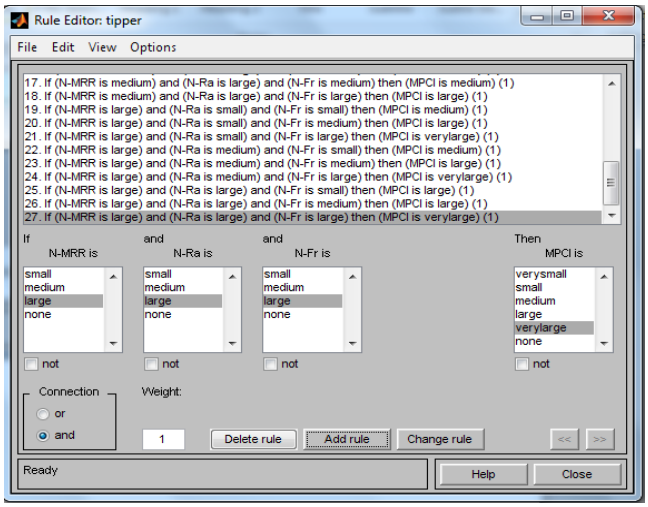

Figure 5.8 Fuzzy Rule-Base

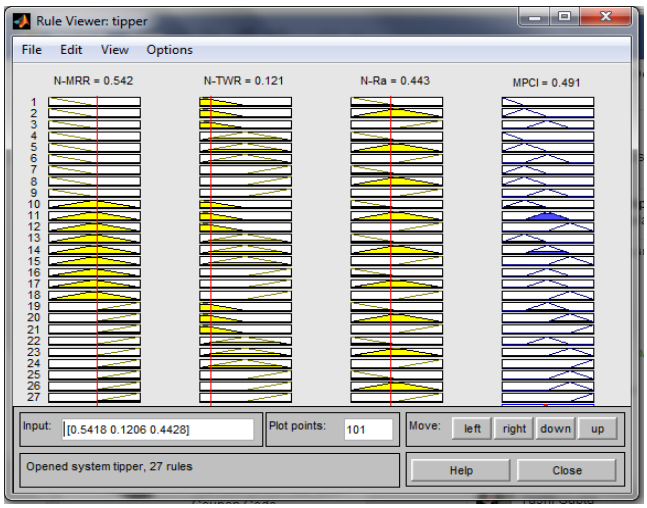

Figure 5.9 Fuzzy rule used in the experimental control

Table 5.9 Optimal value of MPCI

Coating	Spidle Speed (RPM)	Feed (mm/rev)	DOC (mm)	Volume Fr. of fiber (%)	MPCI
PVD	860	0.396	1.5	30	0.7528

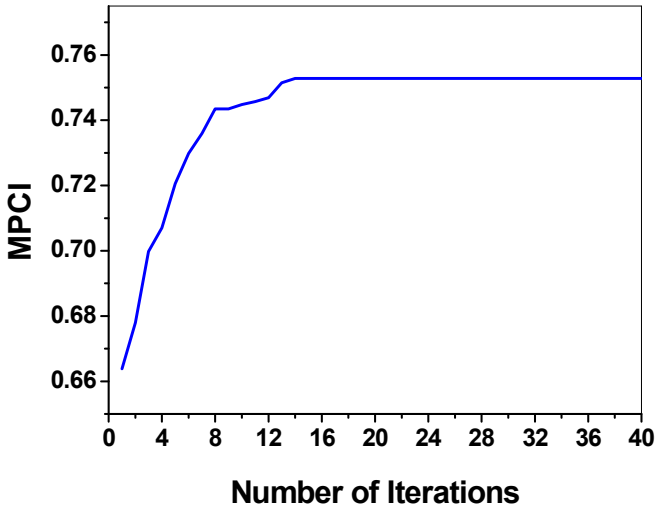

Figure 5.10 Convergence Curve of MPCI

5.6 Conclusions

In this study, GFRP has been machined under dry condition using PVD coated and CVD coated tool cutting tools. Multi objective optimization is used to obtain optimal process parameters. Fuzzy inference system coupled with ICA is used for obtain optimal process parameters. The work also highlighted the performance characteristics comparison between PVD coated tool and CVD coated tool. The following conclusions can be drawn from this study.

- Coating of tool material, depth of cut and volume fraction of fibre is significant factor for MRR, coating of tool material, spindle speed and depth of cut is significant for flank wear and spindle speed, feed rate and volume fraction of fibre is significant factor for surface roughness.
- PVD coated tool is more efficient as compare to CVD in case of flank wear because the maximum value of flank wear for PVD coated tool is 93.87 µm and maximum value of flank wear for CVD coated tool is 162.33 µm.
- The optimal setup for process parameters is PVD coated tool, spindle speed is 860 RPM, feed rate 0.396, depth of cut 1.5 volume fraction of fibre is 30%.

Chapter 6

Executive Summary and Conclusions

6.1 Introduction

The research reported in this thesis consists of three parts: the first part provides the description of the simulation model for turning of Inconel 718 and validation with experimental values, second part reports the experimental investigation on turning of Inconel 718 using CVD and PVD coated tools and last part focusses on comparative study of CVD and PVD coated tool on experimental investigation of turning of GFRP composite.

6.2 Summary of findings

The present work not only highlights the simulation model for machining process in turning of Inconel 718 but also examines the effect of process parameter on machining evaluation performance characteristics in detail for both Inconel 718 and GFRP composites. In simulation modelling, flank wear has been estimated using Usui's model for turning of Inconel 718 with CVD coated tool of tungsten carbide (WC). The present work also aims to study the machinability aspects of Inconel 718 and GFRP composite under dry condition using PVD coated and CVD coated cutting tools of tungsten carbide. The machining performance characteristics such as MRR, surface roughness and flank wear have been evaluated in dry turning of Inconel 718 and GFRP both. In order to obtain the optimal parametric combination, fuzzy inference system coupled with ICA has been used. The major findings are as follows:
Simulation modelling of turning of Inconel 718:

- Simulation modelling is one of the convenient means to predict the machining performance characteristics without restoring to costly experimentation.
- The simulation approach enables to predict the tool wear and material removal rate at any given cutting time as cutting tool geometry is constantly updated in FEM simulation through DEFORM 3D.
- In case of CVD coated tool, the percentage relative error between experimental and simulation predicted value of flank wear and MRR is below 7%. In most instances, simulation predicts higher value for flank wear and MRR than experimental values. However, simulation can appreciably save costly experimental time, cost, and resources.
- This study confirms the ability of the DEFORM 3D simulation model to predict the flank wear and MRR in case of CVD coated tool.
- During turning process, the maximum temperature at tool tip-work piece interface is 1100°C at spindle speed of 1020 RPM, depth of cut of 1 mm and feed rate of 0.08 mm/rev.

- In experiments, the value of flank wear varies from 211.25 µm to 350.76 µm whereas it varies from 219.25 µm to 365.32 µm in simulation.
- Analysis of variance suggests that the most influencing factors are spindle speed, depth of cut and feed rate in case of MRR whereas spindle speed and depth of cut are the most influencing factors in case of flank wear.

Dry turning of Inconel 718

- PVD (single layer coating: AlTiN) coated tool is more efficient as compared to CVD (four layers coating: TiN, Al_2O_3, TiCN, TiN) coated tool in case of flank wear.
- Fuzzy inference system (FIS) coupled with ICA is suitable for finding the optimal process parameters.
- The optimal setting of process parameters for CVD coated tool is spindle speed 400 RPM, depth of cut 1mm and feed rate 0.08 mm/rev and for PVD coated tool is spindle speed 1000 RPM, depth of cut 1 mm and feed rate 0.2 mm/rev.

Dry turning of GFRP composite

- The coating of tool material, depth of cut and volume fraction of fibre are significant factors for MRR, coating of tool material, spindle speed and depth of cut are significant for flank wear and spindle speed, feed rate and volume fraction of fiber are significant factors for surface roughness.
- PVD coated tool is more efficient as compared to CVD in case of flank wear because the maximum value of flank wear for PVD coated tool is 93.87 µm whereas maximum value of flank wear for CVD coated tool is 162.33 µm.
- The optimal setup for process parameters is PVD coated tool, spindle speed of 860 RPM, feed rate of 0.396 mm/rev, depth of cut of 1.5 mm and volume fraction of fibre 30%.

The work highlights the important contribution of each factor on the output response (MRR, flank wear and surface roughness). Tables 6.1, 6.2 and 6.3 show the significant factors for the responses.

Table 6.1 Significant factors for turning of Inconel 718 using CVD coated tool

Responses	Significant terms
Material removal rate	Spindle speed, depth of cut, feed rate
Flank wear	Spindle speed, depth of cut
Surface roughness	Spindle speed, depth of cut, feed rate

Table 6.2 Significant factors for turning of Inconel 718 using PVD coated tool

Responses	Significant terms
Material removal rate	Spindle speed, depth of cut, feed rate
Flank wear	Spindle speed, depth of cut, feed rate
Surface roughness	Spindle speed, depth of cut, feed rate

Table 6.3 Significant factors for turning of GFRP composite

Responses	Significant terms
Material removal rate	Coating of tool material, depth of cut, volume fraction of fibre
Flank wear	Coating of tool material, Spindle speed, depth of cut
Surface roughness	Spindle speed, feed rate, volume fraction of fibre

Table 6.4, 6.5 and 6.6 show the optimum setting of process parameters in turning of both Inconel 718 and GFRP composites. To achieve this, present work utilizes the FIS coupled with ICA for optimization. The suitability of fuzzy inference system (FIS) lies in converting all the responses into an equivalent single response known as multi performance characteristics index (MPCI). The multiplicative relation between MPCI and process parameters is obtained by non-linear regression analysis. The generated equation is used as fitness function in ICA for determining optimum setting for process parameters.

Table 6.4 Optimum setting for turning of Inconel 718 (CVD coated)

Spindle speed (RPM)	Depth of cut (mm)	Feed rate (mm/rev)
400	1	0.2

Table 6.5 Optimum setting for turning of Inconel 718 (PVD coated)

Spindle speed (RPM)	Depth of cut (mm)	Feed rate (mm/rev)
1000	1	0.2

Table 6.6 Optimum setting for turning of GFRP composite

Coating	Spidle Speed (RPM)	Feed (mm/rev)	DOC (mm)	Volume Fr. of fiber (%)
PVD	860	0.396	1.5	30

6.3 Major contribution of the research work

- A finite element based numerical model has been developed for predicting the turning responses of Inconel 718 using DEFORM 3D software. The predicted models are validated through experimental observations. The model can be successfully used to predict the performance characteristics in turning. This can help the tool engineers to reduce the experimental efforts.
- The proposed hybrid approach for multi-response optimization of turning process using fuzzy inference system coupled with imperialist competitive algorithm can help the practicing engineers to simultaneously optimize several responses. The method uses one of the efficient multi-criteria decision making method along with a latest evolutionary approach. The proposed method being quite generic can be applied to fields other than turning process.
- As the effect of control parameters on performance characteristics in conventional turning process has been explored in detail, the suggested process parametric setting helps to ease for planning of turning operation.
- It is found that behavior of PVD coated tool is superior than CVD coated tool in all the considered performance characteristics both in dry turning of Inconel 718 and GFRP.

6.4 Limitations of the study

In spite of advantages obtained through proposed study, the following may be treated as limitations of the study since they have not been addressed in this study;

- Interactions between the process parameters are not considered.
- During turning process, the machine vibration is not considered.
- The study on tool wear like crater wear and notch wear of tool insert are not considered.

6.5 Scope for future work

- To develop a work piece model of GFRP composite using Solid Works and CATIA.
- To study machinability of GFRP composite using coated (PVD and CVD) and uncoated tools for different fiber orientation.
- To determine optimal parameter setting using multi response optimization techniques, response surface methodology, with some new evolutionary techniques such as Harmony search method, Bat algorithm etc.

REFERENCES

Abhishek, K., Datta, S., Mahapatra, S.S., Mandal, G. and Majumdar, G. (2013) Taguchi approach followed by fuzzy linguistic reasoning for quality-productivity optimization in machining operation. *Journal of Manufacturing Technology Management*. 24 (6). p. 929-951.

Ahmadi, M.A., Ebadi, M., Shokrollahi, A. and Majidic, S.M.J. (2013) Evolving artificial neural network and imperialist competitive algorithm for prediction oil flow rate of the reservoir. *Applied Soft Computing*. 13 (2). p. 1085-1098.

Amini, S., Fatemi, M. H., and Atefi, R. (2013) High Speed Turning of Inconel 718 Using Ceramic and Carbide Cutting Tools. *Arabian Journal for Science and Engineering*. 39 (3) p. 2323-2330.

Arrazola, P.J., Kortabarria, A., Madariaga, A., Esnaola, J.A., Fernandez, E., Cappellini, C., Ulutan, D. and Ozel, T. (2014) On the machining induced residual stresses in IN718 nickel-based alloy: Experiments and predictions with finite element simulation. *Simulation Modelling Practice and Theory*. 41 p. 87-103.

Arrazola, P.J. and Ozel, T. (2010) Investigations on the effects of friction modelling in finite element simulation of machining. *International Journal of Mechanical Sciences*. 52 (1) p. 31-42.

Arsecularatne, J.A., Zhang and L.C., Montross, C. (2006) Wear and tool life of tungsten carbide, PCBN and PCD cutting tools. *International Journal of Machine Tools and Manufacture*. 46 (5) p. 482-491.

Arunachalam, R.M., Mannan, M.A. and Spowage, A.C. (2004) Surface integrity when machining age hardened Inconel 718 with coated carbide cutting tools. *International Journal of Machine Tools and Manufacture*. 44 (14) p. 1481-1491.

Atashpaz-Gargari, E. and Lucas, C. (2007) Imperialist competitive algorithm: an algorithm for optimization inspired by imperialistic competition, in: IEEE Congress on Evolutionary Computation, CEC, p. 4661-4667.

Attanasio, A., Ceretti, E., Fiorentino, A., Cappellini, C. and Giardini, C. (2010) Investigation and FEM-based simulation of tool wear in turning operations with uncoated carbide tools. *Wear*. 269 (5-6) p. 344-350.

Aurich, J.C. and Bil, H. (2006) 3D Finite Element Modelling of Segmented Chip Formation. *CIRP Annals-Manufacturing Technology*. 55 (1) p. 47-50.

Bashiri, M. and Bagheri, M. (2013) Using Imperialist Competitive Algorithm in Optimization of Nonlinear Multiple Responses. *International Journal of Industrial Engineering and Production Research*. 24 (3). p. 229-235.

Bhatt, A., Attia, H., Vargas, R. and Thomson, V. (2010) Wear mechanisms of WC coated and uncoated tools in finish turning of Inconel 718. *Tribology International*. 43 (5-6) p. 1113-1121.

Bharti, P.S., Maheshwari, S. and Sharma, C. (2012) Multi-objective optimization of electric-discharge machining process using controlled elitist NSGA-II. *Journal of Mechanical Science and Technology*. 26 (6). p. 1875-1883.

Bhoyar, Y.R. and Kamble, P.D. (2013) Finite element analysis on temperature distribution in turning process using DEFORM 3D. *International Journal of Research in Engineering and Technology*. 2 (5) p. 901-906.

Bose, P.K., Deb, M., Banerjee, R. and Majumder, A. (2013) Multi objective optimization of performance parameters of a single cylinder diesel engine running with hydrogen using a Taguchi-fuzzy based approach. *Energy*. 63 (December). p. 375-386.

Cantero, J.L., Diaz-Alvarez, J., Miguelez, M.H. and Marin, N.C. (2013) Analysis of tool wear patterns in finishing turning of Inconel 718. *Wear*. 297 (1-2). p. 885-894.

Chinchanikar, S. and Choudhury, S.K., (2013) Wear behaviours of single-layer and multi-layer coated carbide inserts in high speed machining of hardened AISI 4340 steel. *Journal of Mechanical Science and Technology*. 27 (5). p. 1451-1459.

Ceretti, E., Lazzaroni, C., Menegardo, L. and Altan, T. (2000) Turning simulations using a three-dimensional FEM code. *Journal of Materials Processing Technology*. 98 (1) p. 99-103.

Chang, C.-S. (2006) Turning of glass-fiber reinforced plastics materials with chamfered main cutting edge carbide tools. *Journal of Materials Processing Technology*. 180 (1-3). p. 117-129.

Choudhury, I.A. and El-Baradie, M.A. (1998) Machinability of nickel-base super alloys: a general review. *Journal of Materials Processing Technology* 77 (1-3) p. 278-284.

Costes, J.P., Guillet, Y., Poulachon, G. and Dessoly, M. (2007) Tool-life and wear mechanisms of CBN tools in machining of Inconel 718. *International Journal of Machine Tools and Manufacture*. 47 (7-8) p. 1081-1087.

Davim, J.P. and Mata, F. (2007) New machinability study of glass fibre reinforced plastics using polycrystalline diamond and cemented carbide (K15) tools. *Materials and Design*. 28 (3). p. 1050-1054.

Davim, J.P., (2010) *Machining of Hard Materials*. United States of America:Springer.

Dandekar, C.R. and Shin, Y.C. (2012) Modeling of machining of composite materials: A review. *International Journal of Machine Tools and Manufacture*. 57 (June). p. 102-121.

Devillez, A., Schneider, F., Dominiak, S., Dudzinski, D. and Larrouquer, D. (2007) Cutting forces and wear in dry machining of Inconel 718 with coated carbide tools. *Wear*. 262 (7-8) p. 931-942.

DEFORM 3D Version 6.1 (sp1) (2007) User Manual. SFTC, Columbus, Ohio State.

Duan, H. and Huang, L. (2014) Imperialist competitive algorithm optimized artificial neural networks for UCAV global path planning. *Neurocomputing*. 125 (February). p. 166-171.

Enayatifar, R., Yousefi, M., Abdullah, A. H. and Darus, A. N. (2013) MOICA: A novel multi-objective approach based on imperialist competitive algorithm. *Applied Mathematics and Computation*. 219 (17). p. 8829-8841.

Ezilarasan, C., Senthil kumar, V.S. and Velayudham, A. (2014) Theoretical predictions and experimental validations on machining the Nimonic C-263 super alloy. *Simulation Modelling Practice and Theory*. 40 p. 192-207.

Ezugwu, E.O., Wanga, Z.M. and Machadop, A.R. (1998) The machinability of nickel-based alloys: a review. *Journal of Material Process Technology*. 86 (1-3) p. 1-16.

Ezugwu, E.O., Fadare, D.A., Bonney, J., Da Silva, R.B. and Sales W.F. (2005) Modelling the correlation between cutting and process parameters in high-speed machining of Inconel 718 alloy using an artificial neural network. *International Journal of Machine Tools and Manufacture*. 45 (12-13) 1375-1385.

Fagan, M.J. (1992) *Finite Element Analysis: Theory and Practice*. Longman, New York, ISBN 0-582-02247-9.

Fahad, M., Mativenga, P.T. and Sheikh, M.A. (2012) A comparative study of multilayer and functionally graded coated tools in high-speed machining. *International Journal of Advanced Manufacturing Technology*. 62 (1-4). p. 43-57.

Fan, Y., Hao, Z.P., Zheng, M., Sun, F.L. and Yang, S.C. (2013) Study of surface quality in machining nickel-based alloy Inconel 718. *International Journal of Advanced Manufacturing Technology*. 69 (9-12) p. 2659-2667.

Groover, M.P. (2002) *Fundamentals of Modern Manufacturing: Materials, Process and Systems*, 2ndEdition, New York, United States of America:John Wiley and Sons.

Hanafi, I., Khamlichi, A., Cabrera, F.M., Lopez, P.J.N. and Jabbouri, A. (2013) Fuzzy rule based predictive model for cutting force in turning of reinforced PEEK composite. *Measurement*. 45 (6). p. 1424-1435.

Homami, R.M., Tehrani, A.F., Mirzadeh, H., Movahedi, B. and Azimifar, F. (2014) Optimization of turning process using artificial intelligence technology. *International Journal of Advanced Manufacturing Technology*. 70 (5-8) p. 1205-1217.

Hussain, S.A., Pandurangadu, V. and Palanikumar, K. (2011) Machinability of glass fiber reinforced plastic (GFRP) composite materials. *International Journal of Engineering, Science and Technology*. 3 (4). p. 103-118.

Idoumghar, L., Cherin, N., Siarry, P., Roche, R. and Miraoui, A. (2013) Hybrid ICA-PSO algorithm for continuous optimization. *Applied Mathematics and Computation*. 219 (24). p. 11149-11170.

Inta, M., Muntean, A., Brindasu, P.D. and Borza, S. (2010) Modelling of tool wear in turning operation. *Academic Journal of Manufacturing Engineering*. 8 (3) p. 49-55.

Jafarian, F., Amirabadi, H. and Fattahi, M. (2013) Improving surface integrity in finish machining of Inconel 718 alloy using intelligent systems. *International Journal of Advanced Manufacturing Technology*. 71 (5-8) p. 817-827.

Karpat, Y. and Ozel, T. (2007) Multi-objective optimization for turning processes using neural network modeling and dynamic-neighborhood particle swarm optimization. *International Journal of Advanced Manufacturing Technology*. 35 (3-4). p. 234-247.

Khan, M.A. and Kumar, A.S. (2011) Machinability of glass fibre reinforced plastic (GFRP) composite using alumina-based ceramic cutting tools. *Journal of Manufacturing Processes*. 13 (1). p. 67-73.

Khamel, S., Ouelaa, N. and Bouacha, K. (2012) Analysis and prediction of tool wear, surface roughness and cutting forces in hard turning with CBN tool. *Journal of Mechanical Science and Technology*. 26 (11). p. 3605-3616.

Khidhir, B. A. and Mohamed, B. (2010) Study of Cutting Speed on surface roughness and chip formation when machining nickel-based alloy. Journal of Mechanical Science and Technology. 24 (5) p. 1053-1059.

Kini, M. V. and Chincholkar, A.M. (2010) Effect of machining parameters on surface roughness and material removal rate in finish turning of ±30° glass fibre reinforced polymer pipes. *Materials and Design.* 31 (7). p. 3590-3598.

Krishnamoorthy, A., Boopathy, S.R., Palanikumar, K. and Davim, J.P. (2012) Application of grey fuzzy logic for the optimization of drilling parameters for CFRP composites with multiple performance characteristics. *Measurement*. 45 (5). p. 1286-1296.

Kumar, S., Gupta, M., Satsangi, P.S. and Sardana, H.K. (2011) Modeling and analysis for surface roughness and material removal rate in machining of UD-GFRP

using PCD tool, *International Journal of Engineering, Science and Technology*. 3 (8). p. 248-270.

Kumar, S., Gupta, M. and Satsangi, P.S. (2013) Multiple-response optimization of turning machining by the taguchi method and the utility concept using uni-directional glass fiber-reinforced plastic composite and carbide (k10) cutting tool. *Journal of Mechanical Science and Technology*. 27 (9). p. 2829-2837.

Lian, K., Zhang, C., Shao, X. and Gao, L. (2012) Optimization of process planning with various flexibilities using an imperialist competitive algorithm. *International Journal of Advanced Manufacturing Technology*. 59 (5-8). p. 815-828.

Li, B. (2012) A review of tool wear estimation using theoretical analysis and numerical simulation technologies. International Journal of Refractory Metals and Hard Materials. 35 p. 143-151.

Lorentzon, J. and Jarvstrat, N. (2008) Modelling tool wear in cemented-carbide machining alloy 718. *International Journal of Machine Tools and Manufacture*. 48 (10) p. 1072-1080.

Lorentzon, J., Jarvstrat, N. and Josefson, B. L. (2009) Modelling chip formation of alloy 718. *Journal of Materials Processing Technology*. 209 (10) p. 4645-4653.

Madou, M.J. (1997) *Fundamentals of Micro-fabrication*. United States of America:CRC Press.

Majumder, A. (2013) Process parameter optimization during EDM of AISI 316 LN stainless steel by using fuzzy based multi-objective PSO. *Journal of Mechanical Science and Technology*. 27 (7). p. 2143-2151.

Mkaddem, A., Soussia, A. B. and Mansori, M. E. (2013) Wear resistance of CVD and PVD multilayer coatings when dry cutting fiber reinforced polymers (FRP). *Wear*. 302 (1-2). p. 946-954.

Nouari, M. and Ginting, A. (2006) Wear characteristics and performance of multi-layer CVD-coated alloyed carbide tool in dry end milling of titanium alloy. *Surface and Coatings Technology*. 200 (18-19). p. 5663-5676.

Niknam, T., Fard, E.T., Pourjafarian, N. and Rousta, A. (2011) An efficient hybrid algorithm based on modified imperialist competitive algorithm and K-means for data clustering. *Engineering Applications of Artificial Intelligence*. 24 (2). p. 306-317.

Olovsjo, S., Hammersberg, P., Avdovic, P., Stahl, J.-E. and Nyborg, L. (2012) Methodology for evaluating effects of material characteristics on machinability theory and statistics-based modelling applied on Alloy 718. *International Journal of Advanced Manufacturing Technology*. 59 (1-4). p. 55-66.

Palanikumar, K., Karunamoorthy, L., Karthikeyan, R. and Latha B. (2006) Optimization of Machining Parameters in Turning GFRP Composites Using a Carbide

(K10) Tool Based on the Taguchi Method with Fuzzy Logics. *Metals and Materials International*. 12 (6). p. 483-491.

Palanikumar, K. (2008) Application of Taguchi and response surface methodologies for surface roughness in machining glass fiber reinforced plastics by PCD tooling. *International Journal of Advanced Manufacturing Technology*. 36 (1-2). p. 19-27.

Palanikumar, K., Latha, B., Senthilkumar, V. S. and Karthikeyan, R. (2009) Multiple Performance Optimization in Machining of GFRP Composites by a PCD Tool using Non-dominated Sorting Genetic Algorithm (NSGA-II). *Metals and Materials International*. 15 (2). p. 249-258.

Pawade, R. S. and Joshi S. S. (2011) Multi-objective optimization of surface roughness and cutting forces in high-speed turning of Inconel 718 using Taguchi grey relational analysis (TGRA). *International Journal of Advanced Manufacturing Technology*. 56 (1-4) p. 47-62.

Pervaiz, S., Deiab, I., Wahba, E.M., Rashid, A. and Nicolescu, M. (2014) A coupled FE and CFD approach to predict the cutting tool temperature profile in machining. *Procedia CIRP*. 17 p. 750-754.

Pittala, G.M. and Monno M. (2010) 3D finite element modeling of face milling of continuous chip material. *International Journal of Advanced Manufacturing Technology*. 47 (5-8) p. 543-555.

Pusavec, F., Hamdi, H., Kopac, J. and Jawahir, I. S. (2011) Surface integrity in cryogenic machining of nickel based alloy-Inconel 718. *Journal of Materials Processing Technology*. 211 (4) p. 273-283.

Ranganathan, S. and Senthilvelan, T. (2011) Multi-response optimization of machining parameters in hot turning using grey analysis. *International Journal of Advanced Manufacturing Technology*. 56 (5-8). p. 455-462.

Sabour, M.H., Eskandar, H. and Salehi, P. (2011) Imperialist Competitive Ant Colony Algorithm for Truss Structures. *World Applied Sciences Journal*. 12 (1). p. 94-105.

Sait, A.N., Aravindan, S. and Haq, A.N. (2009) Optimisation of machining parameters of glass-fibre-reinforced plastic (GFRP) pipes by desirability function analysis using Taguchi technique. *International Journal of Advanced Manufacturing Technology*. 43 (5-6). p. 581-589.

Sardinas, R.Q., Santana, M.R. and Brindis, E.A. (2006) Genetic algorithm-based multi-objective optimization of cutting parameters in turning processes. *Engineering Applications of Artificial Intelligence*. 19 (2). p. 127i 133.

Schintlmeister, W., Wallgram, W., Kanz, J. and Gigl, K. (1989) Cutting tool materials coated by chemical vapor deposition. *Wear*. 100 (1-3). p. 153-169.

Shabgard, M.R., Badamchizadeh, M.A., Ranjbary, G. and Amini, K. (2013) Fuzzy approach to select machining parameters in electrical discharge machining (EDM) and ultrasonic-assisted EDM processes. *Journal of Manufacturing Systems*. 32 (1). p. 32-39.

Seheikh-Ahmad, J.Y. (2009) *Machining of Polymer Composites*, United States of America:Springer.

Senthilkumaar J.S., Selvarani P. and Arunachalam R.M. (2012) Intelligent optimization and selection of machining parameters in finish turning and facing of Inconel 718. *International Journal of Advanced Manufacturing Technology*. 58 (9-12). p. 885-894.

Talatahari, S., Azar, B.F., Sheikholeslami, R. and Gandomi, A.H. (2012) Imperialist competitive algorithm combined with chaos for global optimization. *Communications in Nonlinear Science and Numerical Simulation*. 17 (3). p. 1312-1319.

Tamizharasan, T. and Kumar, N.S. (2012) Optimization of cutting insert geometry using DEFORM-3D numerical simulation and experimental validation, *International Journal of Simulation Modelling*. 11 (2) p. 65-76.

Tanase, I., Popovici, V., Ceau, G. and Predincea, N. (2012) Cutting edge temperature prediction using the process simulation with DEFORM 3D software package. *Proceedings in Manufacturing Systems*. 7 (4) p. 265-268.

Tay, A.O., Stevenson, M.G. and Davis, G.V. (1974) Using the finite element method to determine temperature distributions in orthogonal machining. *Proceedings of the Institution of Mechanical Engineers*. 188 (1) p. 627-638.

Teimouri, R., Baseri, H. and Moharami, R. (2013) Multi-responses optimization of ultrasonic machining process. *Journal of Intelligent Manufacturing*. (August). [DOI 10.1007/s10845-013-0831-1].

Teti, R. (2002) Machining of Composite Materials, *CIRP Annals-Manufacturing Technology*. 51 (2). p. 611-634.

Thakur, D.G., Ramamoorthy, B. and Vijayaraghavan, L. (2009) An experimental analysis of effective high speed turning of superalloy Inconel 718. *Journal of Materials Sciences*. 44 (12) p. 3296-3304.

Thakur, D.G., Ramamoorthy, B. and Vijayaraghavan, L. (2010) Investigation and optimization of lubrication parameters in high speed turning of superalloy Inconel 718. *International Journal of Advanced Manufacturing Technology*. 50 (5-8) p. 471-478.

Thakur, D.G., Ramamoorthy, B. and Vijayaraghavan, L. (2012) Effect of cutting parameters on the degree of work hardening and tool life during high-speed

machining of Inconel 718. *International Journal of Advanced Manufacturing Technology*. 59 (5-8) p. 483-489.

Thakur, D.G., Ramamoorthy, B. and Vijayaraghavan, L. (2009) Machinability investigation of Inconel 718 in high-speed turning. *International Journal of Advanced Manufacturing Technology*. 45 (5-6) p. 421-429.

Thakur, D.G., Ramamoorthy, B. and Vijayaraghavan, L. (2009) A Study on the Parameters in High-Speed Turning of Superalloy Inconel 718. *Materials and Manufacturing Processes*. 24 (4) p. 497-503.

Thirumalai, R. and Senthilkumaar, J.S. (2013) Multi-criteria decision making in the selection of machining parameters for Inconel 718. *Journal of Mechanical Science and Technology*. 27 (4). p. 1109-1116.

Upadhyaya, G.S. (2001) Materials science of cemented carbides-an overview. *Materials and Design*. 22 (6). p. 483-489.

Umer, U., Qudeiri, J.A., Hussein, H.A.M., Khan, A.A. and Al-ahmari, A.R. (2014) Multi-objective optimization of oblique turning operations using finite element model and genetic algorithm. *International Journal of Advanced Manufacturing Technology*. 71 (1-4). p. 593-603.

Usui, E., Shirakashi, T. and Kitagawa, T. (1984) Analytical prediction of cutting tool wear. *Wear*. 100 (1-3) p. 129-151.

Uhlmann, E., Schulenburg, M. G. and Zettier, R. (2007) Finite element modeling and cutting simulation of Inconel 718. *Annals of the CIRP*. 56 (1). p. 61-64.

Umbrello, D., (2013) Investigation of surface integrity in dry machining of Inconel 718. *International Journal of Advanced Manufacturing Technology*. 69 (9-12) p. 2183-2190.

Vaz Jr., M., Owen, D. R., Kalhori, J. V., Lundblad, M. and Lindgren, L.-E. (2007) Modelling and simulation of machining processes. *Archives of Computational Methods in Engineering*. 14 (2) p. 173-204.

Wertheim, R. (1998) Developpment and application of new cutting tool materials, in: Proceedings of the Conference on Improving Machine Tool Performance. San Sebastian. Spain. July. p. 303-313.

Yang, S.H. and Natarajan, U. (2010) Multi-objective optimization of cutting parameters in turning process using differential evolution and non-dominated sorting genetic algorithm-II approaches. *International Journal of Advanced Manufacturing Technology*. 49 (5-8). p. 773-784.

Yen, Y.C., Sohner, J., Lilly, B. and Altan, T. (2004) Estimation of tool wear in orthogonal cutting using the finite element analysis. *Journal of Materials Processing Technology*. 146 (1) p. 82-91.

Yousefi, M., Darus, A.N. and Mohammadi, H. (2012) An imperialist competitive algorithm for optimal design of plate-fin heat exchangers. *International Journal of Heat and Mass Transfer*. 55 (11-12). p. 3178-3185.

Yue, C. X., Liu, X. L., Pen, H. M., Hu, J. S. and Zhao, X. F. (2009) 2D FEM estimate of tool wear in hard cutting operation: Extractive of interrelated parameters and tool wear simulation result. *Advanced Materials Research*. 69-70 p. 316-321.

Zebala, W. and Slodki, B. (2013) Cutting data correction in Inconel 718 turning. *International Journal of Advanced Manufacturing Technology*. 65 (5-8). p. 881-893.

Zhao, H., Barber, G.C. and Zou, Q. (2002) A study of flank wear in orthogonal cutting with internal cooling. *Wear*. 253 (9-10) p. 957-962.

Zhou, J., Bushlya, V., Avdovic, P. and Stahl, J. E. (2012) Study of surface quality in high speed turning of Inconel 718 with uncoated and coated CBN tools. International Journal of Advanced Manufacturing Technology. 58 (1-4) 141-151.

Zhu, D., Zhang, X. and Ding, H. (2013) Tool wear characteristics in machining of nickel-based super-alloys. *International Journal of Machine Tools and Manufacture*. 64 (January) p. 60-77.

List of Publications

Papers Accepted for Publication

- **Rajiv Kumar Yadav**, Kumar Abhishek, Siba Sankar Mahapatra, A Simulation Approach for Estimating Flank wear and Material Removal Rate in Turning of Inconel 718, *Simulation Modelling Practice and Theory.* DOI: 10.1016/j.simpat.2014.12.004.
- **Rajiv Kumar Yadav**, Kumar Abhishek, Siba Sankar Mahapatra, Numerical Simulation and Parametric Optimization in turning of Inconel718, *Procedia Engineering.*

Published Papers

- Suman Chatterjee, Kumar Abhishek, **Rajiv Kumar Yadav**, S.S. Mahapatra, Optimization of Drilling Process Parameters by Harmony Search Algorithm, *IEEE Xplore-Recent Advances and Innovations in Engineering (ICRAIE)*. DOI: 10.1109/ICRAIE.2014.6909278.
- Kumar Abhishek, Suman Chatterjee, **Rajiv Kumar Yadav**, Rajesh Kumar Verma, Saurav Datta, Siba Sankar Mahapatra and Pradip Kumar Pal, A Fuzzy-ICA Based Hybrid Approach for Parametric Appraisal in Machining (Turning) of GFRP Composites, *International Journal of Basic and Applied Science Research (IJBASR),* Vol. 1, 2014, pp. 15-19.
- Suman Chatterjee, Kumar Abhishek, Siba Sankar Mahapatra, Saurav Datta, **Rajiv Kumar Yadav**, NSGA-II Approach of Optimization to Study the Effects of Drilling Parameters in AISI-304 Stainless Steel, *Procedia Engineering*, Vol. 97, 2014, pp. 78-84.

International Conference

- **Rajiv Kumar Yadav**, Kumar Abhishek, Siba Sankar Mahapatra, ñNumerical Simulation and Parametric Optimization in turning of Inconel718ò, 4th Nirma University International Conference on Engineering, (NUiCONE)-2013, Gujarat, November 28-30, 2013.